PROCESS OPTIMIZATION IN MACHINING

PROCESS OPTIMIZATION IN MACHINING: AN APPLIED RESEARCH APPROACH

BY

SIMON OOMEN-HURST

B.ENG. (MECH. ENG.)

A Thesis Submitted to the School of Graduate Studies in Partial Fulfilment of the Requirements for the Degree Master of Applied Science.

MASTER OF APPLIED SCIENCE (2012) MCMASTER UNIVERSITY

(MECHANICAL ENGINEERING) HAMILTON, ONTARIO,

CANADA

TITLE: PROCESS OPTIMIZATION IN MACHINING: AN APPLIED RESEARCH APPROACH

AUTHOR: SIMON OOMEN-HURST

B.ENG (MECH ENG) MCMASTER UNIVERSITY

SUPERVISOR: DR. S. VELDHUIS

NUMBER OF PAGES: xii, 120

ACKNOWLEDGEMENTS

The success of this work was supported heavily by the amazing people in the MMRI and Mechanical Engineering department at McMaster University.

First and foremost, I'd like to thank Dr. Veldhuis for his support and encouragement, as well as for his endless efforts which provide myself and my fellow researches with such rich opportunity in the MSL. I would also like to specially thank Mr. Maneesh Khanna for his technical support, as well as his experience and guidance, which has been invaluable in navigating the intricacies of collaborative industrial research.

I would also like to thank Dr. M.D. Abad, Dr. G. Fox-Rabinovich, and Dr. Julia Dosbaeva for their expertise and support in this research, as well as Mr. Terry Wagg, Mr. Jim McLaren, Mr. JP Talon, Mr. Mark MacKenzie Mr. Ron Lodewyks, and Mr. Joe Verhaege for their training and technical support throughout my work.

I would also like to acknowledge Siemens Power Generation Canada and Precision-Tech ltd., as well as NSERC and CANRIMT for their financial contributions.

Finally, I would like to thank my fellow graduate students, Mr. Mark Dubois, Mr. Jeremy Boyd, and Mr. Kevin Tanaka for their thoughts and feedback throughout my research.

ABSTRACT

The objective of this research was to work with industrial partners to develop and apply innovative and intelligent improvement to their production processes in order to achieve a higher level of productivity and quality while lowering cost.

Two projects were completed and are discussed in this work. The first project was focused on improving tooling in a milling process of high value parts by varying coatings and geometries of the tooling. The second project involved implementing statistical process control (SPC) using control charts and process capability metrics through customized software.

In the first project, the industrial partner was experiencing rapid wear of tools when milling NiCrMoV steel. A detailed material characterisation study revealed the likely cause was the presence of un-tempered martensite having high hardness. Cutting tools were then chosen to compare the performance of tools with varying rake angle and coating; where all other geometry/features were identical. It was found that the best performing tooling had a relatively more aggressive rake angle at 16º, and a PVD coating consisting of TiAlN + Al_2O_3 + ZrN; showing a tool life 300% greater than the baseline tooling. Inspection of the worn tools by SEM, EDX, and Raman spectroscopy revealed that the Al_2O_3 and ZrN coating layers detached long before the failure.

In the second project, software was developed collaboratively with an industrial partner for a CNC turning process. The process was semi-automated, and used 100% inspection of parts. Part measurement data was recorded by the software, allowing for SPC to be applied to identify common-cause sources of variation. The software was then able to make offset recommendations in real-time to correct for variation. Providing process history for quality assurance (QA) also allowed for identifying of several areas for improvement in the process which were corrected, considerably reducing variability.

TABLE OF CONTENTS

LIST OF FIGURES

LIST OF TABLES

CHAPTER 1. INTRODUCTION

Manufacturing in Ontario generated $258 billion in 2011, down significantly from its high in 2007 at $287 billion (Statistics Canada, 2012). Though activity is recovering, international competition remains a threat to Canadian manufacturers. Regions which are able to compete based on low labour cost and few regulatory hurdles put pressure on domestic manufactures to reduce prices and costs. As Canada values its worker's rights and mandates fair compensation, Canadian manufacturers must focus on innovation to remain competitive in the global market.

The research completed and discussed in this body of work holds the potential to assist Canadian manufacturers, specifically in the area of machining, in taking steps towards achieving the goals of increased productivity and quality, as well as lowered cost. The two projects in this work highlight different areas of machining where leveraging advanced knowledge and technology will improve process control and improve productivity.

The first project focuses on tooling in a machining process. By intelligently analysing the performance of tooling and characterising the workpiece material, it is possible to select tooling which can vastly exceed the performance and life of previous tools. An increased tool life means that the tool can be used to produce more parts and needs to be replaced less frequently. Tool replacement is a time intensive activity which halts production and triggers the need for manual labour, and so minimizing the need for this helps improve productivity and lower cost. A better performing tool can also allow a process to operate at higher speeds, allowing a machine to produce more parts than before. This increases productivity and capacity without capital cost. A more reliable tool which fails less often allows a process to become automated, improving productivity and lessening the need for low-value added manual labour thus driving down cost and allowing labour to focus on high-value added activities.

The second project focuses on assisting manufacturing companies in taking the first step towards automation in their processes. In order to automate a process, it must first be understood. Once it is understood, it needs to be controlled. Once it can be controlled, then it can be automated. This project focused on providing a software based tool which can collect the data necessary to understand a process and provide first-steps toward controlling it. By understanding their process, a company no longer is operating in a “fire-fighting” mentality where operations are not inspected or analysed until a production problem is identified and needs to be corrected immediately. When a process is understood, production problems can be identified and corrected early on, before they become major issues which significantly hinder productivity. As well, areas for potential increases in productivity or quality are easily identified and support for improvement activities can be made using production data.

1.1 RESEARCH PROJECT DESCRIPTIONS, MOTIVATION AND OBJECTIVES

The vast majority of the work described was completed in cooperation with industrial partners. These projects were generated by manufacturing companies identifying goals relating to process problems or potential areas of improvement. These goals align with the research strengths of the Machining Systems Lab (MSL) and specific researchers within it. The manufacturer and researchers then work collaboratively to pursue a solution, leveraging both the extensive knowledge of the research group and production experience and resources of the industrial partner. Through this process, the industrial partner gains a knowledge based improvement to their process and the research group gains knowledge, funding and opportunities to find applications for their basic science work.

The body of work described in this thesis is very much in-line with this vehicle for research. Two major projects were completed, having very different research content but both pursuing the same goal: aiding Canadian industry by

providing research and knowledge based improvements for their processes which achieved real world results. Each project is briefly described, along with the objectives for each in the following sections.

1.1.1 PROJECT 1: COMPARISON OF HARD COATINGS AND TOOL GEOMETRIES

Description

The first project was done in collaboration with Siemens Power Generation Canada. The plant manufactured large-scale power generation turbines in the range of 100 MW – 500 MW outputs, and worked extensively with high-temperature and corrosion resistant steels, which are challenging to machine. The project focused on a side-milling operation used to machine dove-tail slots into large compressor disks which hold compressor blades. After implementing a new material type for the compressor disk, the process began to show very high rates of tool wear. Siemens sought the aid of the McMaster Manufacturing Research Institute (MMRI) to improve the life of the tools.

Motivation

The industrial motivation for this project is described first. Siemens found that tool wear had significantly accelerated after implementing the new material type for the disk. The operators found that tools would wear out before completing a single cutting pass, presenting significant technical risk to the part should an insert fail catastrophically during cutting. Additionally, the frequent changing of inserts on the tooling was hindering production considerably. Therefore, Siemens required a solution to improve the life of their tooling.

This project provided an opportunity to advance the research groups knowledge on tool life in stainless steel-like materials; with specific focus on application of tooling coatings to resist the dominant wear mechanisms found in this process.

Objectives

The three main research objectives for this project are discussed in the paragraphs below.

The first objective was to understand and characterize the wear mechanisms which were causing the accelerated tool wear. This involved a detailed material and microstructure analysis.

The next step was to perform machining trials with the current tooling and additional tooling which varied in either geometry or coating composition. The objective of this stage was to empirically identify the best performing tooling through machining trials which closely resemble the actual cutting process.

The final objective was to correlate insert performance to their differences in geometry and coating through characterisation and analysis of the worn inserts.

1.1.2 PROJECT 2: PROCESS MONITORING

Description

This project was done in collaboration with a mid-volume automotive manufacturing company producing CNC machined parts. Their processes are semi-automated and do not include process control, and require significant operator attention and interaction. In an attempt to improve and better understand their process, they entered into a collaborative project with the MMRI to develop a software based solution to monitor one of their high-volume production cells. The software would interface with their existing gauges and CNC machines to monitor trends in parts, identify problems in production, and provide valuable process history for quality control purposes.

Motivations

Understanding exactly what is happening in a production process is not straight-forward. Without a software based solution, it is extremely difficult and time consuming to monitor the process. Doing so would require nearly 100% inspection, record, and analysis of parts which is costly, time consuming and the additional duties required of the operator would heavily impact production rates. Therefore, in an attempt to achieve a high level of process understanding, and eventually control, the MMRI worked collaboratively with the company to develop a software package to monitor, analyze and control a test production cell.

The motivation for the MMRI was to develop software which could aid in quantifying process improvements. It is often difficult to quantify the exact improvement associated with implemented recommendations made by the MMRI for industry. This is problematic both because it hinders research efforts if long-term results of specific improvements are not available and it is more difficult to quantify economic impact of improvements in order to attract future research collaboration with industry. Therefore, having software which can track the performance of a process over weeks or months after a process improvement and report these changes in a useful form would be extremely valuable to the research group and the industrial partner.

Objectives

The objective for this project was to produce software which could be implemented for on-line process monitoring and control. The software should have a modular structure, so that it can easily and quickly be adapted to industrial needs, and should provide valuable feedback on process improvements in order to quantify those improvements in terms of metrics such as tool life, production rates, scraped part rates, etc.. The process should also have the ability to analyze production data in real time to provide useful feedback in the form of

specification limit alerts, offset recommendations or other process specific parameters.

CHAPTER 2. BACKGROUND

This section provides the necessary background information required to understand and follow the described work. This section is not intended to be exhaustive, and so in the interest of brevity some information is left to the interested reader to pursue. This is especially prevalent in the sections covering the basics of cutting theory, which are well established and published in numerous sources.

2.1 TOOLING HISTORY

High speed steel constituted the majority of cutting tools until the invention of cemented carbide as a cutting tool material in 1923 (Guo, et al., 2010). Though more brittle, its superior hardness and abrasion resistance led to significant increases in tool life and productivity in machining. The next major advancement in tooling was the introduction of wear-resistant and lubricious coatings, starting in 1971.

Coating deposition was first done through chemical-vapour deposition (CVD), followed by physical vapour deposition some years later. TiC, TiN and Al_2O_3 were among the first materials to be used for coating inserts to enhance wear and thermal resistance. In addition, combining these coatings allowed for even further enhancements for tool performance by combining the advantages of each.

Eventually PVD methods for applying coatings began to replace CVD as the deposition temperatures involved in PVD are significantly lower, at around 500ºC compared with 1000ºC for CVD. Furthermore the range of materials that can be deposited with PVD process is far greater than CVD based processes. This provides the end user with greater flexibility when designing a coating. TiAlN also gained popularity for its high speed capabilities and heat resistance. Al_2O_3 coatings have remained popular as well, benefiting from substantial

improvements in deposition techniques to significantly improve its mechanical properties and bonding through phase control and microstructural refinement (M'Saoubi & Ruppi, 2009). In recent years, duplex deposition methods combining both CVD and PVD have been developed and provide excellent performance on difficult to machine materials such as stainless steels, exotic materials and super-alloys (Votsch, et al., 2004) (Schiller, et al., 2004) (Grzesik, 1999).

Cutting edge geometry has also been an area of prolonged and intense study due to the significant effect it can have on tool life and performance (Maranhao, et al., 2010) (Gunay, et al., 2004). Tool features such as the chip breaker and rake angle influence the specific cutting energy behaviour of the tool, and even slight modifications to these geometries can affect both cutting force and tool life significantly.

2.2 CUTTING THEORY

This section will provide a brief overview of the theory necessary to understand the forces involved in machining.

2.2.1 ORTHOGONAL CUTTING

In order to greatly simplify analysis of cutting forces, the assumption of orthogonal cutting is often made. This simply means that the metal cutting operation is done with a tool that is uniform in the direction perpendicular to cutting, as shown in Figure 2.2-1(a). Figure 2.2-1(b) shows the more complex case where the tool is not uniform in the perpendicular direction and is known as oblique cutting.

The orthogonal cutting assumption has been shown to be a reasonably accurate simplification of oblique metal cutting (Shaw, 1997), and is therefore widely used due to its relatively lower complexity. The assumption allows for force predictions and calculations to be completed in just two dimensions.

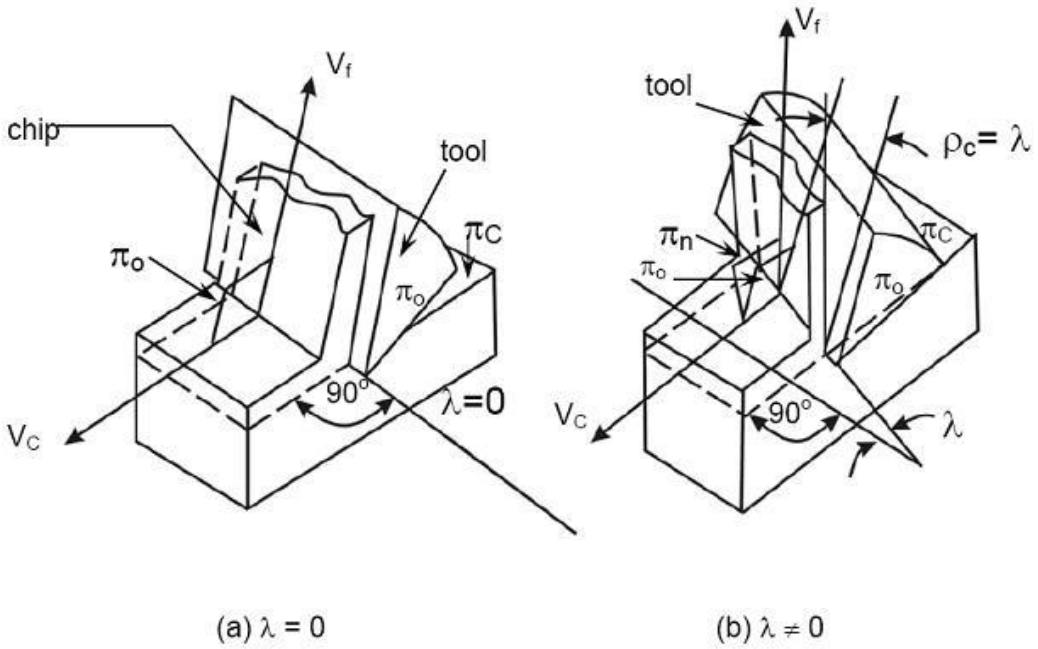

Figure 2.2-1 – Orthogonal cutting (a) vs. oblique cutting (b) (Parthasarathy, 2011)

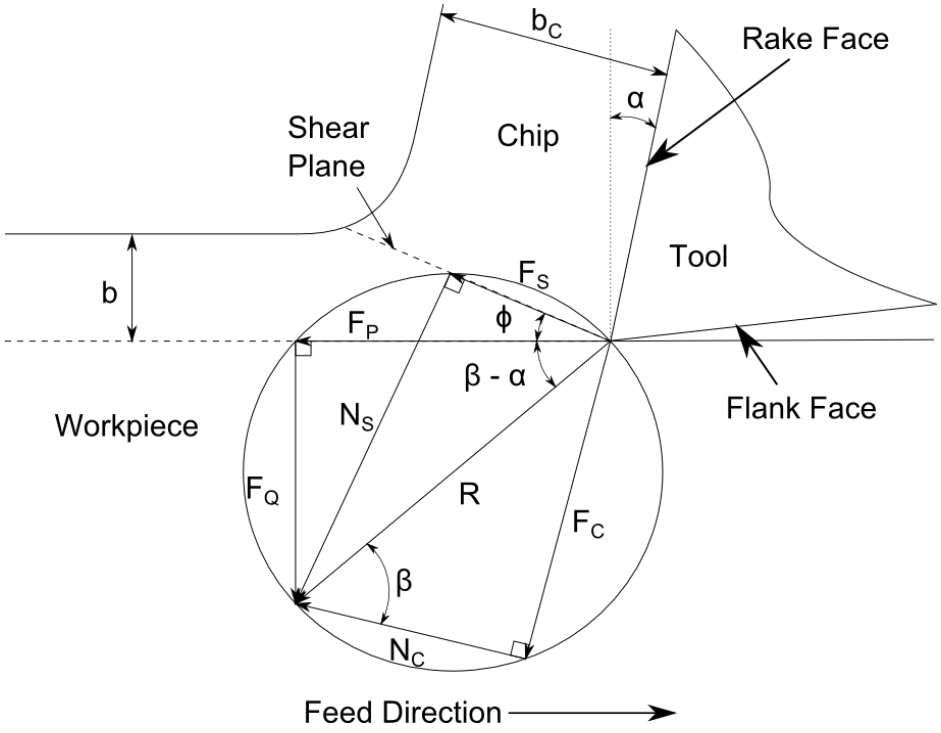

Figure 2.2-2 – Cutting forces diagram for orthogonal cutting according to Merchant's model

2.2.2 CUTTING FORCE ESTIMATION IN ORTHOGONAL CUTTING

Using the orthogonal assumption discussed in the previous section, useful cutting force calculations can be made to predict the forces seen by the tool during cutting. The nomenclature for this section is explained below. See Table 2.2-1 and Figure 2.2-2 for an explanation of these terms.

Table 2.2-1 – Nomenclature for force equations

Term	Meaning
Rake Face	The face of the tool that is in contact with the chip
Flank Face	The face of the tool which faces the machined surface of the workpiece
Feed Direction	The direction which the workpiece travels past the tool
b	Un-cut chip thickness or depth of cut
$\mathbf{b_C}$	Cut-chip thickness
$\boldsymbol{\phi}$	Shear angle; defined as the angle between the feed direction and the shear plane
$\boldsymbol{\alpha}$	Rake angle; defined as the angle between the rake face and vertical (shown as positive)
$\boldsymbol{\beta}$	Average friction angle; defined as the average friction angle between the tool's rake face and the moving chip
$\mathbf{F_p}$	Cutting force; force acting on the tool in the direction of feed
$\mathbf{F_Q}$	Thrust force; force acting on the tool perpendicular to the feed direction
$\mathbf{F_S}$	Shear force; the force acting in the direction of the shear plane
$\mathbf{N_S}$	Normal shear force; the force acting normal to the shear plane
$\mathbf{F_c}$	Friction force; the frictional force generated on the rake face
$\mathbf{N_c}$	Rake face normal force; the normal force acting perpendicular to the rake face
R	Resultant force

Merchants model is a well established, widely published, and widely referenced theory in the field of machining. For this reason, the interested reader is directed to (Shaw, 1997), (Altintas, 2012) and (Stephenson & Agapiou, 1997) to learn more regarding Merchant's cutting force model. For the purposes of this

work, it is sufficient to know that Merchant's model approximates forces well, though often over-estimates magnitudes and therefore provides conservative estimates (Eggleston, et al., 1959).

In the following work, it is necessary to understand three forces involved in milling. The three are essentially cutting force (F_p) and thrust force (F_Q) for two faces, as shown in Figure 2.2-3. Cutting is occurring on both the axial and radial faces of the tool, and applying the orthogonal assumption means that there will be a cutting force and a thrust force for each. The cutting force for both edges act in the same direction, and can be represented as a resultant cutting force. The thrust forces for each face act perpendicular to the face. In this work, the axial thrust force is described as the "thrust force", and the radial thrust force is described as the "side force".

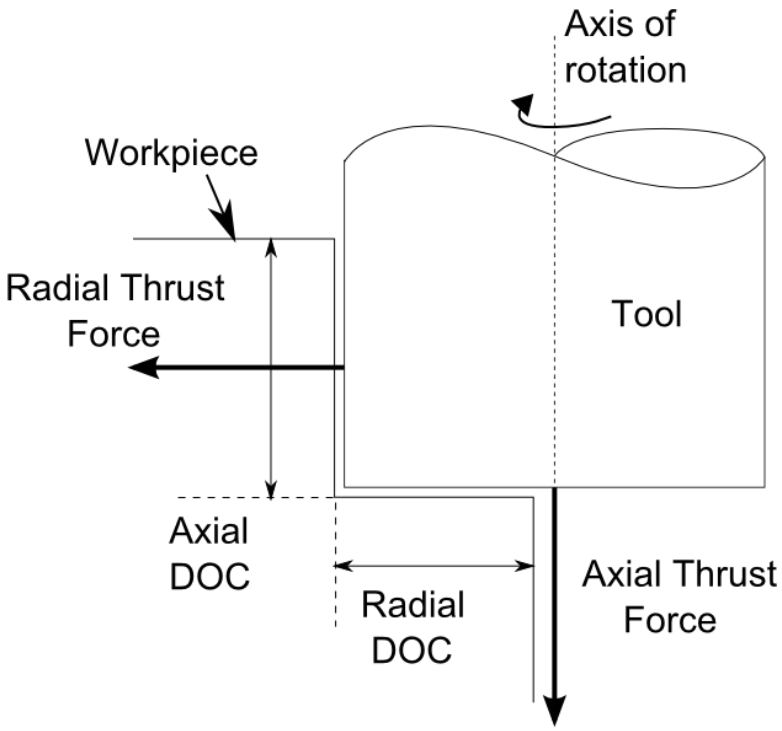

Figure 2.2-3 – Cutter showing both axial and radial engagement with a workpiece

2.2.3 TOOL WEAR MECHANISMS

There are several types of wear that a tool may experience during cutting, depending on the conditions and process. A fairly exhaustive list of wear types are shown in Figure 2.2-4 and are discussed in Table 2.2-2. Though wear types can vary widely, the five main mechanisms which are responsible for these wear types are:

1) Abrasive Wear – A mechanical wear mechanism where hard particles (or a hard bulk material) scratch and abrade the tool, slowly wearing it away
2) Adhesive Wear – A chemical or mechanical wear mechanism where workpiece material will weld to the tool under the high pressure and temperature conditions in the cutting zone; this workpiece material will then break away from the tool, and with it removing a small (or sometimes large) chunk of tool material as well
3) Diffusion – A chemical wear mechanism where tool material will diffuse into workpiece material; this mechanism occurs mostly at high temperatures and depends on affinity between material and workpiece (example: diamond cutting tools will diffuse readily into low-carbon steels due to the workpiece's strong affinity for carbon)
4) Oxidation – A chemical wear mechanism where tool material will oxidize (burn) due to high heat and exposure to oxygen in the atmosphere
5) Mechanical Load – A mechanical wear mechanism where tool loading exceeds the capabilities of the tool, causing it to break

The mechanisms discussed above are correlated to the wear types in Table 2.2-2.

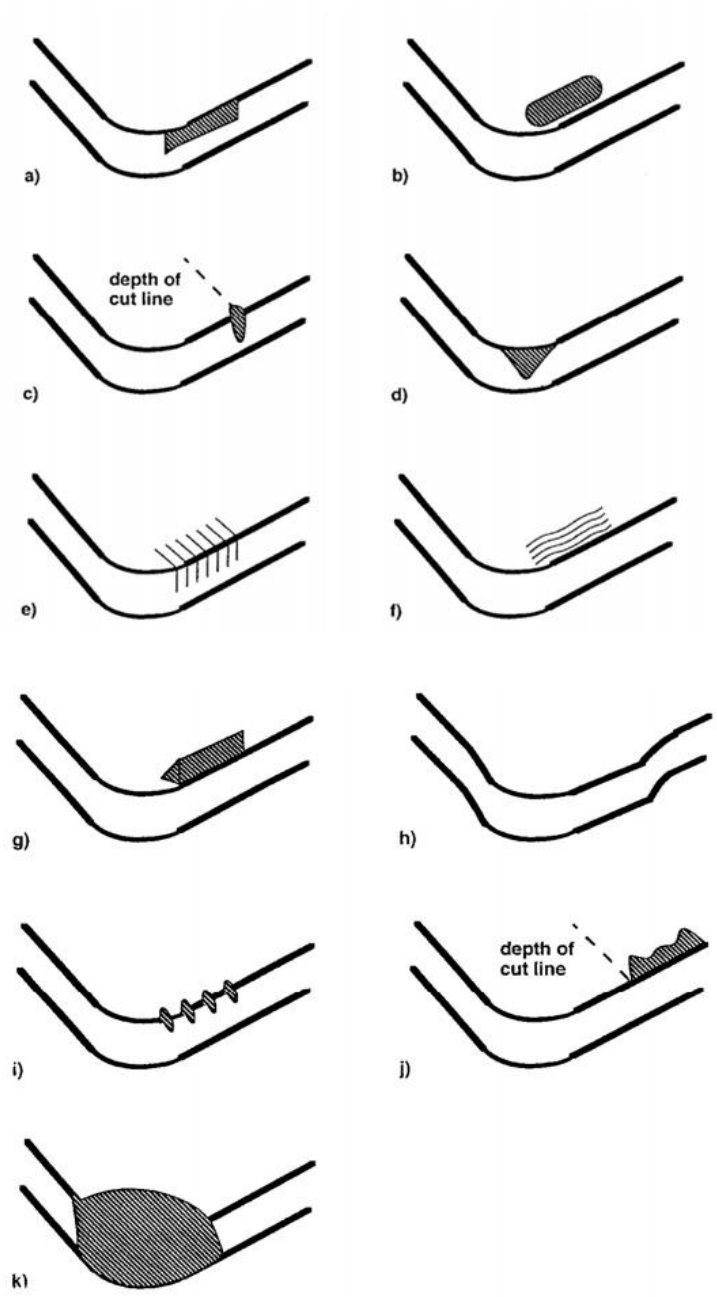

Figure 2.2-4 – Tool wear types: (a) Flank wear; (b) Crater Wear; (c) Notch wear; (d) Nose Wear; (e) Comb cracking (thermal); (f) Parallel cracking (mechanical); (g) Built-up edge; (h) Gross plastic deformation; (i) Minor chipping; (j) Chip hammering; (k) Major chipping/gross fracture (Stephenson & Agapiou, 1997)

Table 2.2-2 –Wear Mechanisms (Stephenson & Agapiou, 1997)

Type	Mechanism	Description
Flank Wear (a)	Abrasive	Caused by rubbing of the flank face on the machined surface
Crater Wear (b)	Diffusion Adhesion	At elevated temperatures the tool material will begin to diffuse into the workpiece material causing craters to form; alternatively the craters may form due to micro-chipping as tooling layers are sheared away by localized adhesion effects
Notch Wear (c)	Oxidation	This wear type typically occurs in turning or other processes where the majority of the tool is continuously embedded in workpiece material and therefore not exposed to oxygen in the surrounding atmosphere. However, at the depth of cut line the tool is exposed and the elevated tool temperatures cause notch wear to form due to oxidation along that line
Nose Wear (d)	Abrasive Oxidation	Nose wear typically occurs in turning operations on the relief face of the tool, and is a combination of flank wear and notch wear. The relief face allows oxygen to reach near to the cutting edge allowing oxidation wear to occur in addition to abrasive wear resulting in flank wear.
Comb Cracking (e)	Mechanical (thermal)	In brittle tools, temperature gradients developed on the cutting tool may cause thermal stresses on the surface of the tool which will can cause or accelerate cracking of the tool or coatings.
Parallel Cracking (f)	Mechanical	Especially prevalent in interrupted cutting such as milling, mechanical cracking may occur in brittle tools due to impact loading on the tool's cutting edge. Repeated impacts initiate crack propagation which weaken the cutting edge of the tool and may lead to chipping or gross fracture
Built Up Edge (g)	Adhesive	Due to high temperature and loads occurring in the cutting zone, workpiece material can weld to the tool. If the degree of adhesion is large, the tool material may build up on the tool's cutting edge, effectively increasing the size of the tool. Eventually the built up edge will reach a critical size, at which point it may break away harmlessly, or may fracture a large piece of tool material, often resulting in tool failure.

Gross Plastic Deformation (h)	Mechanical	This type of wear is most common in ductile tooling materials, such as high speed steel. Due to high heat and loading, the tool material may deform, changing the tool geometry, depth of cut and other important process parameters.
Minor Chipping (i)	Mechanical Adhesive	Minor chipping can be the eventual result of residual cracks caused by either thermal (comb cracking) or mechanical (parallel cracking) wear types, and is especially prevalent in interrupted cutting, such as milling. It can also be the result of adhesive wear, were the level of adhesion is small and so fractured tool material remains minimal.
Chip Hammering (j)	Mechanical Abrasion	Chip hammering occurs when the formation of the chip is not well controlled. The chip curls up, away from then tool and is then forced back down to strike and abrade the tool away from the cutting zone.
Gross Fracture (k)	Mechanical Adhesion	Catastrophic failure of the tool by massive chipping/gross fracture can occur for a number of reasons. If mechanical loading on the cutting edge far exceeds the capacity of the tool to support it can cause this. As well, the breaking off of a large built up edge can cause gross fracture as previously discussed. Severe thermal or mechanical cracking can also lead to this wear mechanism.

2.3 NiCrMoV MATERIAL AND TOOL CHARACTERISATION

In industry, simply comparing tool lives through machining trials is often sufficient to see some improvement over existing tool performance. However, in order to better capture these benefits it is useful to do a detailed study of the worn tools. Drawing correlations between tooling performance and its properties provides a powerful tool for intelligently modifying tooling selections to maximize process performance and efficiency.

It is also beneficial to do material characterisation studies on workpieces. This will lend understanding to the wear mechanisms seen on tooling by

correlating them to properties of the material that are well known to cause issues in machining.

2.3.1 MICRO-HARDNESS

Testing for hardness using a standard Vickers micro-hardness test (formerly known as a diamond pyramid hardness test) is an effective way to investigate material hardness and homogeneity (Kalpakjian & Schmid, 2006). Wear rates in metal cutting have long been shown to be inversely proportional to hardness of the tooling material (Rabinowicz, 1995), and so having some measure of the workpiece hardness is necessary for any tool wear study.

2.3.2 MICROSTRUCTURE – OPTICAL AND SEM METHODS

The microstructure of a material plays a very significant role in both tool wear mechanisms and wear rates as it heavily affects the mechanical properties of steels. This microstructure can sometimes be identified through visual inspection with the aid of optical and scanning electron microscopy. A polished and etched sample of workpiece material observed by these means will reveal the grain structure and give insight into how it might affect tool wear.

The materials concerned in this body of work are NiCrMoV steels, which are similar to the family of stainless steels. NiCrMoV steels are capable of heat treatment by both quenching and precipitate hardening (McHaughton, et al., 1991), and are often tempered or subjected to artificial aging to improve toughness, strength and to reduce brittleness.

2.4 SUPER-CLEAN STEELS

The term “superclean” describes steels that have been produced to have very low levels of non-metallic inclusions or contaminants such as silicon, sulfur, phosphorus, manganese, arsenic and antimony. This is done through careful control of the steelmaking process to limit the level of contaminants.

2.4.1 HARDNESS AND MACHINABILITY OF NiCrMoV STEEL

NiCrMoV hardness values have been found to range from 230 – 350 HV (Ryu, et al., 1997), (Wittig & Joshi, 1990), (Shige, et al., 2001). Micro-hardness has also been found to increase with increasing levels of purity, meaning lower levels of non-metallic inclusions (Coutsouradis, 1994). Initially during the development of high-purity NiCrMoV steels for use in power generation, machinability was a concern; though (Bachelet, 1990) reports that no significant machining issues were seen.

One goal of producing high-purity NiCrMoV steels is to reduce sulphur levels, an additive which is typically associated with improved machinability. Thus, it is expected that minimizing the inclusion of this element would decrease machinability. However, (McHaughton, et al., 1991) reports:

> *“..very low sulfur steels are supposed by some to be more difficult to machine, but the evidence accumulated with all the trial and production rotor forgings of superclean 3.5NiCrMoV steel does not support this supposition.”*

As discussed in this work, issues surrounding the machining of these steels related to increased abrasive tool wear were observed, and so other factors aside from steel chemical composition alone must be a factor. One possibility may be heat treatment, as (Gates, et al., 1987) reports that the mechanical properties of NiCrMoV, as with most stainless steels, can vary widely depending on heat treatment.

2.5 STATISTICAL PROCESS CONTROL (SPC) METRICS

As noted by (Kalpakjian & Schmid, 2006), manufacturing inherently involves sources of variability, including:

- Wear on tooling
- Machinery condition (age, maintenance, quality etc)
- Condition of metalworking fluids
- Environmental conditions (temperature, humidity etc.)
- Incoming material variation (hardness, dimensional changes, etc)
- Operator skill and attention

Some of these can be tracked and minimized (common-cause variation) while others are more random (special cause variation) making them difficult to track. Statistical process control is the application of statistical tools to a process with the goals of minimizing common-cause sources of variability in the process output and understanding the underlying causes of special cause variation.

By implementing SPC in real-time, non-random variation in a process, such as tooling wear and environmental conditions, can be identified and corrected automatically.

In this body of work, SPC was implemented in a process using two SPC metrics: a weighted moving average, and process capability.

The weighted moving average was calculated using seven data points with a linearly decreasing weighting:

$$\bar{x} = \sum_{i=1}^{7} n_i \frac{(7-i)}{7}$$ **Equation 2.5-1**

Process capability is a measure of how data variability in a process compares to the specification limits set on the process. This requires some

understanding of control charts. A sample control chart showing some necessary terminology is shown in Figure 2.5-1 and explained in Table 2.5-1.

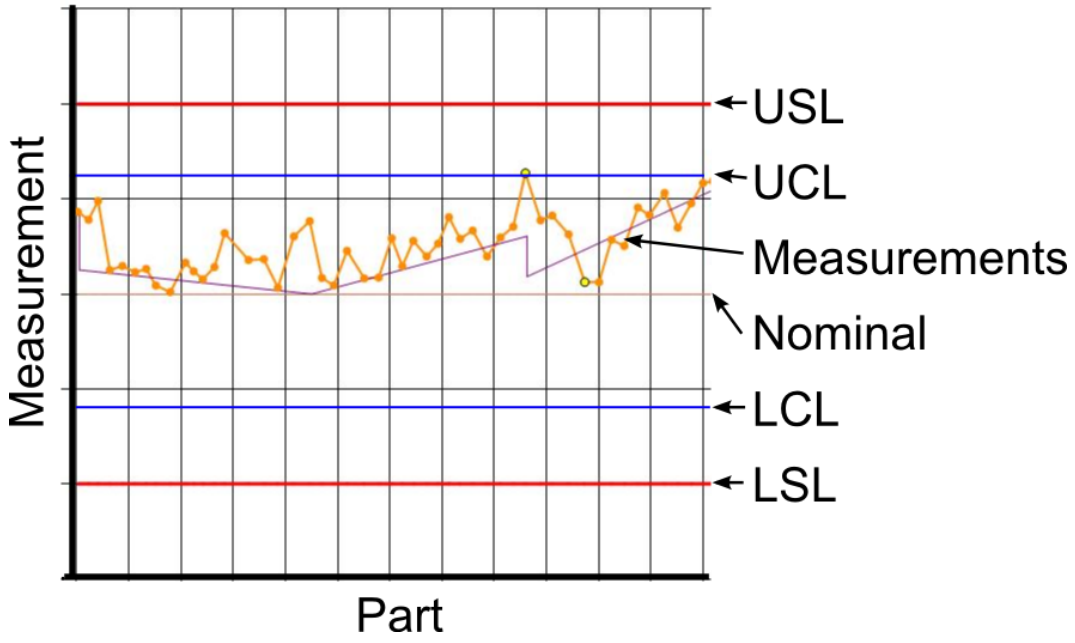

Figure 2.5-1 – Sample control chart

Table 2.5-1 – Explanation of control chart terminology

Feature	Description
USL/LSL Upper/Lower Specification Limit	This is a value, often denoted by a tolerance limit on a part or feature; any measurement beyond these limits mean the part must be scrapped or repaired
UCL/LCL Upper/Lower Control Limits	These are limits set intelligently by quality control using SPC; when a part or process average exceeds these limits it means that the process is out of control and requires corrective action; alternatively, this even is sometimes due to a special-cause variation and does not require attention

Process capability is a metric which is calculated using the process variability (standard deviation) as well as the specification limits (often times simply being the tolerance range on a part). The formula for calculating process capability follows (Chandra, 2001):

$$c_P = \frac{UCL - LCL}{6\sigma}$$ **Equation 2.5-2**

However, the above metric assumes that the process mean is centered between the UCL and LCL. Therefore, if it is not centered, perhaps due to an improper tool offset, c_p will over-estimate the capability of the process. Therefore, a modified index is used to better represent a non-centered process:

$$c_{PK} = min\left[\frac{UCL - \bar{x}}{3\sigma}, \frac{\bar{x} - LCL}{3\sigma}\right]$$ **Equation 2.5-3**

This value gives an estimate of the number of parts which are falling between the specification limits, and therefore are often used to calculate number of defects per million opportunities (DPMO). Some process capability values along with their DPMO estimates are shown in Table 2.5-2.

Table 2.5-2 – Process capability and DPMO

Process Capability (C_{PK})	Sigma level	DPMO*
0.33	1	317311
0.50	1.5	133614
0.67	2	45500
0.8	2.4	16395
1.0	3	2700
1.33	4	63
1.50	4.5	7
1.67	5	1
2.00	6	0.002

*These values are calculated using the probability density function for a normal distribution

C_{PK} requirements vary significantly between applications; a safety critical application may require a C_{PK} value exceeding 2.0, where automotive production often targets 1.3 minimum and 1.67 ideally (ISO spec. TS16949). These values are set on a case-by-case basis between customers and suppliers, though the values above are common to the automotive manufacturing industry.

It should be noted that one limitation in the use of process capability indices is they require that the data be normally distributed. Therefore, normality testing should be completed on sample data in order to determine how closely it fits a normal distribution. If a set of data is not normally distributed, the capability indices will either overestimate capability resulting in potential production problems going un-noticed and higher than expected DPMO; or under-estimate capability which will trigger unnecessary efforts to correct variability which is not actually occurring.

Statistical process control and Process capability are well established topics and further information for the interested reader can be found in (Chandra, 2001) and (Tennant, 2001).

CHAPTER 3. COMPARISON OF HARD COATINGS AND TOOL GEOMETRIES

The body of research discussed in this chapter focuses on tool wear studies for NiCrMoV steel through a collaborative project with Siemens Power Generation Canada. The results of this work were peer-reviewed and published in Tribology International, and this chapter closely follows this publication (Oomen-Hurst, et al., 2012) with the contributions of others to this research clearly indicated. NiCrMoV steels have properties which make them suitable for the power generation industry, though recently they have seen increased usage in aerospace and automotive industries as well (Salemi & Abdollah-zadeh, 2008).

NiCrMoV steels are designed to resist temper embrittlement, a phenomenon that occurs in NiCrMoV steels which reduces the toughness of the steel. Temper embrittlement occurs after prolonged exposure to operating temperatures between 350ºC and 575ºC, commonly found in gas and steam turbine applications (Gates, et al., 1987). This is accomplished by careful production of the steel to minimize levels of non-metallic inclusions or contaminants such as silicon, sulphur, phosphorus, manganese, arsenic and antimony which are known to negatively impact the mechanical properties of the steels, such as fracture toughness (Schlicht, et al., 1988). The goal of this is to produce steel which is resistant or immune to temper embrittlement by reducing the levels of non-metallic inclusions which are thought to be a major cause of temper embrittlement.

Problems arise in machining of NiCrMoV steels due to high hardness, high toughness, and inconsistent microstructure, which contribute to accelerated tool wear and chipping. NiCrMoV steel is often used for large rotor forgings for gas or steam turbines and is extremely expensive and time consuming to produce. It is therefore critical that cutting insert selection is carefully completed to minimize the risk of an insert failing mid-cut, which could potentially damage the rotor.

This body of work was divided into three phases, and each is briefly described:

--- Phase 1: Material Characterisation

In order to understand what may be causing the severe tool wear, a material characterisation study was conducted on material samples. Optical methods, SEM, hardness testing, and XRD were all performed to identify material properties which may have been responsible for the accelerated tool wear.

--- Phase 2: Experimental Testing

Once potential causes of tool wear were identified in Phase 1, new tooling was selected and lab scale tool wear testing was conducted to investigate the relative performance of several tools. Through flank wear measurements and cutting forces, tools were worn to failure and their performances compared. The best performing tool was then identified and recommended.

--- Phase 3: Tool Wear Characterisation

In order to augment and advance the knowledge base of the MMRI research group, the mechanisms of the tool wear in each tool from Phase 2 were investigated. Optical, SEM, Ramen spectroscopy, and XRD methods were used to investigate the worn tools and aid in understanding how and why the tools showed such large differences in performance.

Phase 1 drew heavily on the expertise of McMaster researchers Dr. German S. Fox-Rabinovich and Dr. Julia Dosbaeva in order to extract meaningful results from the material characterisation. Phase 2 was completed by the author, while phase 3 was done with extensive collaboration with the publication's second author, Dr. M. D. Abad. Results and discussion which were the result of Dr. Abad's contributions will be clearly noted as such in the following sections.

3.1 MATERIAL CHARACTERISATION

The NiCrMoV steels are ultra-high strength, low alloy martensitic steels and combine good hardenability with high ductility, high strength, high fatigue strength and creep resistance. Problems arise in machining of this steel due to its high hardness and toughness, as well as its inhomogeneous microstructure (Jallad & Ben-Amotz, 2002). Despite having critical and wide ranging applications, the material is relatively new and few studies have been done to quantify its machinability (Yang, et al., 2004) (Chen, et al., 2001).

The industrial partner supplied samples of NiCrMoV steel for the material characterisation step. Specific composition cannot be provided as it is a trade secret. However, for the purposes of analysis, the chemical composition of standard NiCrMoV steel used in power generation applications is provided in Table 3.1-1.

Table 3.1-1 – Chemical composition of typical NiCrMoV steel used in power generation applications

Element	%Weight	Element	%Weight
C	0.25 – 0.30	V	0.08 – 0.15
Si	< 0.04	$Al_{ges\ (total)}$	< 0.010
Mn	< 0.04	As	< 0.008
P	< 0.003	Sb	<0.002
S	< 0.004	Sn	<0.005
Cr	1.50 – 1.80	N	N/A
Mo	0.38 – 0.48	Nb	N/A
Ni	3.30 – 3.70	Cu	N/A

High levels of vanadium, chromium, and molybdenum are consistent with stainless type steels, which show poor machinability due to their high toughness and tendency to increase hardness during heat treatment (Tchizhik, et al., 1998).

3.1.1 MICROSTRUCTURE CHARACTERISATION – SEM AND OPTICAL METHODS

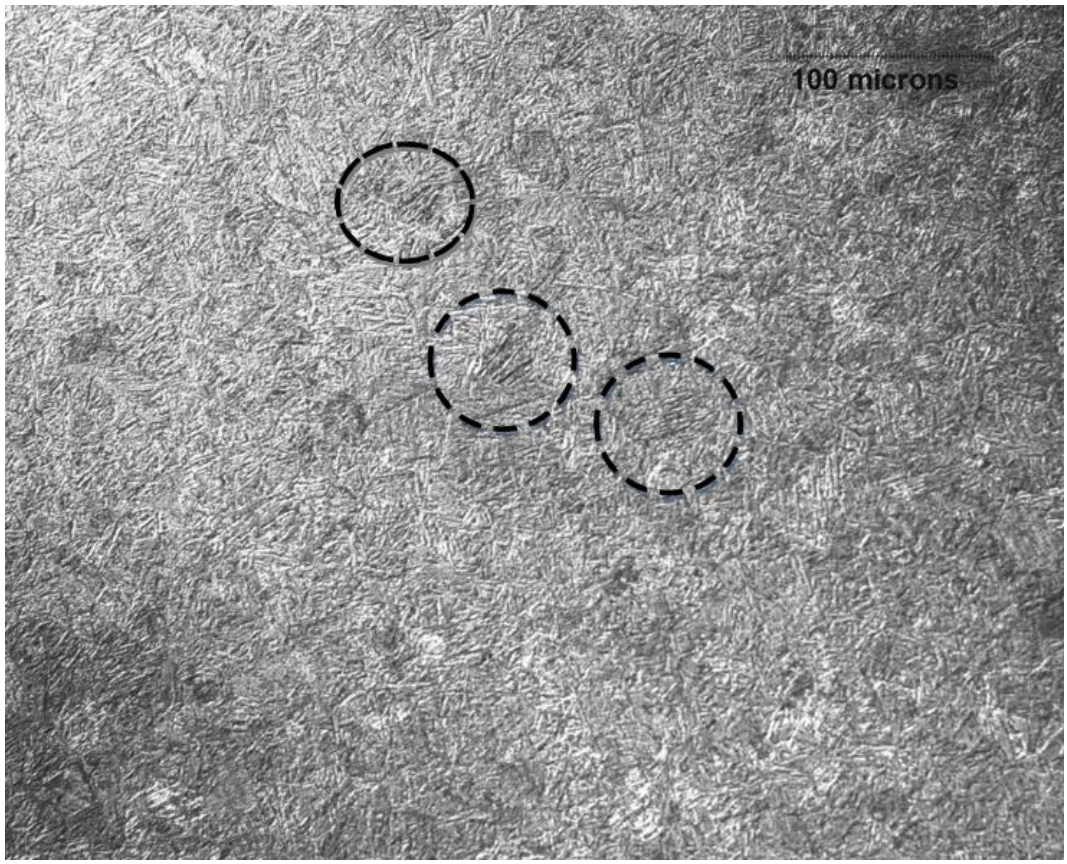

Figure 3.1-1 – Optical image of NiCrMoV steel at 200x magnification; circles indicate non-homogeneous areas in the microstructure

Figure 3.1-1 shows the microstructure of the material sample provided by the industrial partner. Immediately it is clear that the material microstructure is non-uniform. The fine grain, needle-like structure suggests tempered martensite with small areas which are dissimilar to the bulk of the microstructure, these are highlighted by black circles. Their slightly longer and better defined needle shape suggests that these are likely un-tempered martensite (Gates, et al., 1987) (ASM, 2004).

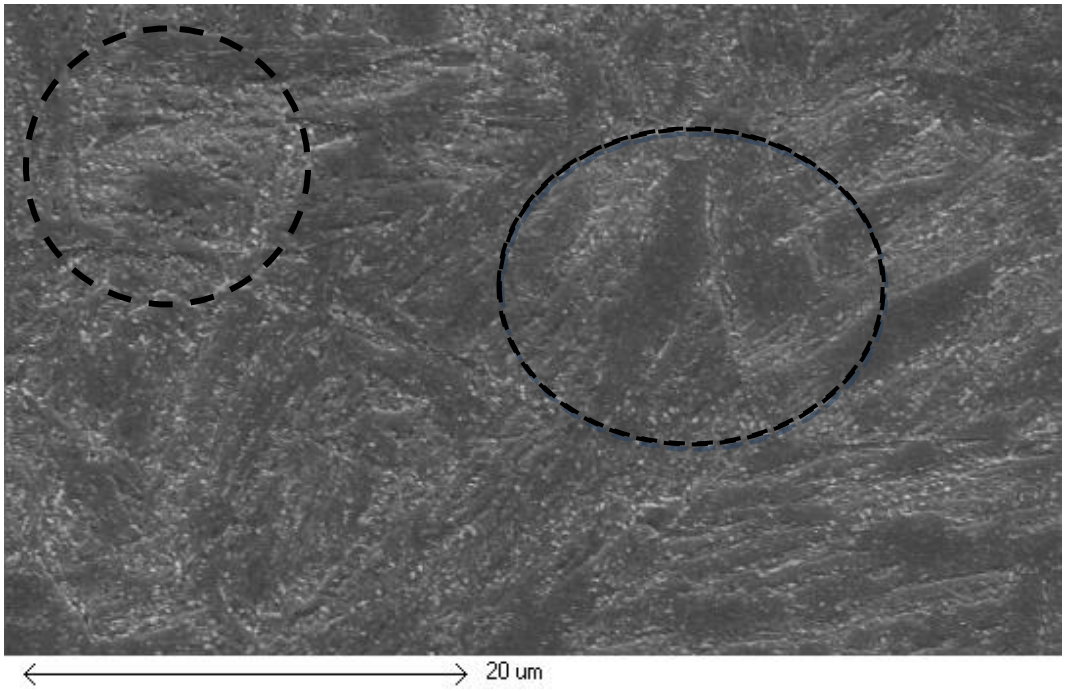

Figure 3.1-2 – SEM image of NiCrMoV sample at 2000x magnification; black circles indicate examples of varied structure

A higher magnification image of the sample at 2000 times magnification is shown in Figure 3.1-2. The highlighted areas in Figure 3.1-2 show different structures, where the area highlighted on the left shows a rough and non-uniform microstructure and the area on the right shows large uniform grains. This confirms the non-homogenous nature of the microstructure which is suggested by Figure 3.1-1.

Additionally, the above figure shows white dots which appear to be precipitates. As grain boundaries are not well defined, it is difficult to speculate on the composition of these precipitates, though these are expected as precipitation hardening is a common heat treatment method for stainless-like materials such as NiCrMoV steel (Kalpakjian & Schmid, 2006).

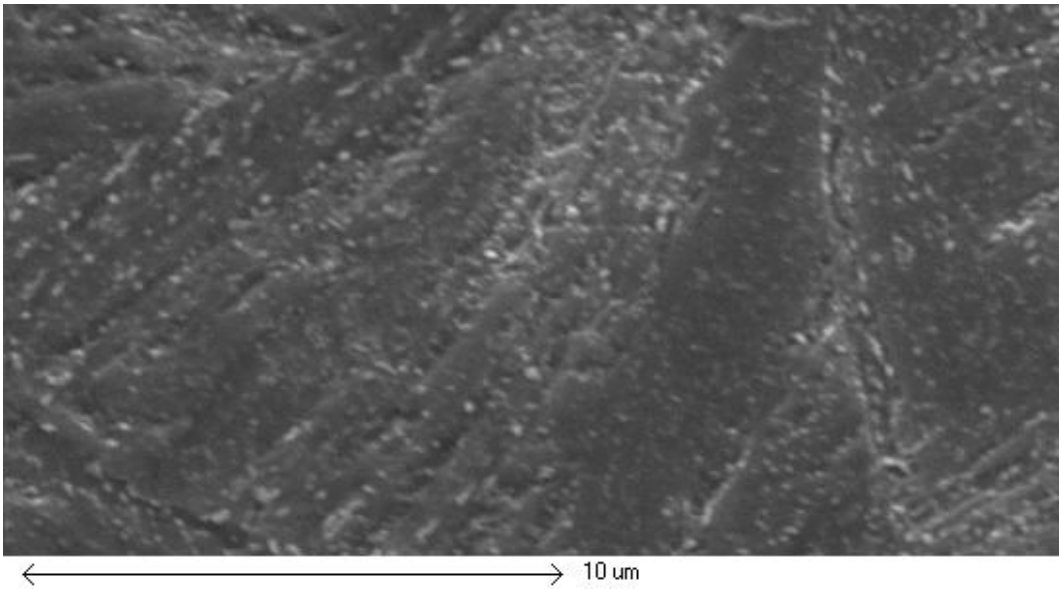

Figure 3.1-3 – SEM image of NiCrMoV sample at 5000x magnification

The higher magnification of the sample in Figure 3.1-3 shows the white precipitates with greater detail. Again, due to the lack of clearly defined boundaries it is difficult to determine whether they are forming on the grain boundaries which is consistent with carbides, or if they are forming on the grains.

3.1.2 MICRO-HARDNESS INDENTATION TESTING

Microhardness testing was completed to investigate the material hardness and uniformity. As noted in Section 2.4.1, micro-hardness testing in the literature showed hardness values between 230 HV – 350 HV.

Standard micro-hardness pyramid indentation tests were done on all three samples with a 10 second dwell and 200 gram-force. The results of this testing is summarized in Table 3.1-2.

The average of 374 HV and maximum of 403 HV are significantly greater than the values found in the literature. Hardness data for a similar, easier to machine steel provided by the industrial partner is listed below for comparison.

Table 3.1-2 – Microhardness testing results for NiCrMoV sample

Trial	Hardness (HV)	Indentation Size		Comments
		X (µm)	Y (µm)	
1	344	32.8	32.8	
2	364	31.9	31.9	
3	394	31.3	30.0	Non-rough area
4	372	31.8	31.3	
5	377	31.2	31.6	
6	403	30.6	30.0	"Solid" area
7	374	31.7	31.3	Rough area
8	367	32.1	31.4	
Average	**374.4**			

Table 3.1-3 – Micro-hardness testing results for free-machining alloy sample

Trial/File Name	Hardness (HV)	Indentation Size	
		X (µm)	Y (µm)
1	288	35.3	36.5
2	296	35.2	35.6
3	291	36.3	35.0
4	303	34.9	35.0
5	296	35.4	35.4
Average	294.8		

Comparing the hardness values of the NiCrMoV steel and the easier-machining alloy displayed in Table 3.1-3, Table 3.1-2 shows that the NiCrMoV steel has an average hardness which is 27% higher, and also has a much higher variance (standard deviation of 5.7 vs. 18.1 for the NiCrMoV steel), which further supports the non-homogeneous nature of the NiCrMoV sample's microstructure. Due to this high variance, further testing was done on the sample.

Random testing was done until a spot with a very high hardness was found. A 6 x 5 grid of hardness tests were then done near the hard spot in an attempt to characterise the size of the hard area.

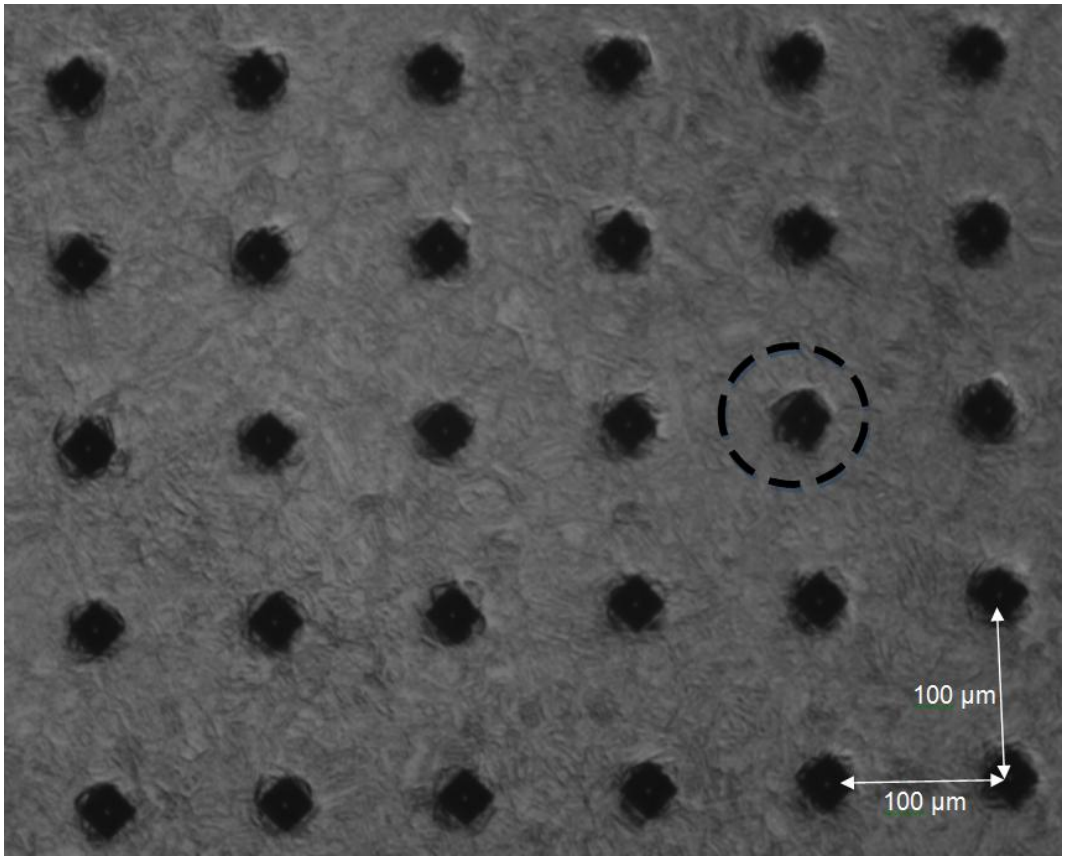

Figure 3.1-4 – Hardness mapping for hard spot on NiCrMoV sample

The initial test that showed high hardness is shown by black circle in Figure 3.1-4. The hardness results are displayed in the surface graph in Figure 3.1-5 which corresponds to the indentation pattern above (light areas correspond to higher hardness).

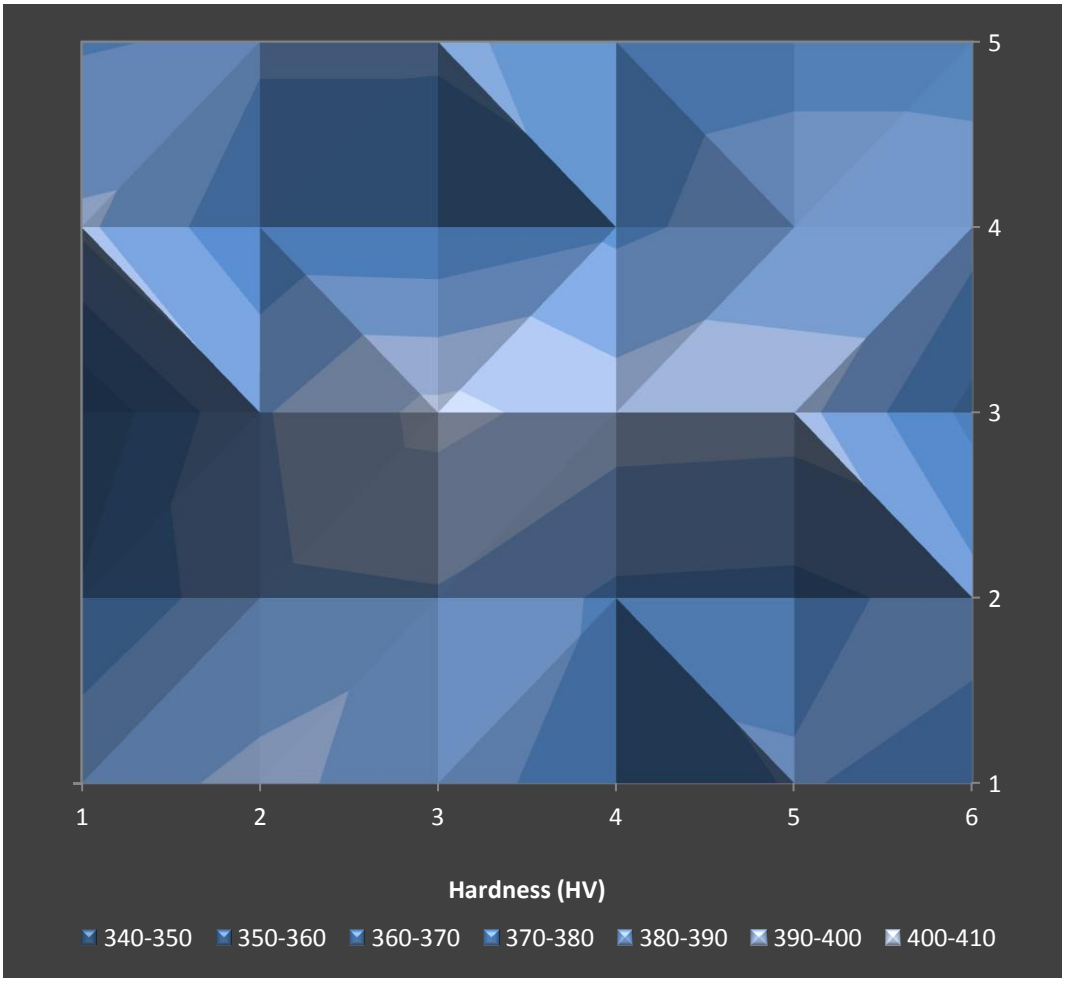

Figure 3.1-5 – Surface profile corresponding to hardness of data obtained in hardness mapping in Figure 3.1-4; light areas correspond to higher hardness

As can be seen in the hardness surface profile in Figure 3.1-5, the high hardness areas are localized and the sample has highly varying hardness even over small distances. The hardness of the sample surface changed significantly over the 100 µm increments used in the test. These results agree with the optical metallographic data of the NiCrMoV sample and again support the non-uniform nature of the steel.

3.1.3 XRD INSPECTION

Due to the inconclusive results in the SEM and optical inspection methods discussed in Section 1.1, X-ray Rontgen Diffraction (XRD) inspection was selected to identify the microstructure of martensite qualitatively with a high degree of certainty and to verify conclusions drawn from SEM and optical methods. Figure 3.1-6 provides a plot comparing the martensite lines of both NiCrMoV and the free-machining sample. This data allows for identification of the crystal structure of the material, which corresponds to ferrite, austenite or martensite. Processed results are shown in Table 3.1-4.

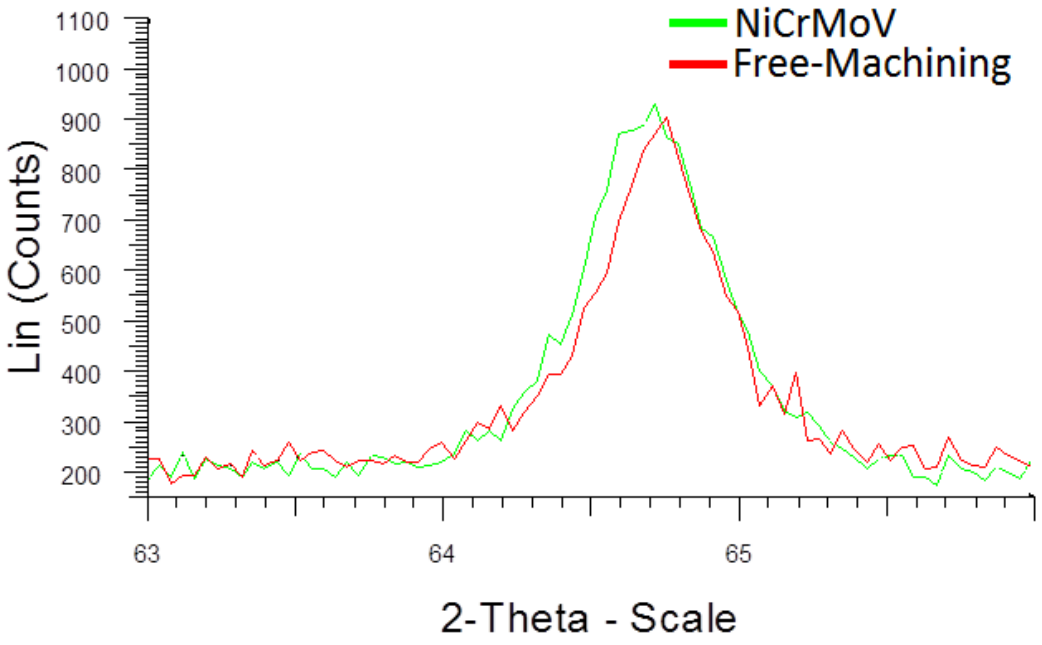

Figure 3.1-6 – X-Ray Rontgen Diffraction comparison plot for NiCrMoV steel sample

Table 3.1-4 – XRD Results

Sample Name	Peaks - FWHM	Hardness
	2-Theta °	HV
NiCrMoV Steel	0.508	374
Free-Machining	0.435	295
Hardened Tool Steel*	N/A	600

*Value included for comparison, from (Tlusty, 2000)

The width of the peaks shown in Figure 3.1-6 correspond to the amount of dissolved carbon in the crystal lattice. During tempering dissolved carbon is allowed to precipitate out of the lattice to form carbides. Therefore, un-tempered martensite contains higher levels of dissolved carbon than tempered martensite. By comparing the widths of the peaks, a relative estimate of the amount of un-tempered martensite can be made between the samples. The widths of the peaks are calculated using FWHM (full width at half maximum) for comparison, and are summarized in Table 3.1-4.

The results of the XRD tests show that there is a correlation between hardness and the FWHM of the XRD results. The test found that there is a significant increase in width of the martensite line in the spectra for the NiCrMoV sample when compared with the free-machining sample. These results clearly indicate a formation of un-tempered martensite in the structure of the NiCrMoV steel.

3.1.4 Material Characterisation Conclusions

Optical and SEM imaging revealed a non-uniform structure which appeared to consist of fine grain tempered martensite, with frequent spots of un-tempered and fine grain martensite. Hardness tests agree with these results showing large variation and high hardness. XRD inspection again showed a higher amount of un-tempered martensite when compared to the free-machining samples, agreeing with previous results. It is believed that these spots of un-tempered martensite and the small grain size may be responsible for the issues seen in machining. The small spots of low-tempered martensite would increase abrasion wear and cause accelerated tool wear when compared with the free machining sample, and agree with observations made by the industrial partner.

3.2 PHASE 2 – EXPERIMENTAL TESTING

Phase one of this work involved a microstructure analysis to help determine why the inserts were wearing much faster than expected. The microstructure investigation showed the NiCrMoV steel to have a relatively higher micro hardness compared to a free-machining alloy the industrial partner had used previously. Further analysis revealed this was likely due to un-tempered martensite which remained intact due to inadequate heat treatment to fully temper the martensite structure.

Phase two of the study was to complete a set of machining trials using current tooling and as well as other candidates to determine which would perform best for machining of the NiCrMoV steel.

3.2.1 EXPERIMENTAL OBJECTIVE AND METRICS

The purpose of this phase was to identify the best performing insert out of three selected for testing in terms of resistance to wear, and therefore tool life.

The performance of each would be measured using two metrics: cutting forces and flank wear. Flank wear was selected as a metric as it is the only wear type which can be feasibly measured between wear trials. Lowered cutting forces have been shown to correlate to improved tool life (Stephenson & Agapiou, 1997), and so cutting force was chosen as a secondary metric to support any trends observed in flank wear.

3.2.2 EXPERIMENTAL PROCEDURE AND SET-UP

The testing done was typical of a standard tool wear testing study. Study material and tooling was obtained from the industrial partner and machined within the MMRI to determine tool life and performance. This section describes the cutting process and experimental set-up.

Material

All experiments were performed with workpieces obtained from the industrial partner, composed of NiCrMoV steel, with the chemical composition noted in Table 3.1-1.

Tooling

Three inserts were selected for testing. Aside from two varied properties, the inserts were identical. The varied properties were chip-breaker groove angle (rake angle), coating, and edge preparation. These properties are summarized in Table 3.2-1, Figure 3.2-1, and Figure 3.2-2 – Cutting edge geometry for C1, C2 and C3 inserts . Insert C2 was similar in coating and geometry to the industrial partner's tooling, and so is selected as the baseline for comparison. Other insert specifications such as specific geometries can be found by referring to (Walter Tools, 2007).

Table 3.2-1 – Cutting insert properties (Walter Tools, 2007)

Name	Walter Prod. ID	Grade	Coating Type	Coating Method	Rake Angle
C1	ADMT120408R-F56	WKP 35	TiCN/Al_2O_3/TiN	CVD	16º
C2	ADMT120408R-D56	WSP 45	TiAlN/Al_2O_3/ZrN	PVD	10º
C3	ADMT120408R-F56	WSM 35	TiAlN/Al_2O_3/ZrN	PVD	16º

The WKP (C1) insert is a CVD coated insert (thickness ~10 mm) and the WSP (C2) and WSM (C3) inserts are PVD coated (thickness ~4 mm) (Walter Tools, 2007). C1 had: (i) an inner TiCN coated layer featuring thermal stability and wear resistance, (ii) a middle coated layer of Al_2O_3 featuring thermal stability and wear resistance, and (iii) an outer coated layer of TiN featuring low friction and welding resistance, and as a wear-indicating layer (M'Saoubi & Ruppi, 2009). C2 and C3 had: (i) an inner layer of TiAlN, (ii) a middle layer of aluminum oxide, and (iii) an outer layer of ZrN.

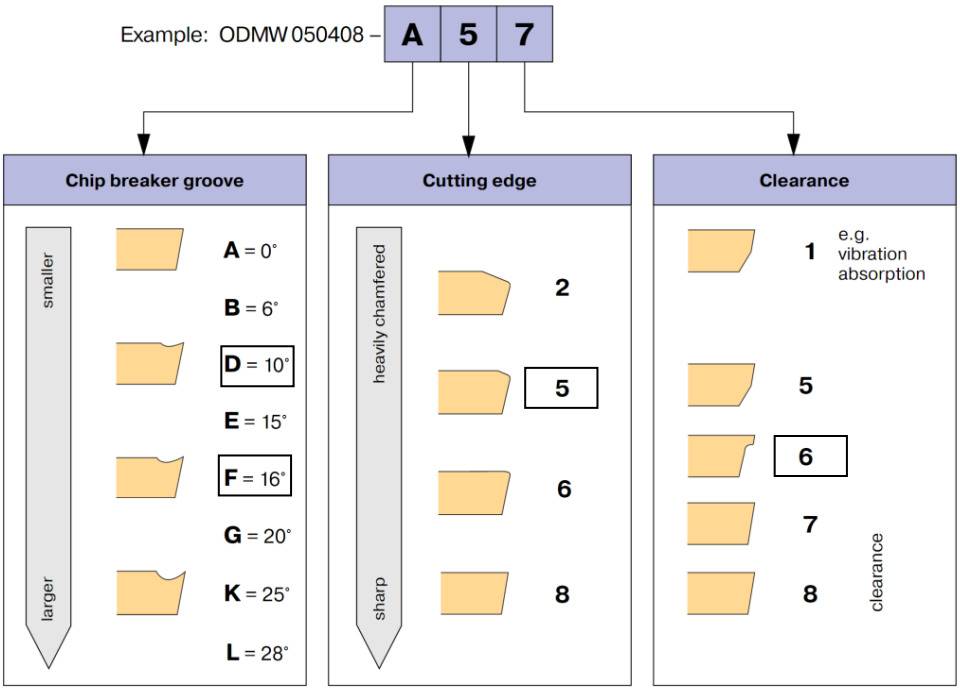

Figure 3.2-1 – Walter Tools chip breaker geometry for inserts (Walter Tools, 2007)

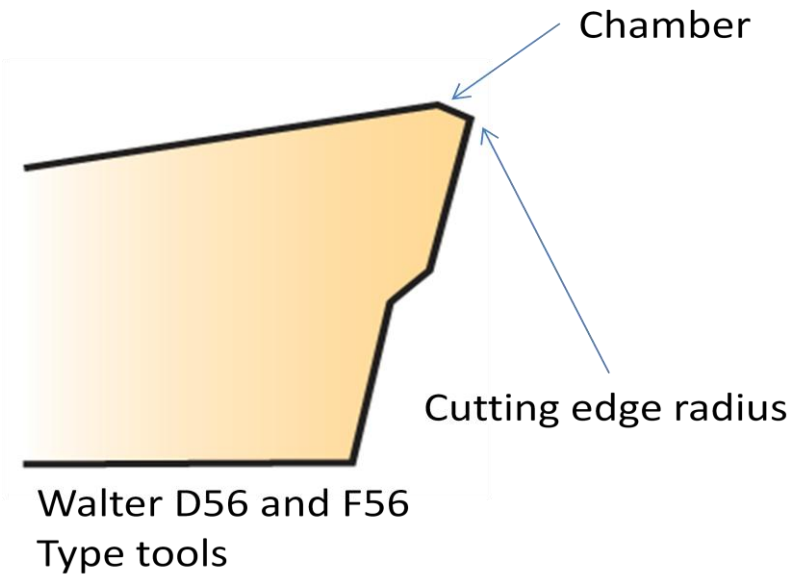

Figure 3.2-2 – Cutting edge geometry for C1, C2 and C3 inserts (Walter Tools, 2007)

Walter documentation suggests that cutting edge preparation is identical for these 3 tools. However, under OM inspection, the chamber on the C2 insert was found to be approximately 130 μm, where the chamber on the C3 insert was found to be approximately 100 μm.

As well, the substrate grades differ slightly. ISO grade designations for C1 and C3 are 35, and C2 is 45. However, these are both considered to be very tough grades and so it is not suspected that this difference had a large impact on insert performance in this study.

Finally, the insert's cutting edge radius was inspected by splitting a tool and inspecting the edge radius under an optical microscope. Preliminary inspection showed that the cutting edge radius for C2 and C3 were of similar size, at approximately 60 μm.

The tool body used was a Walter 1 ¼" 2-flute end mill with a stacked insert configuration (Walter Prod ID: F4138.UW31.031.Z02.43). Only a single insert in the tool body was used for each test.

Cutting Parameters and Procedure

Four trials of each insert type were completed to obtain a small sample set, for a total of 12 cutting tests. The testing was done on a Makino 40 HP 5-axis CNC mill having very high dynamic and static stiffness. A summary of the cutting parameters used can be found in Table 3.2-2; these were selected to reflect the industrial partner's process. Partial tool engagement (shoulder milling) was used for testing.

In the following sections, a pass refers to a single cutting pass on the workpiece. A cutting pass in this case is 255 mm in length, 3 mm wide and 3 mm in depth as shown in Figure 3.2-3. Therefore, a single cutting pass represents

2295 mm^3 of material removed. This process was repeated for each insert until sufficient cutting had occurred to wear the tool to the failure criteria of 300 µm.

Table 3.2-2 – Cutting parameters for testing

Parameter	Value
Type	Milling (heavily interrupted cutting)
Cutting Speed	85 SMM
Cutting Tool	31.75 mm single flute end mill
Radial DOC	3 mm
Axial DOC	3 mm
Chip Load	0.15 mm/tooth
Feed	200 mm/min
Coolant type	Semi-synthetic, Flood

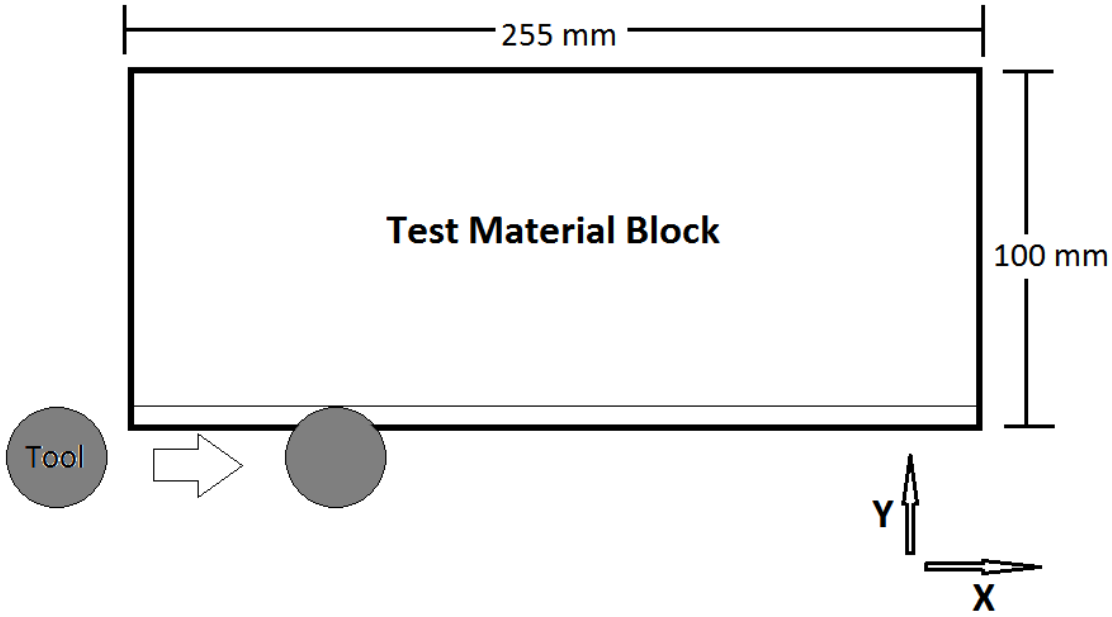

Figure 3.2-3 – Diagram showing a single cutting pass for testing

Data Collection

Flank wear was selected to characterize the tool life of the inserts. Repeated cutting passes were completed up to a flank wear of 300 µm, which is

a generally accepted standard for failure criteria of milling tools. Flank wear measurements and general observation was completed through optical microscopy using a Mitutoyo tool-maker's microscope. The microscope was equipped with an optical crosshair and micrometer stage adjustments, and sample lighting was accomplished through adjustable fibre-optic direct lighting.

Cutting forces were recorded as a supplement to measurements of flank wear. A Kistler 3-axis dynamometer was used for force collection. It is also useful as an independent indicator of performance as it can be used to benchmark the average cutting forces. Three axes of force were recorded during cutting, X, Y, and Z directions. X corresponds to the 'cutting force', which acts in the direction of the movement of the cutting tool, Y to the 'side force', which acts perpendicular to the cutting force and Z to the 'thrust force' which acts parallel to the axis of the tool.

3.2.3 PHASE 2 RESULTS

This section describes the results obtained from completing machining trials in Phase 2. Discussion of these results and attempts to correlate performance of tools to their properties is made in Phase 3.

Tooling Performance

As seen in the following figures, there was markedly different performance achieved by each tool. C2 represents the baseline as it is representative of the industrial partner's tooling before this study was conducted. The tool life of each insert is now described, and is shown in Figure 3.2-4.

Insert C1, having both a different coating and rake angle from the baseline insert C2 (CVD deposited TiCN/Al_2O_3/TiN; 16º rake angle) performed extremely poorly, failing after just 15 cutting passes or ~4 m length of cut.

The baseline insert C2 (PVD deposited TiAlN/Al_2O_3/ZrN; 10º rake angle) performed far better, lasting approximately 50 cutting passes or ~15 m length of cut; an improvement of over 300% over C1.

Insert C3 showed the best tool life of the tested inserts (PVD deposited TiAlN/ Al_2O_3/ZrN; 16º rake angle). C3 lasted an impressive 193 passes before reaching the failure criteria, which was approximately ~50 m cutting length. This is a 1200% improvement over C1, and over a 300% improvement over the baseline tooling, C2.

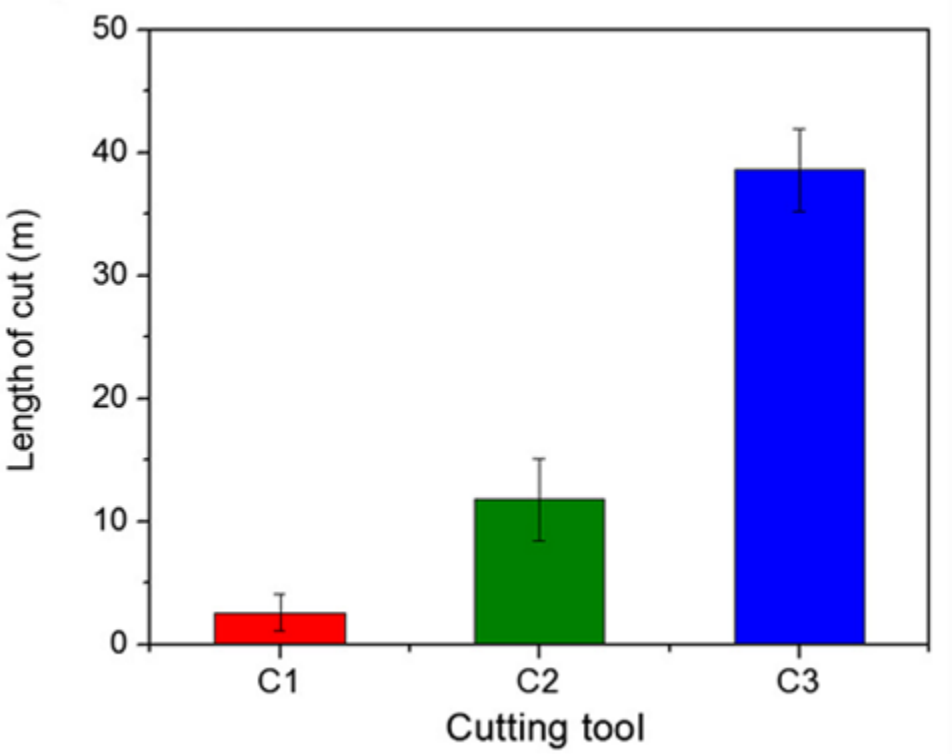

Figure 3.2-4 – Insert performance (tool life)

The measured forces are represented for all the inserts in Figure 3.2-5. The cutting (X) and side (Y) force show very similar trends. The thrust force (Z) varied considerably, though there is a significant amount of clustering around 19–21 N. The C3 inserts exhibited lower average cutting forces in all measured directions. For X, the C3 insert exhibited a 15% decrease in cutting force when

compared to C1 and C2. The cutting force (X), the most dominant force during the cutting process, is plotted vs. length of cut in Figure 3.2-7 for the inserts. In comparing Figure 3.2-6 and Figure 3.2-7, it is clear there is a strong correlation between cutting force and flank wear. As seen in this graph, the cutting forces for the C3 insert remain very steady through testing and only increase once significant wear had occurred. This confirms the extremely low and stable wear seen in flank wear measurements of C3 tools, not showing any significant increase in cutting force until higher wear rates in the 35.7–44.0 m range.

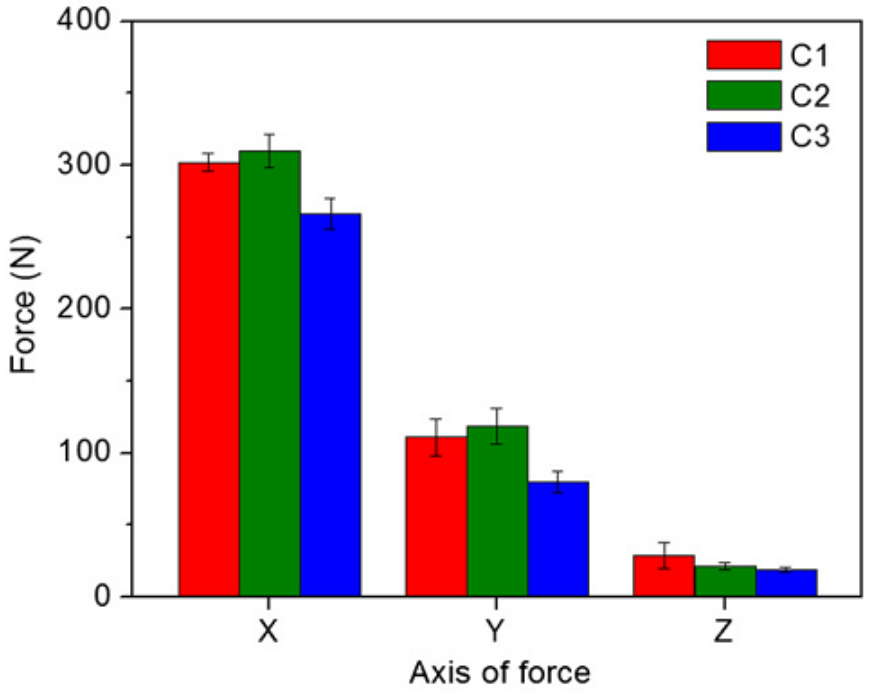

Figure 3.2-5 – Insert performance (cutting force)

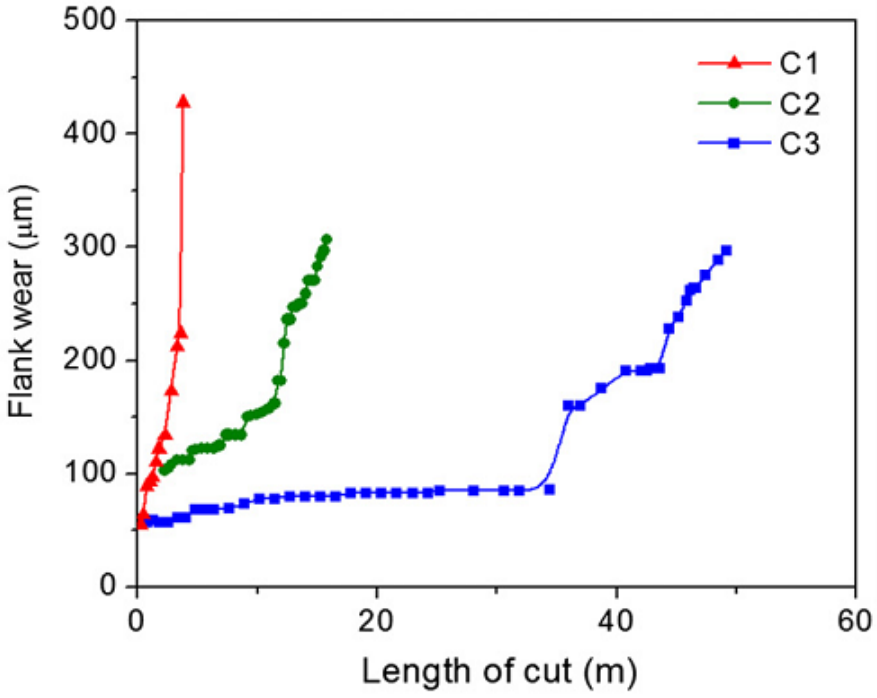

Figure 3.2-6 – Plot of flank wear measurements for each insert over the course of tool life

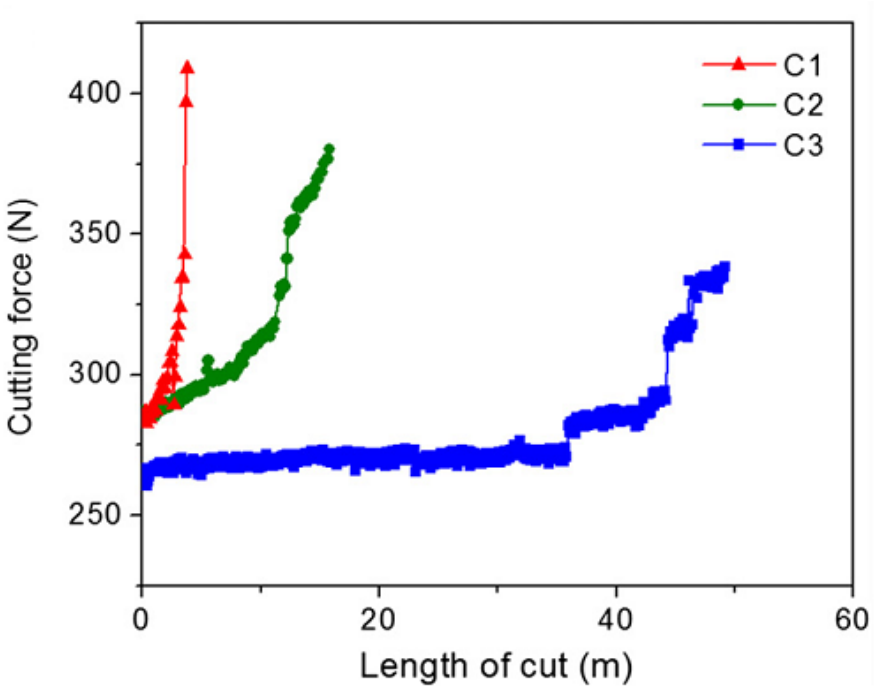

Figure 3.2-7 – Plot of cutting forces for each insert over the course of tool life

Figure 3.2-7 – Plot of cutting forces for each insert over the course of tool life shows the cutting forces for each insert, and C3 does show a significant decrease in cutting force, however this may just be an artifact of the fact that C3 had reduced flank wear compared with the other inserts. This reduced flank wear may have been responsible for the low cutting forces seen. To ensure the lowered force is the result of tool performance and not flank wear, flank wear compared to cutting force is shown in Figure 3.2-8 – Flank wear vs. Cutting forces. For all levels of flank wear, C3 showed lower cutting forces. It is therefore clear that the reduced force is not an artifact of reduced levels of flank wear.

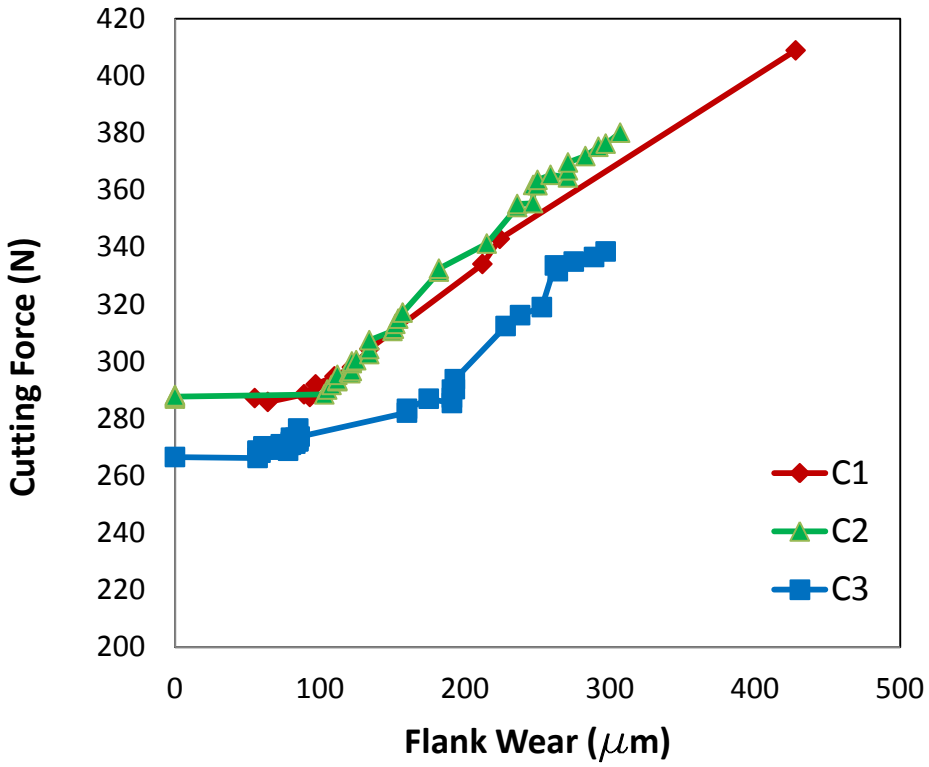

Figure 3.2-8 – Flank wear vs. Cutting forces

From the above figures, it is clear that the C3 insert provided the longest tool life and the lowest cutting forces, improving significantly on the performance of the baseline tooling.

3.3 PHASE 3 – INSERT AND WEAR CHARACTERISATION AND ANALYSIS[1]

This section provides an analysis of wear mechanisms and coatings through SEM, OM, XRD and EDS in an attempt to explain the performances of each insert. For reference, the inserts along with their key properties are summarized in Table 3.3-1. All other insert properties are identical, according to (Walter Tools, 2007).

Table 3.3-1 – Summary of Insert performance and properties

Insert	Coating	Rake Angle	Normalized Tool Life
C1	TiCN/Al_2O_3/TiN (CVD)	16º	0.3
C2	TiAlN/Al_2O_3/ZrN (PVD)	10º	1
C3	TiAlN/Al_2O_3/ZrN (PVD)	16º	3

Initial observation of results show that the best performing insert C3, and the worst performing insert C1 share the same rake angle but differ in coatings. Therefore, the difference in performance is likely due to the coating composition and/or deposition method. It is also clear that the baseline insert C2 and the best performing insert C3 share identical coatings and differ in only rake angle, where C3 has a more aggressive rake angle of 16º. Based on these observations, the following correlations are apparent:

1) The C1 insert's coating was responsible for its poor performance
2) The C3's combination of more aggressive rake angle and relatively more appropriate coating is responsible for its superior performance. Tool geometry determines load and temperature. Coating performance varies depending on load and temperature thus this represents a better combination.

[1] This section draws heavily from (Oomen-Hurst, et al., 2012), a journal article published based on the work described in this chapter, done in collaboration between the author and Dr. M.D Abad (McMaster University), whose work and contributions are noted in the following sections.

The following sections will discuss in detail the characterisation of the wear and inserts in order to support or disprove the correlations stated above.

3.3.1 INSERT CHARACTERISATION – PRIOR TO TESTING[2]

XRD has been used to identify the crystallographic phases of the coated inserts and are shown in Figure 3.3-1(a).

For C1, the main identified phases correspond to Al_2O_3, TiN, and TiCN from the coating and WC from the substrate. Aluminum oxide, also referred to as alumina, has several crystallographic phases and the two most well-known are the α-Al_2O_3, also known as corundum, and γ-Al2O3 (Gupta, et al., 2010), (Edlmayr, et al., 2010), (Ruppi, 2005). The peaks seen in Figure 3.3-1(a) correspond to the α-Al_2O_3 phase (ICCD card no. 001- 12960), (Nagabhushana, et al., 2009). XRD patterns corresponding to TiCN (ICCD card no. 042-1488) and TiN (ICDD card no. 006-0642) (Martínez-Martínez, et al., 2009), (Subramanian, et al., 2011) were also identified.

For the C2 and C3 inserts, ZrN (cubic phase) (ICDD card no. 002-0956) (Silva, et al., 2010) (Moura, et al., 2006) and TiAlN were identified, as expected (cubic phase) (Subramanian, et al., 2011). No peaks corresponding to Al_2O_3 were found in the diffractograms of C2 or C3.

In order to have superficial phase information, Raman spectroscopy has been used to analyze the coatings up to a 5–10 μm depth. Raman spectra of these different cutting tools are shown in Figure 3.3-1(b). The absence of sharp and well defined peaks could be attributed to the local structural disorder of the coatings (Moura, et al., 2006), (Dreiling, et al., 2010) and consequentially the Raman spectra is composed of broadened bands.

[2] XRD and EDS work discussed in this section was primarily collected and analyzed by Dr. M.D. Abad (McMaster University), these results are included as they lend considerable understanding to the underlying mechanisms explaining tool performance

C1 shows several broad bands and sharp peaks. Bands at 263 and 339 cm^{-1} correspond to TiN and/or TiCN (Dreiling, et al., 2010). Bands at 560, 645, 380, 417 and 750 cm^{-1} all correspond to various characteristics of α-Al_2O_3 (Spengler, et al., 1978), (Cheng, et al., 2002), (Wermelinger, et al., 2007), (Dogra, et al., 2011), (Wermelinger, et al., 2007), (Jallad & Ben-Amotz, 2002).

The Raman spectra of C2 is shown in Figure 3.3-1(b) and it is clearly different from C1. ZrN is identified by the 500 cm^{-1} band, and in the low frequency region by two bands centered at around 165 and 220 cm^{-1} (Moura, et al., 2006), (Spengler & Kaiser, 1976). The TiAlN layer was not observed, probably because Raman is a superficial technique and phonons could not be measured from the inner layer. No features of α-Al_2O_3 have been found by Raman in any region. Due to its symmetry, γ-Al_2O_3 does not show active bands by Raman and so could not be detected by this technique (Edlmayr, et al., 2010), (Nagabhushana, et al., 2009), (Cava, et al., 2007).

The presence of α-phase in the C1 insert is clear, as demonstrated by the XRD and Raman results. However, the absence of an Al_2O_3 crystallographic phase in the XRD results and the absence of bands or peaks in the Raman spectra indicates that: (i) No α-phase has been deposited by PVD in C2 or C3, (ii) γ-phase could have been deposited by PVD but its degree of crystallinity is really poor and therefore no XRD pattern was identified, and finally (iii) amorphous Al_2O_3 or another of the meta-stable alumina phases with a low degree of crystallinity has been synthesized by this coating method (Fietzke, et al., 1996), (Klocke, et al., 2008).

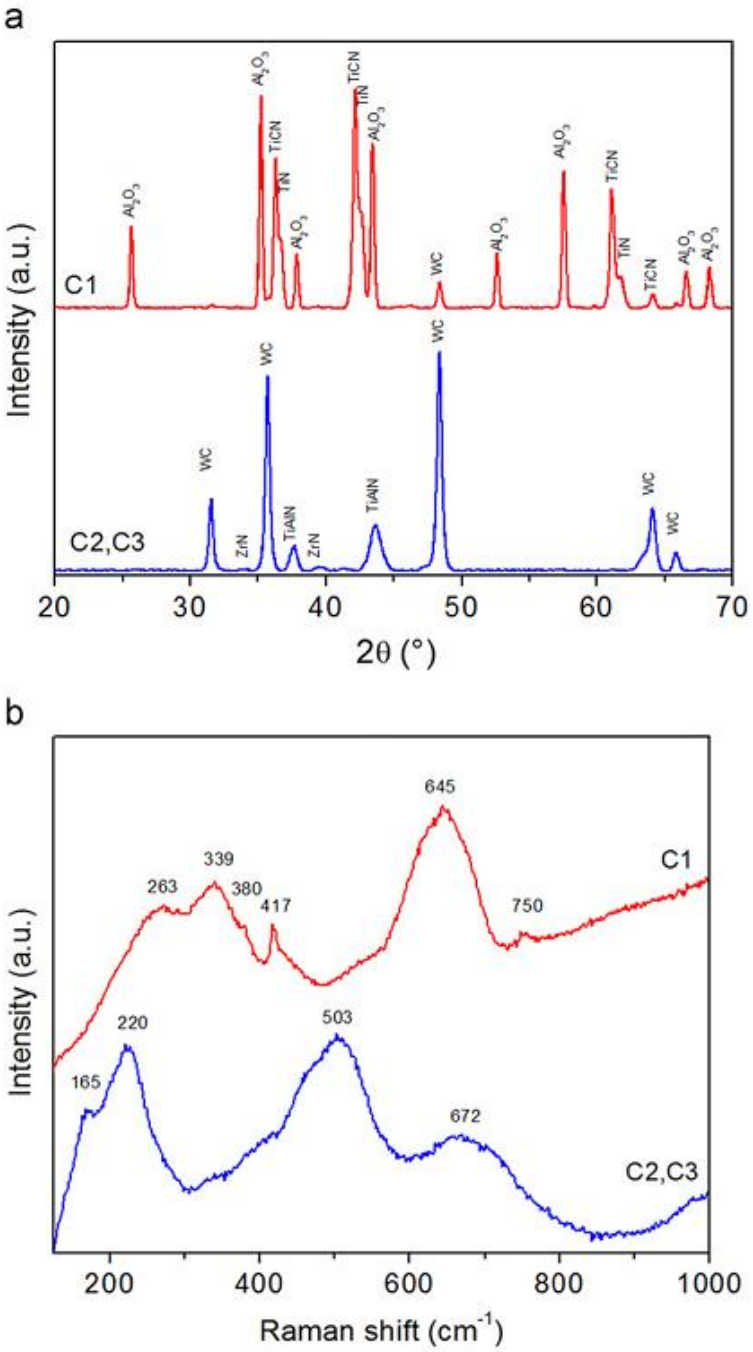

Figure 3.3-1 – XRD difractograms (a) and Raman spectra (b) of the different inserts

3.3.2 FAILURE MODES

Through testing there were two obvious modes of failure, massive chipping and abrasive wear. This section contains SEM and OM images which show these wear mechanisms for each of the insert types.

The C1 inserts wore very rapidly, and displayed both rapid abrasive wear as well as massive chipping which exceeded the failure criteria significantly in a short time. Figure 3.3-2 shows an OM image of a C1 insert at failure, and both the massive chipping and aggressive abrasive wear are visible.

The C2 inserts wore by abrasive wear, and again are pictured in Figure 3.3-2. Note that the majority of wear took place away from the tip of the tool.

The C3 inserts wore by gentle abrasive wear as demonstrated by the image at failure in Figure 3.3-2. Flank wear was again most prevalent away from the tip of the insert, though not as much as C2. Figure 3.3-3 and Figure 3.3-4 highlight the vastly superior performance of the C3 inserts; the first showing a C3 at 110 cutting passes with practically no flank wear at all, compared with the latter showing a C2 insert at failure after only 60 cutting passes.

SEM investigation of the inserts in Figure 3.3-5 through Figure 3.3-7 show C1, C2 and C3 at failure, and agree with the observations made through optical microscopy. The SEM images offer a higher magnification, contrast and a better representation of depth.

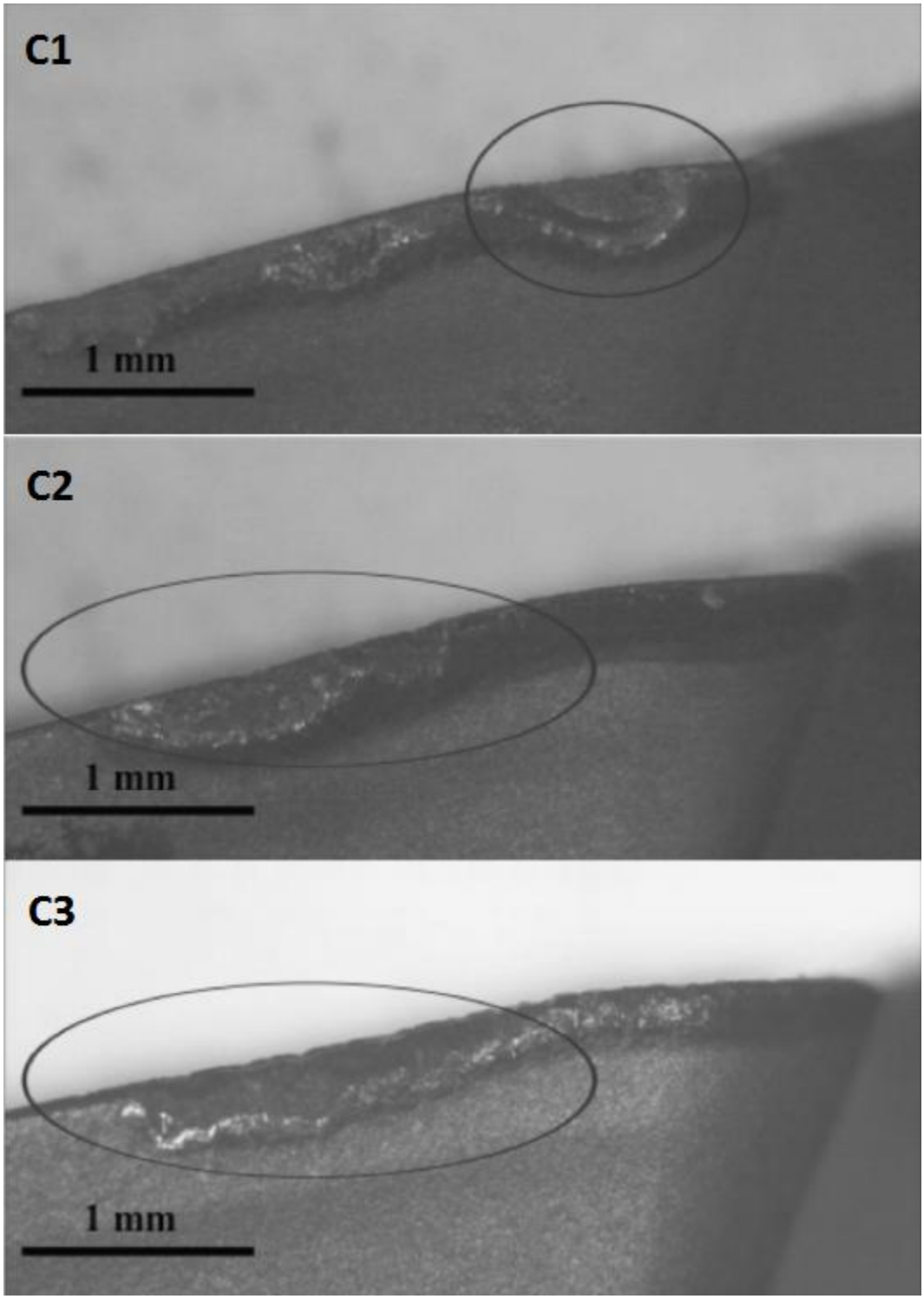

Figure 3.3-2 – Optical Microscopy images of inserts after failure with area of maximum wear highlighted

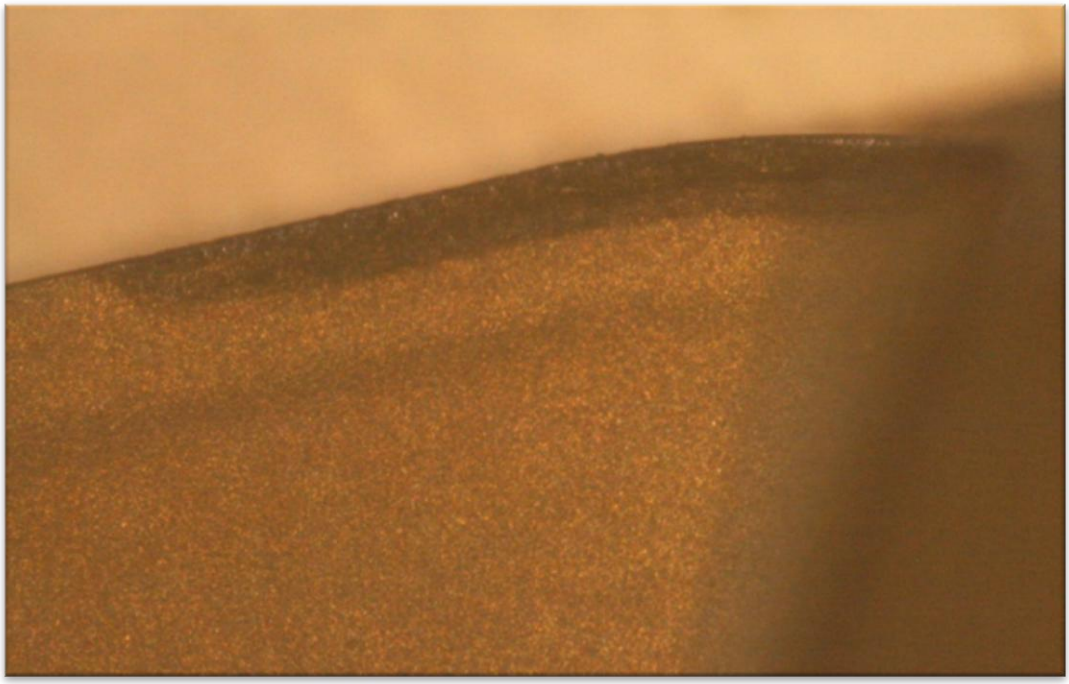

Figure 3.3-3 – C3 insert at 110 passes, ~30 m cutting length, showing almost no visible flank wear

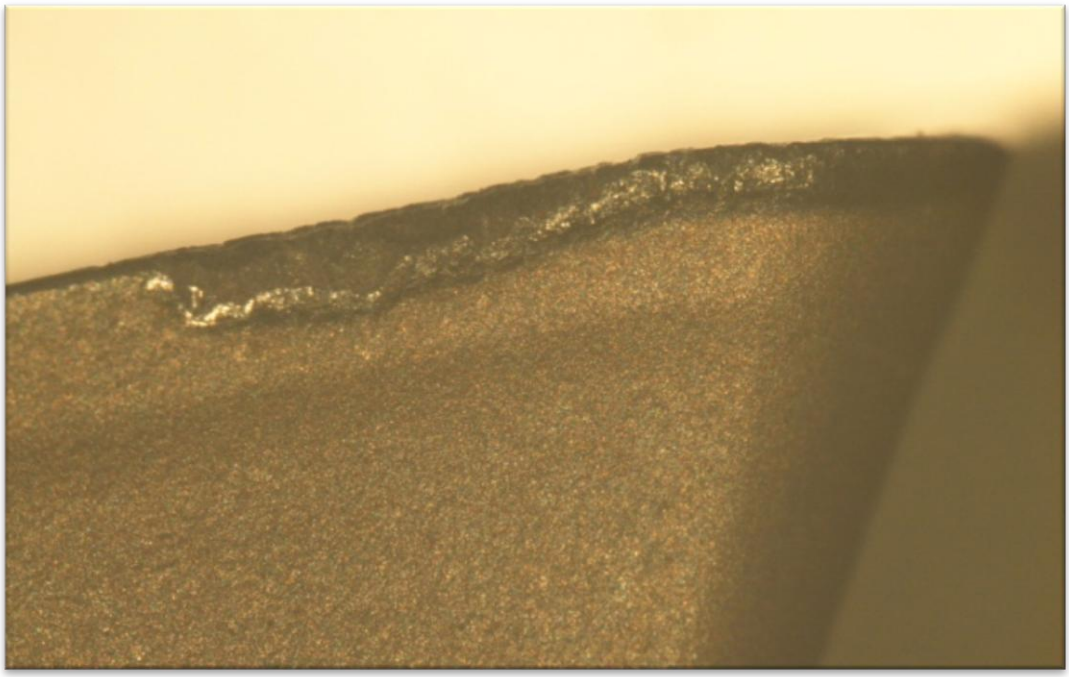

Figure 3.3-4 – C2 insert at 60 passes, ~ 15 m cutting length, this insert has reached failure criteria

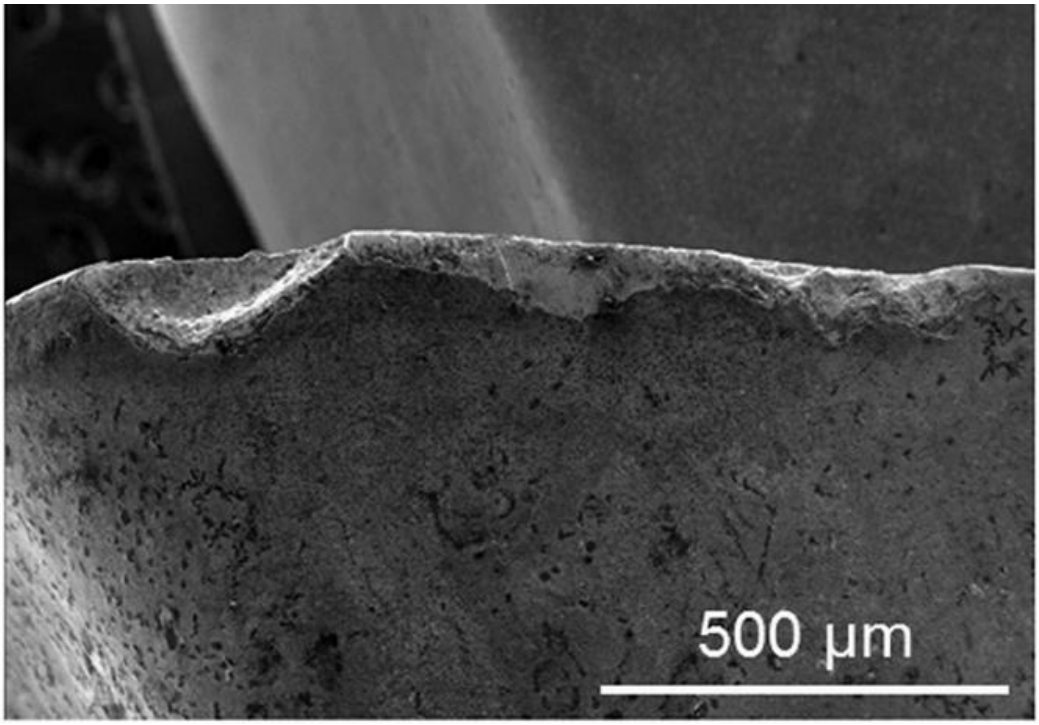

Figure 3.3-5 – SEM image of C1 at failure due to massive chipping and rapid abrasive wear

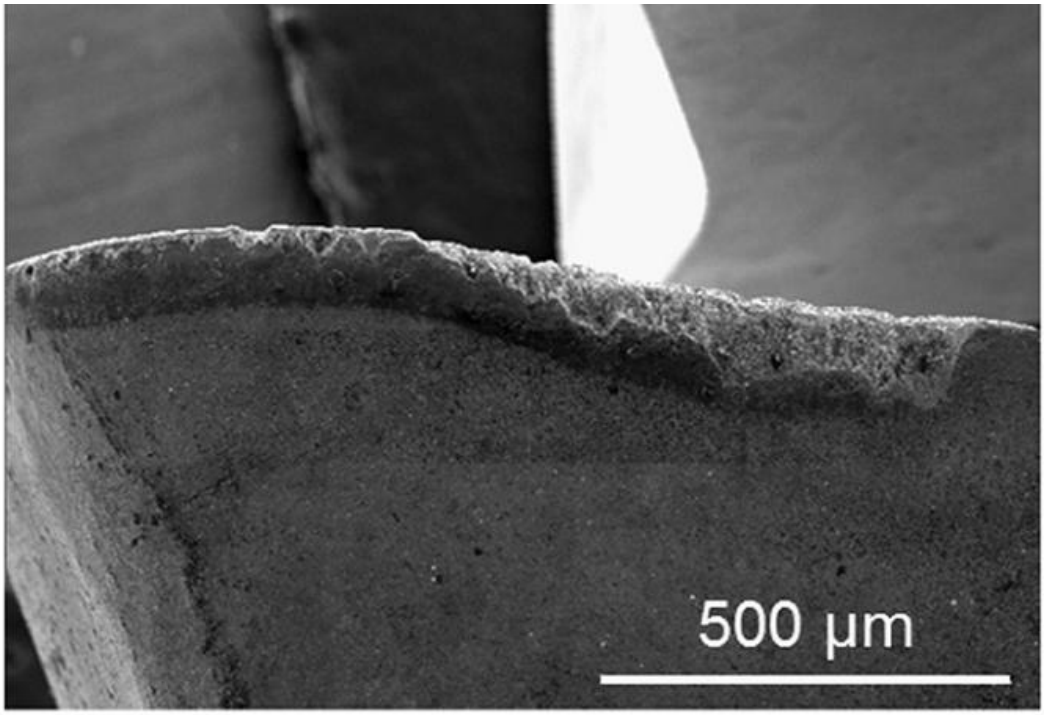

Figure 3.3-6 – SEM image of C2 at failure due to abrasive wear

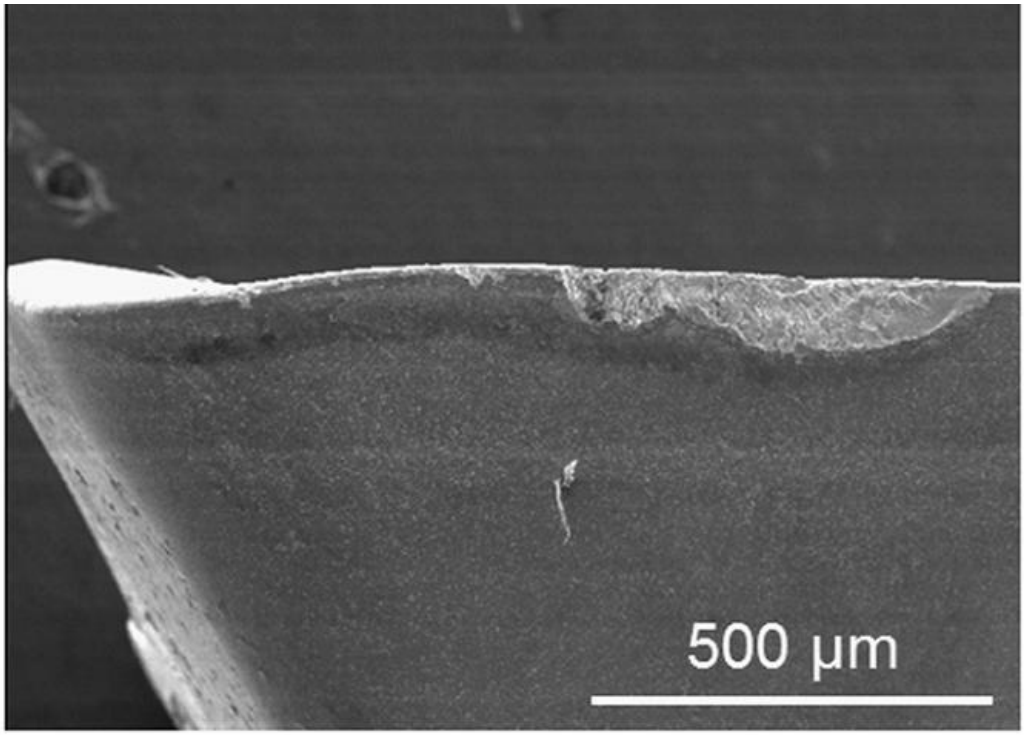

Figure 3.3-7 – SEM image of C3 insert at failure due to gentle abrasive wear

3.3.3 INSERT CHARACTERISATION – POST TESTING[3]

This section discusses SEM, EDX and Raman spectra results which serve to characterise and understand the wear on the inserts at failure. EDX and Raman spectra, as well as SEM images of the inserts at failure were captured and are shown in Figure 3.3-8, Figure 3.3-9, and Figure 3.3-10 to demonstrate the failure mechanisms.

- - - C1 at Failure

SEM micrographs of the tip and flank face of the C1 insert are shown in Figure 3.3-8 (a) and (b), respectively. EDX and Raman analysis have been carried out at three zones of interest, indicated in the micrographs by Roman numerals. By EDX (Figure 3.3-8(c)), it can be seen that Zone I shows the typical

[3] The majority of the data collection and analysis in this section was completed by Dr. M.D. Abad (McMaster University). It is included to aid in understanding the tooling performance.

elements that form the insert coating, as described in Table 3.2-1 which agree with Walter specifications, XRD, and Raman results. The C1 insert was coated with TiCN and α-Al_2O_3 layers, as well as a thin TiN top layer, using CVD deposition. In Zone II, located in the area exposed by massive chipping, only the substrate is observed (WC) and this suggests that total delamination of the coating has occurred in that zone. Zone III, located in the rapid abrasive wear area away from the tip, shows a thick layer of iron adhered to the flank face. Raman spectra of these different areas are shown in Figure 3.3-8(d). Zone I corresponds to the insert coating and has been explained in detail previously. No relevant features are present in the Raman spectra of Zone II, corresponding to the WC substrate and did not show active Raman bands. In Zone III, a broad band at 306 cm^{-1} and peaks at 547 and 670 cm^{-1} the magnetite phase of iron oxide Fe_3O_4 (Shim & Duffy, 2001), (Chamritski & Burns, 2005).

Once the coating had delaminated in Zone II, the WC substrate should have oxidized. However, there is evidence that the transfer layer of iron/iron oxide is partially protecting the underlying tool material from oxidation as seen in (Constable, et al., 2001).

- - - C2 at Failure

Figure 3.3-9 (a) and (b) show two different SEM micrographs of the worn flank surface of C2 at different magnifications. Three different zones were analyzed. Using EDX, the chemical composition of the coating was observed by investigating the unworn area at Zone I. This showed the coating is composed of three different layers; the outer ZrN layer, the aluminum oxide based layer, and the inner TiAlN layer, all deposited by PVD (Walter Tools, 2007). Zone II shows the WC substrate together with small quantities of iron. This iron is contained within the pits, valleys or asperities of the worn and rough surface. Zone III, the closest region to the coating, shows a layer of iron/iron oxide. The analyses of these zones by Raman are shown in Figure 3.3-9(d). Zone I shows the spectra of

the C2 coating as previously detailed. Zone II shows no relevant features, as seen previously for the WC substrate for the C1 insert. In Zone III, Fe_3O_4 was identified by the same method as C1.

- - - C3 at Failure

Figure 3.3-10 (a) and (b) show four different zones on the worn surface of the C3 insert, presented in two SEM micrographs. EDX and Raman results for Zone I showed elements consistent with the composition of the un-worn coating, as seen in C2. In Zone II, EDX identified WC substrate, as well as small quantities of iron and chromium transferred from the workpiece material. Zone III showed a thin layer of iron/iron oxide. Zone IV, the contact zone on the flank face, showed just titanium, aluminum and nitrogen. This region was of particular interest and it will be studied in detail.

Figure 3.3-10 (d) shows the Raman spectra of the different zones. As cited above, Zone I results consisted of un-worn coating elements as expected and agree with C2. Zone II is not represented because the WC substrate does not generate a useful signal as previously discussed. Zone III shows again the formation of magnetite Fe_3O_4, as previously seen. Zone IV shows two broad bands at 270 and 670 cm^{-1}. These bands are associated with the TiAlN coating deposited by PVD (Constable, et al., 1999), (Liew, 2010), (Barshilia & Rajam, 2004). After clearly seeing this TiAlN coating using EDX and Raman spectroscopy, the study of the coatings at an intermediate state of wear, prior to tool failure, is of interest.

- - - C3 Partially Worn

Figure 3.3-11(a) shows a micrograph of a C3 insert which had not yet reached failure. The insert was used for 30 m, and is in the steady state region of wear. The wear on the flank face is minimal, with only some micro-flaking wear marks.

Figure 3.3-11(b) shows a higher magnification SEM micrograph of the square area in (a). Four different areas have been identified: Zones I and II correspond to the coating layer, as seen by EDX in (c). Zones III and IV showed identical EDX spectra with only titanium, aluminum and nitrogen being identified. The Raman spectroscopy results for Zone I show the ZrN bands, as previously seen for this coating type. In Zone II, the closest studied region to the flank wear, the bands associated with ZrN and TiAlN are present. Zones III and IV again showed the TiAlN bands and no characteristics associated with ZrN. Al_2O_3 was not been observed by Raman, possibly because the γ-phase could not be detected by this technique. However, the fact that EDX shows only titanium, aluminum and nitrogen, and not oxygen, indicates that any Al_2O_3 layers have been detached.

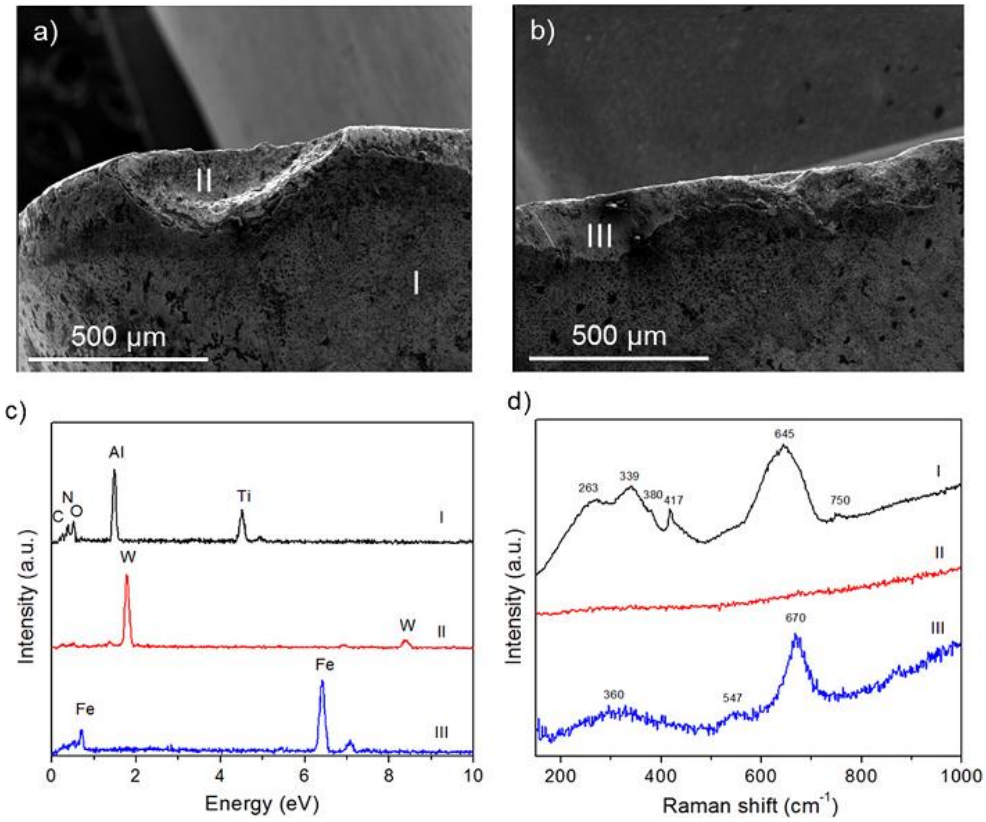

Figure 3.3-8 – SEM images of C1 (a and b), EDX (c) and Raman spectra (d) of indicated zones at failure

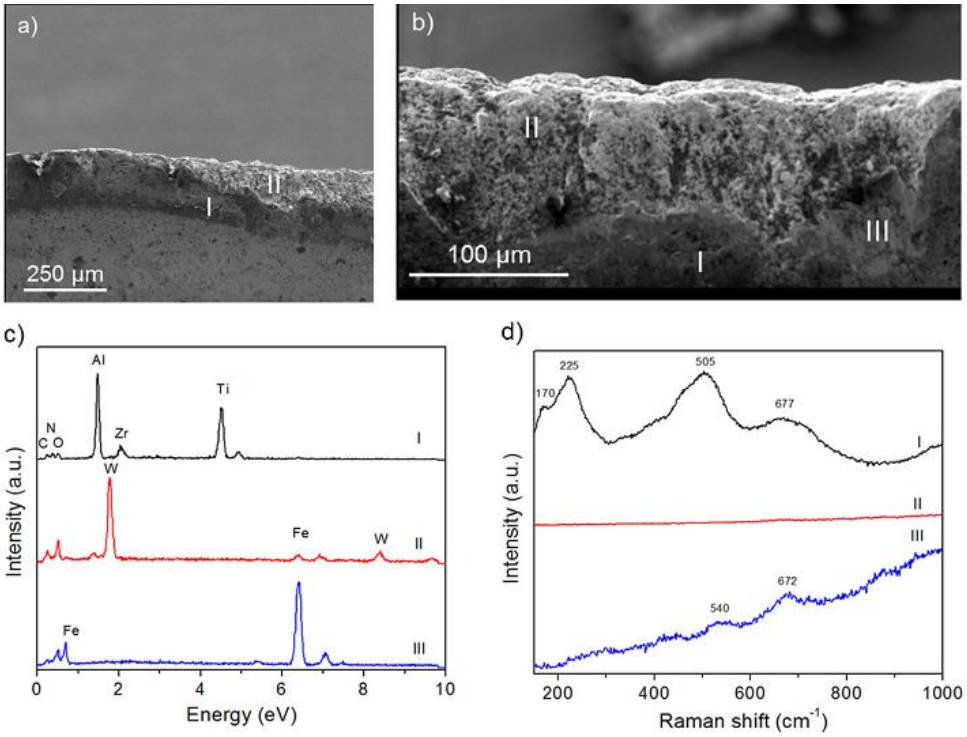

Figure 3.3-9 – SEM images of C2 (a and b), EDX (c) and Raman spectra (d) of indicated zones at failure

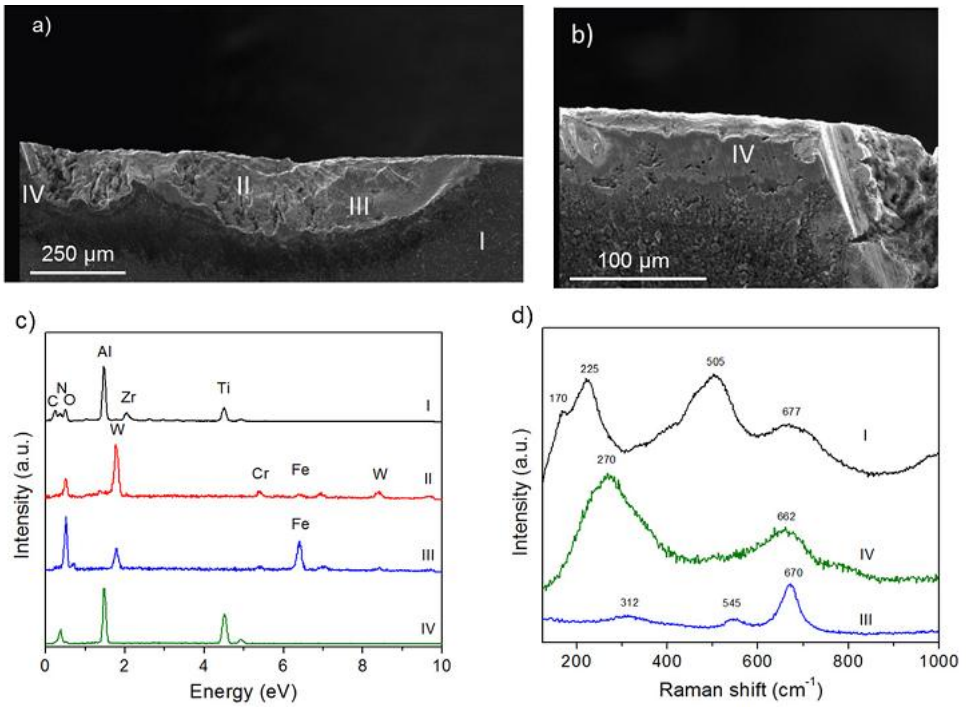

Figure 3.3-10 – SEM images of C3 (a and b), EDX (c), and Raman spectra (d) of indicated zones, at failure

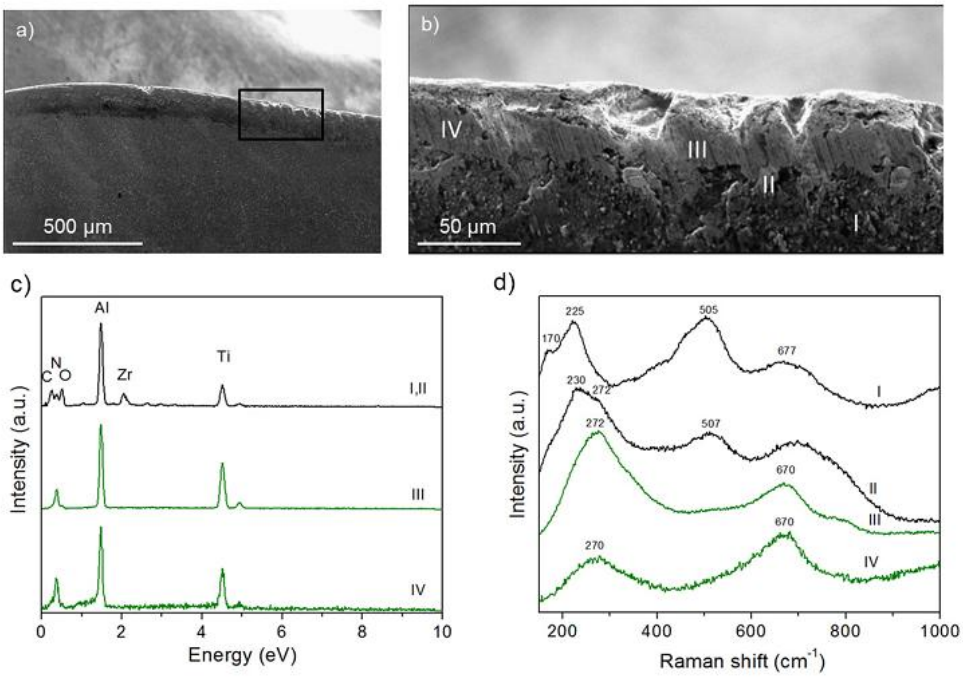

Figure 3.3-11 – SEM images of C3 (a and b), EDX (c), and Raman spectra (d) of indicated zones, in the steady state wear region at approximately 30 m

3.4 DISCUSSIONS

The results show that the tool life varies significantly for the three inserts studied. The C3 insert lasted more than three times longer than the C2 insert, and over 12 times longer than the C1 insert. Two factors were varied between these inserts, the coating composition and the chip breaker groove angle, which alters the effective rake face angle of the tool. In the following sections these factors are investigated and relationships between these and the results are presented.

3.4.1 RAKE ANGLE (CHIP BREAKER GROOVE ANGLE) AND CUTTING EDGE GEOMETRY

As discussed in the previous section, there is a difference in geometry between the C2 insert and the C1 and C3 inserts. The C2 insert has a 10º groove angle, where the other inserts have a more aggressive 16º groove angle. A larger

groove angle corresponds to a more positive rake angle, and a ‘‘sharper’’ tool wedge. As well, the C2 insert has a larger cutting edge chamber compared with C3.

According to widely accepted cutting force models such as Merchant’s; both of these changes in geometry should result in a decrease in cutting forces, which agrees with the results seen with the C2 and C3 tools in Figure 3.2-5 and with similar findings by (Gunay, et al., 2004). However, as both of these factors were varied, it is unclear how significant the impact of each was on the reduce cutting forces.

A reduction in cutting forces is favorable because lower cutting forces will result in lower friction, which in turn results in lower cutting temperatures. The lower cutting temperatures keep the process operating in a more favorable region of the coating which reduces the rate of abrasive wear (Stephenson & Agapiou, 1997). It is supposed that this is due to thermal softening of the coating; specifically the top layers. As a material heats up, its hardness tends to drop. Wear rates have been found to be inversely proportional to hardness (Rabinowicz, 1995), and so a drop in hardness due to thermal softening will likely result in increased wear rates and reduced tool life. Thermal softening may also accelerate plastic deformation of the cutting edge, which would result in a further increase in cutting temperatures, forces, and wear.

A more positive rake angle also reduces the strength of the cutting edge, as there is less material to support it. It also stands to reason that less material near the cutting edge will decrease the capacity for heat conduction, and thereby increase operating temperatures which as discussed previously, may negatively impact tool life.

3.4.2 COATING

Deposition methods may have played a role in the differing performances of the tools. The deposition method for the C2 and C3 inserts was PVD, where the C1 insert was coated using CVD. CVD processes require higher temperatures and typically result in a thicker coating; however, due to the higher temperatures involved, CVD coatings can develop so-called ‘‘cooling cracks’’ due to residual tensile stresses in the coating after cooling (Astrand, et al., 2004). PVD processes require a comparatively lower temperature and result in a thinner coating, but also develop compressive stresses that resist crack initiation and propagations; thus assisting in avoiding premature tool failure. The compressive stresses make the cutting edge tougher, and therefore able to withstand and resist crack propagation.

The CVD coated tool showed very poor performance in this study. It is believed that in spite of having a well designed multi-layer coating structure combining the heat resistance of α-Al_2O_3 and the wear resistance of TiCN, the highly interrupted nature of milling NiCrMoV steel caused cyclic thermal and mechanical loading and overwhelmed the CVD coating. Additionally, the CVD coating may already have been made brittle by ‘‘cooling cracks’’ as previously discussed; further promoting chipping in this process.

The large difference in performance between the inserts suggests that the PVD coating technique may have been more suitable for this heavily interrupted process. The combination of a crack-free coating deposition method, compressive stress, and high abrasive wear resistance gives superior tool performance to the C2 and C3 tools when compared to C1. However, it is believed that the lower temperature used in PVD is responsible for the presence of γ-Al_2O_3 or a poorly crystallized Al_2O_3 phase that was easily removed. This phase could work as a protective thermal barrier, limiting the heat transfer from the tool/chip interface into to the substrate material. However, previously

discussed investigation suggests that this layer had been detached and that the TiAlN layer is primarily responsible for the improved performance of these inserts.

3.5 SUMMARY

The three tools studied for milling of the NiCrMoV steel had markedly different tool lives. Analysis of the results in terms of the coatings applied and the geometries used provides some explanation for these results. The PVD TiAlN/Al_2O_3/ZrN C3 insert outperformed the C2 insert in terms of tool life and force by a factor of three, despite having identical coatings. This improvement is therefore attributed to the more aggressive chip breaker groove angle found on the C3 insert, as well as the reduced size of the cutting edge chamber. Thus, the negative thermal and strength related effects associated with reducing the amount of material near the cutting edge are likely being offset by the benefits of lowering the cutting forces, and thereby reducing heat generation. Overall this results in substantially improved tool life as seen in the presented results.

The CVD deposited TiCN/Al_2O_3/TiN coating (C1) was found to be unsuitable for this application because it was susceptible to chipping and fracture in this highly interrupted cutting process. The C3 insert with the PVD TiAlN/Al_2O_3/ZrN coating showed the best tool life and best wear characteristics for this application due to a more aggressive chip breaker groove angle (16º). It is believed that the TiAlN base coating layer alone is inhibiting the wear process, as the Al_2O_3 and ZrN top layers were detached long before the failure of the tool.

3.5.1 PRODUCTION IMPLICATIONS

By improving the tool life in this process, Siemens can now significantly reduce the technical risk to their parts and accelerate production. With the proposed tooling the frequency of tool changes is now reduced by 67%, greatly

reducing low-value added labour required in this process; as the tooling has 16 inserts which require changing.

Though small compared to the cost of the part, tooling costs are also reduced significantly. On a part having ~30 slots, previously requiring one set of inserts per slot and at ~$15 per tool (Walter Tools, 2007), tooling costs have been reduced from $3,600 to $1,200 per part, a potential savings of $2,400 per part.

However, the real cost savings in this improvement is the time savings and reduced low-value added labour, which is difficult to quantify. Anecdotal data provided by Siemens personnel suggested that this improvement would cut production time from 2 months to 1-2 weeks for this part due to increased reliability in tool life; that is, production could proceed normally because the operator did not have to continuously ensure tooling would not fail mid-cut. This results in a much greater time savings than suggested by tool life improvement alone. At a reasonable combined machine and operator time cost rate of $100/hour, and considering an 8-hour work day, a conservative time savings of 1 month (20 business days) results in a potential savings of $16,000 per part in reduced production cost.

However, the above is a rough estimate, and difficult to quantify with certainty without detailed production data; such data could easily be obtained through the use of a software based solution, such as the one described in Chapter 4 of this work.

Combined, this improvement has the potential to save $18,400 per part and significantly reduces the risk of scraping an extremely valuable part. This provides the industrial partner with the ability to produce parts faster while reducing costs; all through intelligent tooling enhancements.

CHAPTER 4. PROCESS MONITORING

4.1 INTRODUCTION

In mid to high volume manufacturing it is very important for companies to seek continuous improvement in their processes. This action allows a company to stay competitive, retaining and attracting new customers through improved productivity, quality and reduced cost. However, the action of improving these processes is not straightforward. Companies are faced with numerous challenges when seeking to improve or correct a process. In the following paragraphs these major steps are identified along with the challenges in completing each step. These are also outlined in Figure 4.1-1.

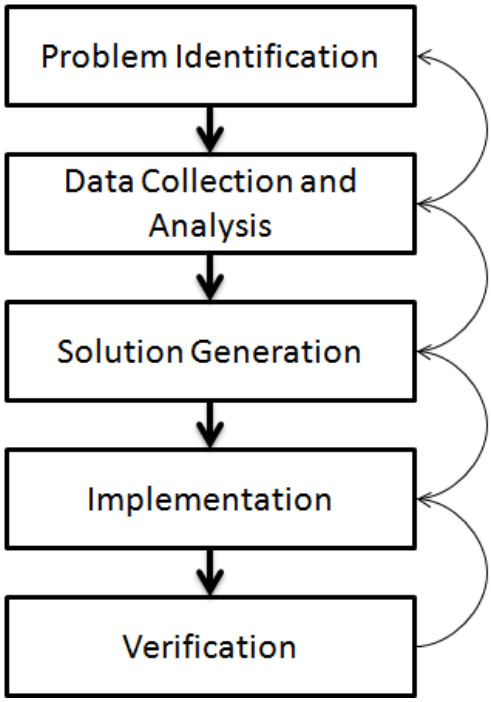

Figure 4.1-1 – Steps in process improvement identification and correction

Identify Potential Improvement

While it may seem straightforward, it is not always easy to identify when a problem is occurring in a manufacturing process. Machine wear or lack of maintenance and inconsistencies between batches of stock material are two examples of unexpected and difficult to measure changes in a process which contribute to scrap parts. Even with quality assurance measures in place, parts may still slip by un-noticed until comprehensive and careful study of large samples of produced parts is conducted.

Data Collection and Analysis

In order to better understand the problem and help identify sources or potential improvement avenues, it is necessary to observe the process from as many perspectives as is practical. These include:

--- Process Inputs

- Machine conditions: temperature variation, wear of critical components such as axis slides and encoders
- Environmental conditions: shop temperature and humidity, as well as contaminants such as particulate matter often found in machining of cast iron parts
- Stock Material: changes in chemistry, hardness, heat treatment or size of stock parts

--- Process, In-situ:

- Operator/Human interaction: Standard procedures, operator habits, areas of the process that introduce random error due to a lack of strict guidance on how to perform duties
- Machining Process: NC programs/tool paths, machining parameters including federate scheduling,

- Tools: tool wear rates, wear mechanisms, tool run-out, tooling changes

--- Process Outputs:

- Part measurements, control charts, process capability metrics
- Waste material, swarf (chips), scrap or out of tolerance parts

From this list it is clear that there are many variables that could potentially cause problems in production or be candidates for improvement. It should also be clear that all of the variables above require a great deal of resources to investigate. All steps require HQP resources, and many also require advanced and expensive instrumentation. In the short term, allocating financial and HQP resources to what is seen as low-value added efforts is difficult for a company to justify. This is a major barrier to seeking these types of improvements for manufacturers, who typically are forced into a mentality of “fire-fighting”, where they only correct problems when they occur rather than proactively preventing them.

Solution Generation

The next step is to take the gathered data and ensure it does indeed correlate to some aspect of the problem. For example, if parts are consistently being machined to the wrong dimension over a specified time, the problem can be traced back to tool wear or temperature induced machine errors depending on the time constant. For example as the machine warms up, the structure, slides, and bearings expand which may cause unintended dimensional error.

The pursuit of a solution again requires extensive HQP inputs, and may also require iteration of the Data Collection and Analysis steps once new information or ideas are generated. As in the previous step, the lost opportunity cost associated with a manufacturing company taking HQP away from high-value added production and new product development projects to fix or improve a process which has a relatively simple error is significant.

Solution Implementation

All of the previous steps require some level of interruption to the production process; however this step has the potential to require the largest down-time for a production or manufacturing cell. This, again, is a significant barrier as any down-time on a production cell has a high cost in both lost production and overhead.

Verification

The final step in the process is verifying that the solution has been implemented properly and effectively. This is typically done by comparing data from before and after the improvement related to the specific metric which showed a problem was present.

Often times completing the above process is very time consuming, requires a high level of knowledge, specialized instrumentation and triggers substantial costs. Therefore, a cost and time effective aid in tackling this process is of great usefulness and value to small and medium sized companies who do not have large financial and personnel resources.

4.2 PROJECT DESCRIPTION

In an attempt to meet the needs of manufactures who are interested in improving their processes, a process monitoring approach in the form of a software program was developed in collaboration with an industry partner.

4.2.1 PROCESS DESCRIPTION

The process that was selected to develop the approach is the mid-volume production of automatic transmission synchronizing rings, as pictured in Figure 4.2-4.

A general, semi-automated process which can be used to produce such a part is described below:

1) Near-finished blanks are loaded into the machine by operators
2) Through automated means, the parts are mounted onto idle CNC spindles
3) One feature is machined, as indicated in Figure 4.2-2.
4) The previously active spindles are unloaded through automated means.
5) The parts exit the machine on a conveyer, from which an operator retrieves them
6) The parts are placed into a gauge, pictured in Figure 4.2-3, which measures the diameter and the height of the final part, as indicated in Figure 4.2-2. The operator then makes a judgement on whether the part is within tolerance or not based on the indicator readings.
7) The operator, as they make judgements on parts, makes memory based tool offsets on the machine

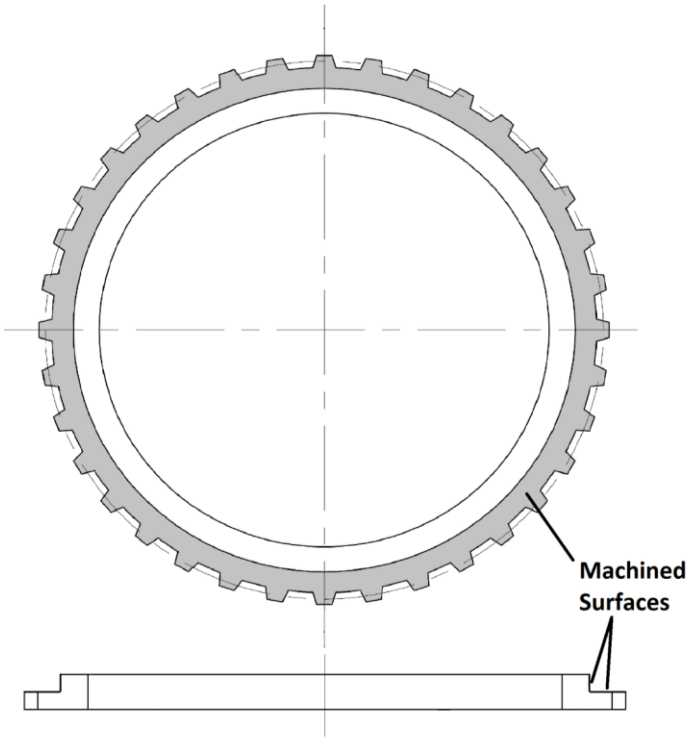

Figure 4.2-1 – CNC machined part geometry, showing machined surfaces

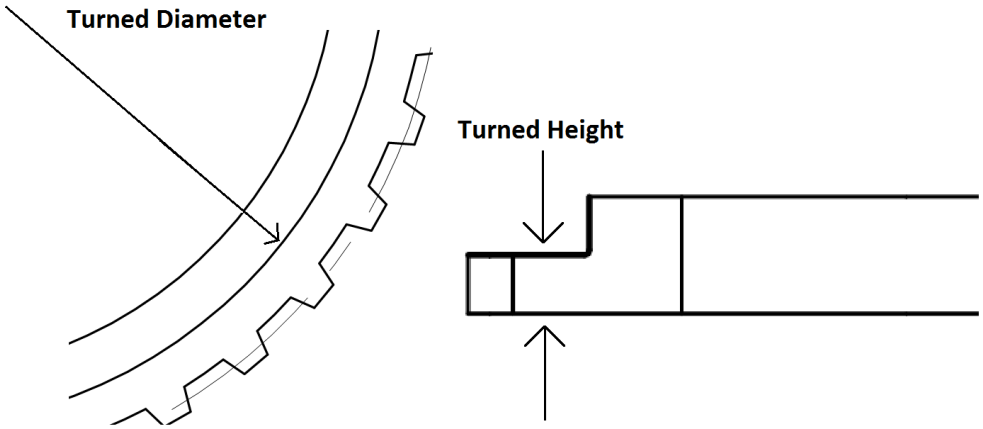

Figure 4.2-2 – Machined dimensions on part

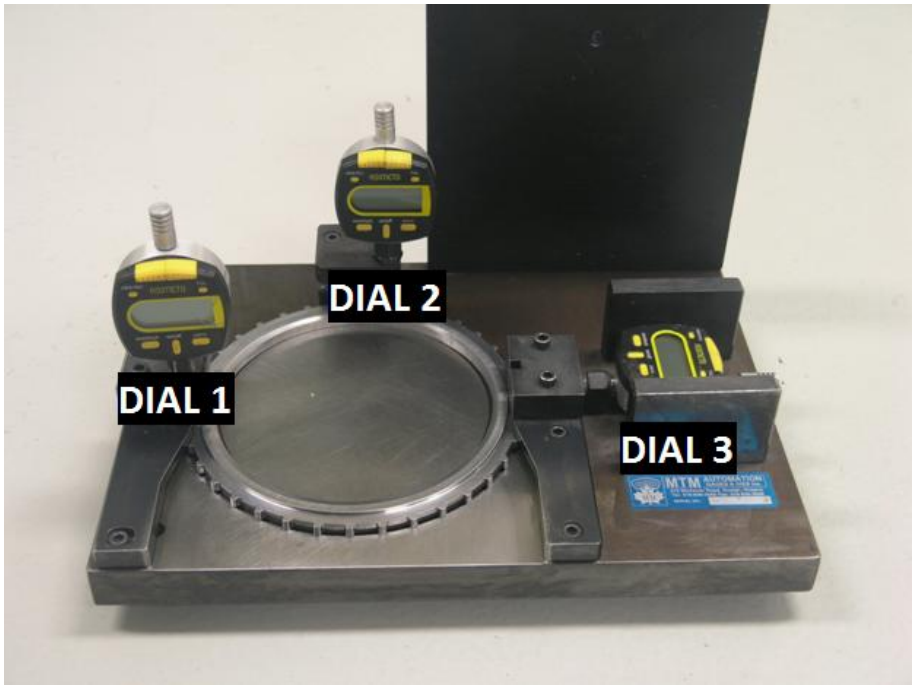

Figure 4.2-3 – Gauge used for measuring synchronizing ring parts; dials 1 and 2 measure height and dial 3 measures diameter

Figure 4.2-4 – Production Part

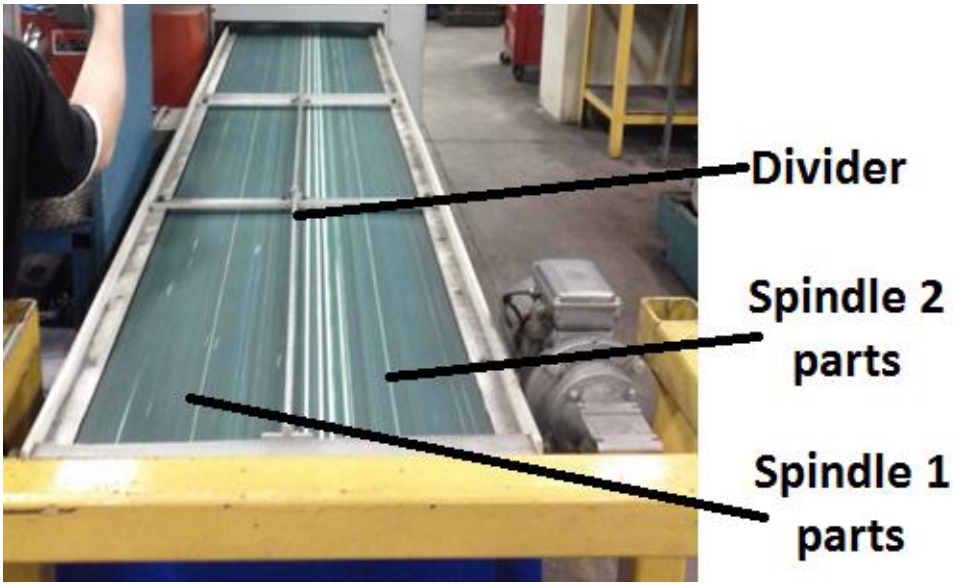

Figure 4.2-5 – Production cell conveyer which delivers parts to the operator for gauge inspection; note the divider was not installed until Phase 2 of software implementation, as discussed in section 4.5.2.

A flowchart of the responsibilities of the operator is shown in Figure 4.2-6 along with the planned shift of these responsibilities to the software.

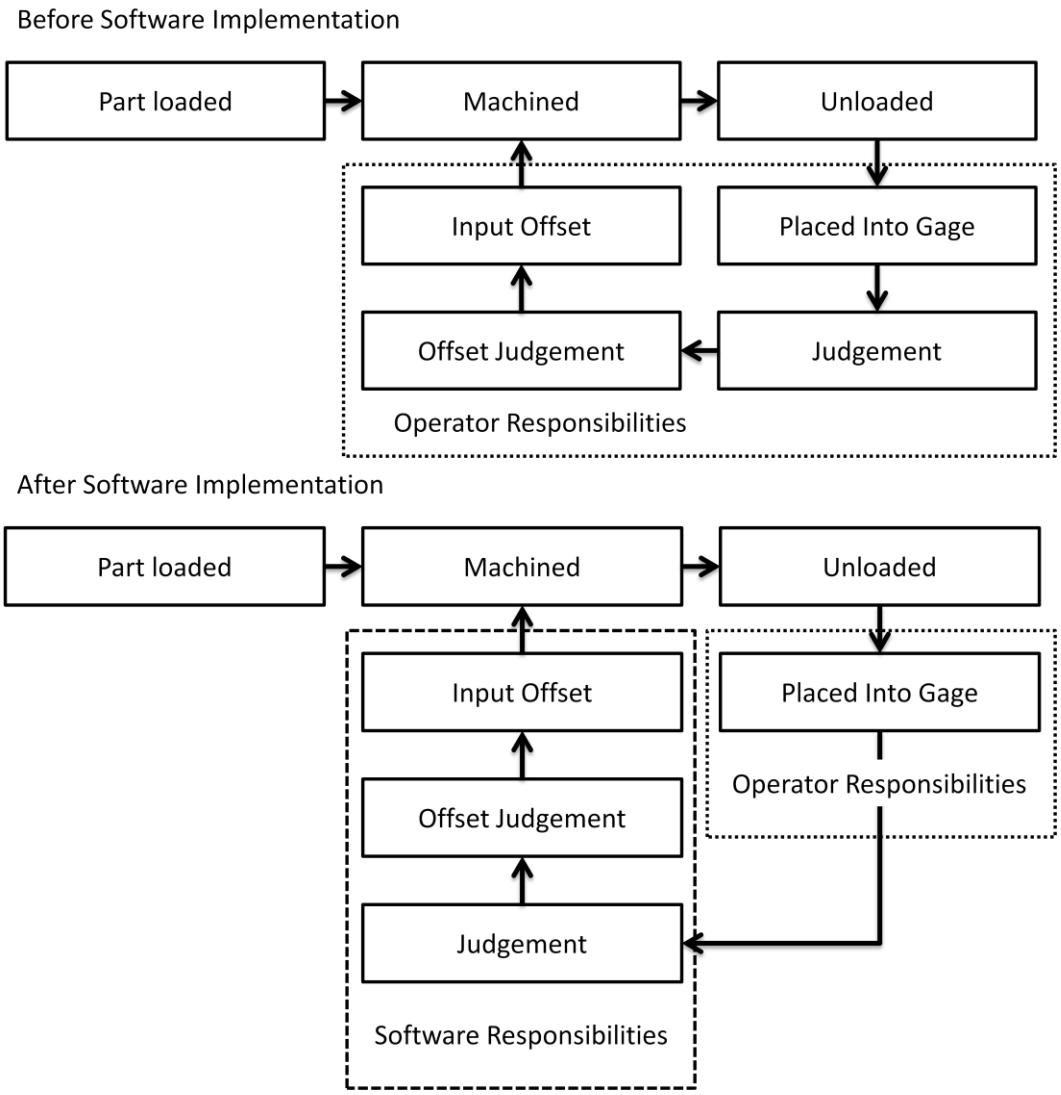

Figure 4.2-6 – Top: Operator responsibilities before software implementation. Bottom: Operator and Software responsibilities after implementation.

4.2.2 PROCESS IMPROVEMENTS

The production process described in section 4.2.1 has several areas that would benefit from improvement, as identified through process analysis outlined in the introduction of this chapter. These are highlighted and described below as improvement goals:

--- Goal 1 – Remove Part Confusion

In step 7, the operator could easily confuse which spindle a part was machined on. This is especially prevalent when the operator falls behind the production rate of the machine, which will continue to deliver parts to the conveyer until the process is paused. If the operator does not know which spindle a part came from, there is no way to make good offset judgements.

The goal is to reduce or eliminate this error to ensure that every part's measurements are attributed to the correct spindle.

--- Goal 2 – Gauge Improvement

Step 8 involves the operator using the gauge to measure the machined dimensions on the part. It was identified that gauge repeatability was one area which had the potential for significant improvement. Due to flatness issues in the blanks, measurements may not be accurate as the flatness variation will contribute to height readings due to improper gauge design, as shown in Figure 4.2-7. In this situation, rotating the part to measure a different angular location along the circumference of the machined surface resulted in variation, occasionally larger than the acceptable tolerance.

Goal 2 is to improve the gauge to negate the influence of flatness error in the parts on measurements.

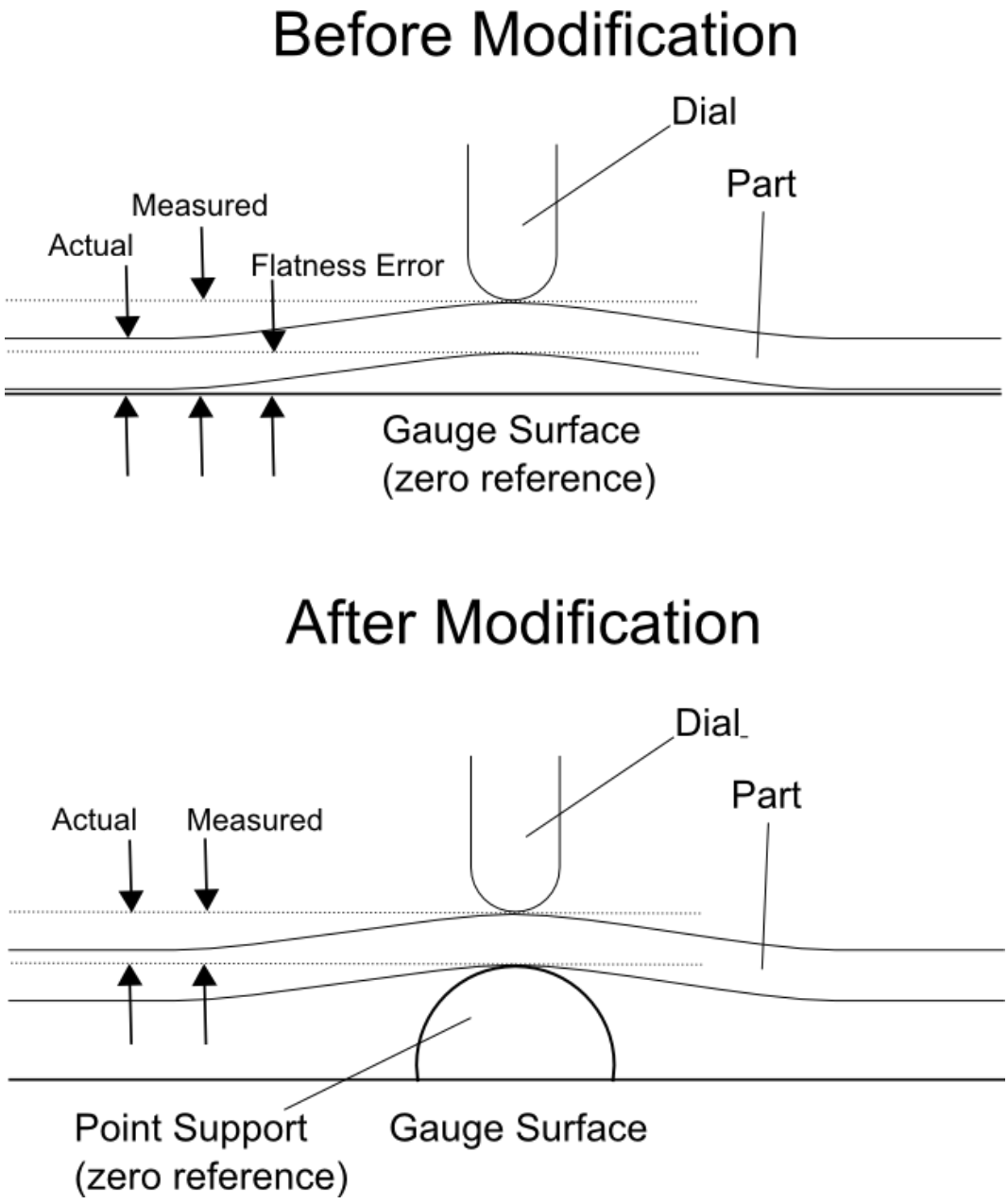

Figure 4.2-7 – Flatness error contributing to height readings

--- Goal 3 – Eliminate Operator Part Judgement

The gauge described in step 7 has three dial indicators, which necessarily must face horizontally. This makes them difficult to read, and in this fast paced cell, misreading or neglecting to read all three dials are easy mistakes for the operator to make.

The third goal is to eliminate the need for the operator to have to read and make a judgement on whether the part is in tolerance or not.

--- Goal 4 – Automate Offset Judgement

Currently the offset judgement process for operators is unspecified. Speaking with the operators reveals they all have their own methods. These are typically based on experience, intuition and a limited memory of measured parts. Occasionally operators will make offsets too frequently, with an inappropriate magnitude which either does not have a large enough impact or over-corrects.

The final goal is to remove the need for operators to make offset judgements, as the necessary inputs to make good judgements are not feasible to implement without the aid of automation and software.

Achieving the goals listed above would provide significant improvement in the process. It would relieve the operator of difficult responsibilities such as offset adjustment, and reduce scrap and variability in parts.

4.3 SOFTWARE DEVELOPMENT

In order to meet the goals described in Section 4.2.2, a software based approach was adopted. The purpose was to produce a modular Statistical Process Control (SPC) package, having an efficient and easy-to-use interface which does not impede the operator and provides valuable quality control information as well as online process feedback. The goals served as objectives for the software's performance.

4.3.1 PROCESS PERFORMANCE METRIC

A widely accepted method of measuring process performance is to use statistical process control metrics such as process capability, as discussed in

Section 2.5. In the following sections, the performance of the process is measured using a non-centered process capability index: C_{pk}.

4.3.2 Software Interface and Operator Interaction

The interface shown below in Figure 4.3-1 was developed in cooperation with the industry partner. The interface with the operator took some time and effort to develop. The reason for this is that it is critical that interfacing with the software does not significantly increase the amount of time it takes for an operator to process a part. This is discussed in detail in section 4.3.3.

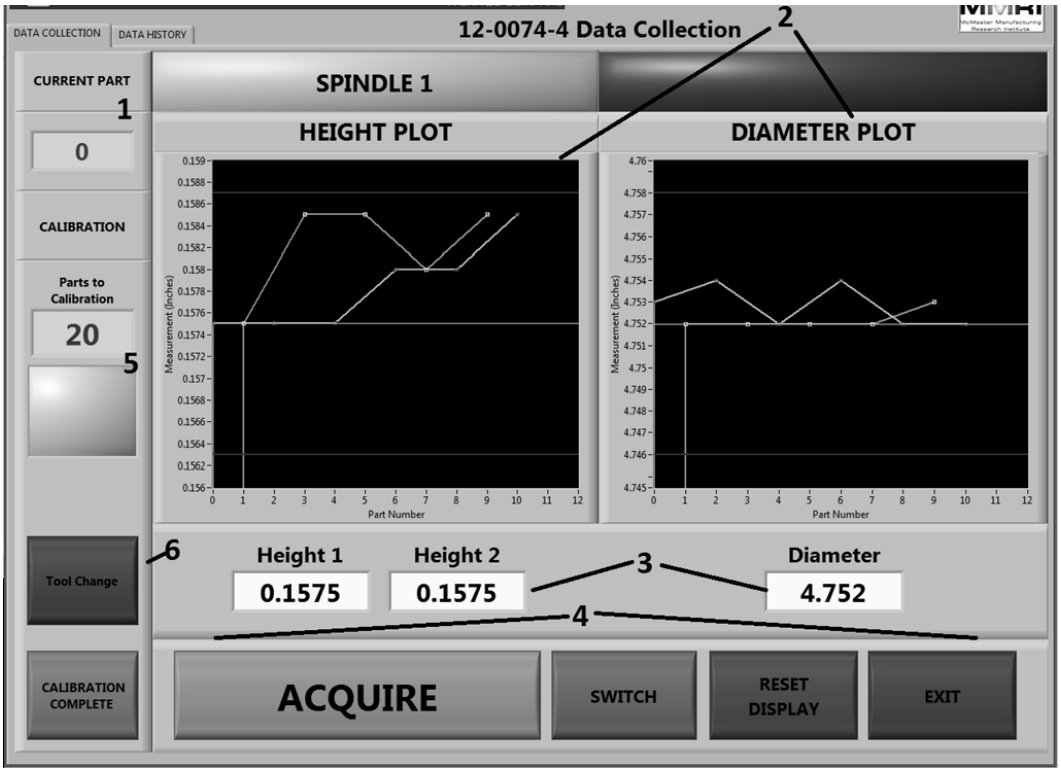

Figure 4.3-1 – Software interface

4.3.3 Software Requirements

There are numerous requirements of the software in order for it to be useful and provide value to both the industrial partner and research efforts. These requirements fall under five areas: Operator interface and interaction; data

collection and storage; on-line process analysis; offline process analysis; and long-term process analysis. These requirements are discussed below along with the software features which satisfy them.

Operator Interface and Interaction

There are two main objectives the software interface must achieve: it must provide the operator with sufficient information without overwhelming them and it must have a high degree of automation. If the software requires large amounts of user input, it greatly diminishes its usefulness. Something as seemingly unobtrusive as moving a mouse to interact with the software can cause significant delays to operator duties. In order to ensure the software operated as passively as possible, requirements were developed based on co-operative analysis of the process with the industry partner. The requirements as well as how they are integrated and met by the software, are discussed below:

--- Requirement 1: Minimize use of Mouse

In many processes the operators are required to be using both hands simultaneously. Therefore, requiring them to frequently use a hand to use a mouse to interact with the software is disruptive.

In order to meet this requirement, the vast majority of interaction with the software is completed through a designated button pad which is located within easy reach of the operator. Use of the mouse is required for operations such as tool changes, however during these tasks the operator has idle time and so this does not hinder them in a significant way.

--- Requirement 2: Data Display and Judgement Aid

The purpose of the data plots and measurement displays on the software interface are to aid the operator in their duties. However, it is a difficult balance

between providing too much information which may overwhelm an operator, and providing too little information to be useful.

This requirement is met by providing the operator with control charts of all part measurements for the previous 10 parts measured. This provides a quick, colour-coordinated and easily interpreted visual interpretation of the process in real time which helps the operator identify sudden changes which require further attention. The real-time gauge measurements are also displayed. These have a far higher visibility than the read-outs on the dials themselves, and therefore reduce the chance of the operator misreading or neglecting to read these values.

Data Collection and Storage

In order to provide valuable information on the process history, data and process events such as tool changes and CNC cutting depth offset adjustments need to be recorded.

--- Requirement 1: Detailed Data Recording

For future analysis of processes and to help identify issues in production, it is necessary to record data with a high level of detail. The software accomplishes this by recording data in real time. This ensures that if the software stops for any reason; all measurements are recorded and are not lost. The data is also recorded with all necessary information such as date, time, part number, etc.

All events that may affect trends in control charts are also recorded; these include: gauge calibration, offset adjustments, tool changes, sub-group switching, and resets. Program starts, exits and errors are also recorded for debugging.

On-line Process Analysis

In-line with goal 3 in Section 4.2.2, on-line process analysis is used to track part measurements and estimate process performance.

--- Requirement 1: Estimate Offsets

Commonly, operators are required to make offsets when they feel they are necessary. Often times these offsets are sub-optimal, and at worst have no beneficial impact; this is because it is exceptionally difficult for an operator to make an optimal judgement without the aid of current data and the ability to perform calculations. The software must be able to replace this duty and provide accurate offset recommendations based on past performance.

--- Requirement 2: Automatic Offset Adjustment

Once the software judges that an offset should be made, it should be able to do this without aid from the operator in order to be as passive and automated as possible.

Automatic offset adjustment is straightforward for most CNC machines, and can be made through built-in Ethernet or com ports. However, this level of automation will take some time to reach as industrial partners would like to be certain that the offset recommendations are consistently reliable. There is considerable potential for increasing variability if offsets are poor, or in the worst case - an extremely large offset could cause the machine to crash potentially resulting in significant repair costs and down time.

--- Requirement 3: Reject Invalid/Outlier Measurements

For a multitude of reasons, occasionally a part may be massively out of tolerance due to special cause variation. Such parts should be detected and rejected as their inclusion will greatly influence the quality of offset recommendations as they are outliers which do not reflect the trends occurring in the process.

The software accomplishes this by removing a data point if it is out of tolerance by 200% or more. As it is extremely rare that a measurement this far

out of tolerance occurs legitimately, the large majority of these measurements are rejected, as demonstrated by the lack of outliers in the data.

Offline Process Analysis

Manufactures which produce automotive parts are often required to meet certain SPC requirements for their production. However, tracking these requirements, such as process capability, is not straightforward. 100% inspection, recording and processing of part measurements is difficult and extremely time consuming without a software solution. The industrial partner also requires a method to create control charts from the stored data for quality control purposes.

--- Requirement 1: Generation of Control Charts

In order to have a visual representation of the process and track process history, the ability of the software to take stored process data and create a control chart from it is necessary.

A separate software module has been developed for this purpose, and a screen capture is pictured in Figure 4.3-2. This module allows the user to select a previously generated data set, which are then plotted as control charts. Examples of these outputs can be found in the later sections of this chapter.

--- Requirement 2: SPC Metrics

Along with control charts, industrial partners are interested in the specific SPC requirements set by their customers.

The software module incorporates this functionality, and displays several SPC metrics required by the industrial partner. The module was designed to be flexible, and so if the software is implemented in different processes with new SPC requirements, they are easily and quickly added into the output.

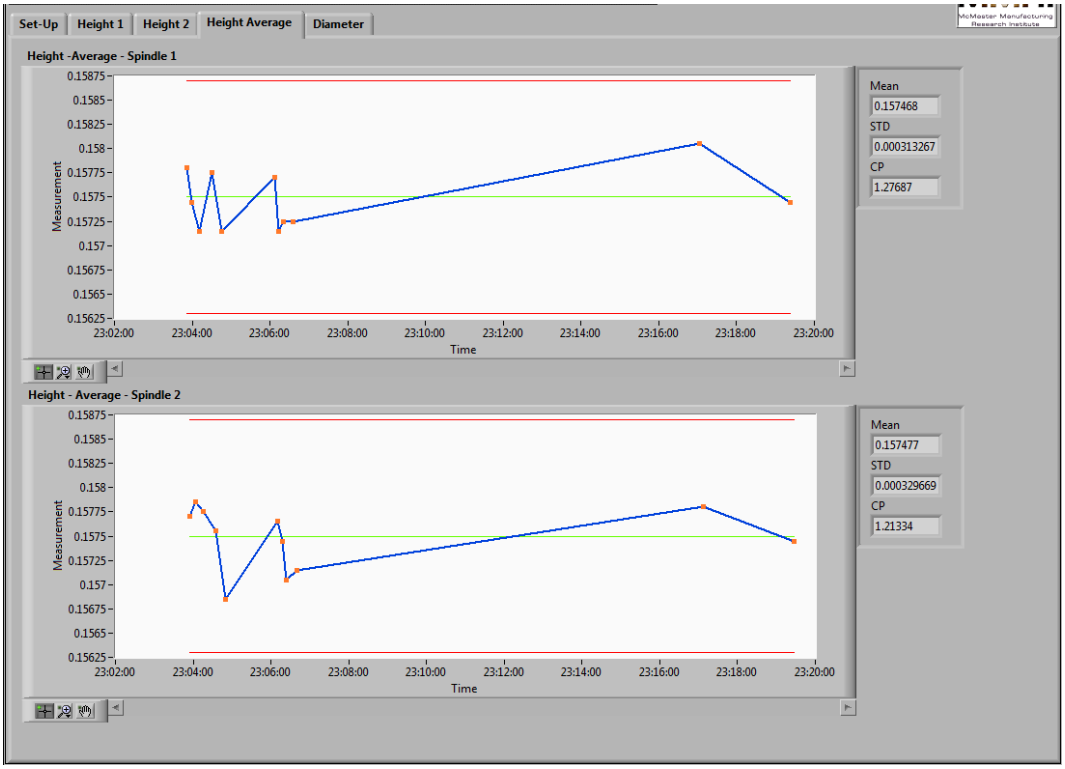

Figure 4.3-2 – Screen capture of control chart data display module

Long-Term Process Analysis

The MSL research group within the MMRI at McMaster University focuses heavily on industrial projects, where improvements are sought and identified in the lab and transferred to an industrial partner's production. However, it is clear that improvements in the lab do not always follow in-lab performance once implemented in production. While in almost all projects there is clear improvement, quantifying it accurately is a challenge as was discussed in Chapter 3 and Section 3.5.1.

--- Requirement 1: Track the long-term performance of recommended improvements

In order to aid in quantifying these improvements, a software based solution to track part measurements, production rates, tool life and other performance metrics would be extremely useful to the MSL and MMRI.

The software developed currently has the functionality to track part measurements, production rates, tool life, and operator actions. If implemented in a production cell along with recommendations developed through one of the MSL's industrial research projects, this software would be able to track the performance before and after implementation to help quantify quality, cost and productivity improvements. This quantification would make clear the benefits, cost savings, or production gains from the partnership, which in turn would encourage further collaboration.

4.4 RESULTS CONSIDERATIONS

There are several considerations and assumptions the reader should be made aware of before presenting the results of this work. These are discussed in this section.

4.4.1 CHANGE IN TEST CELL

The reader should also be made aware that approximately 9 months into the project, it was decided to move the software implementation to a different production cell. This was due to flatness issues in the incoming material. Some improvements were made in the cell; however, additional improvement was complicated by these flatness issues. Though the flatness was within tolerance of the part, identifying additional process improvements was very difficult as the variation in the flatness masked and dominated all other variation. Therefore, production was moved to a cell which had a similar production process. These part blanks did not have flatness issues. In the results sections to follow, it will be made clear when the transition was made between cells.

4.4.2 SPINDLE GROUPING

The terms "Spindle 1" and "Spindle 2" which are used extensively in the results section are misleading; in reality the data in the results section is the

result of multiple spindles being grouped into data sets labeled as “Spindle 1” and “Spindle 2”. However, there are only two cutting tools and so offsets are made to the tools only. Effectively, this means the operator (and after implementation, the software) only has to track offsets for two spindles according to the current production set-up. This spindle grouping is shown in Figure 4.4-1; real spindles 1 and 2 are grouped and henceforth referred to as “Spindle 1”. Similarly, real spindles 3 and 4 are grouped and referred to as “Spindle 2”.

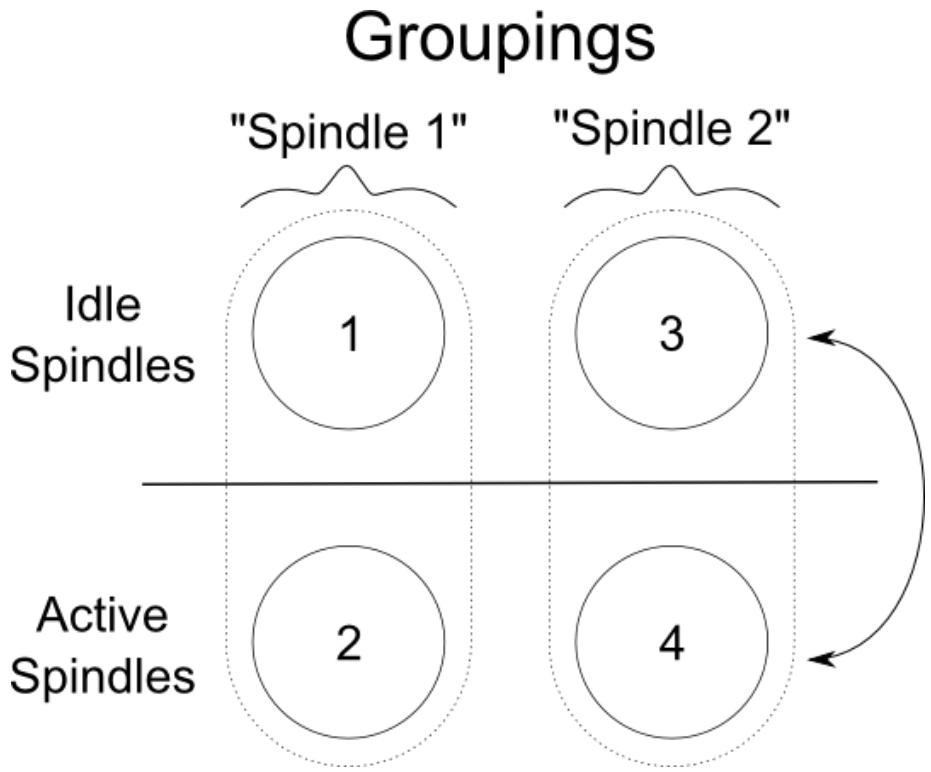

Figure 4.4-1 – Explanation of grouping of four spindles into two groups, and reference convention for the groups

Whether there is significant variation between the grouped spindles which share a single offset was not exhaustively verified. However the industrial partner assured that they had investigated this previously and the variation between spindles was negligible and much of the difference between “spindles 1 and 2” (which in reality represent spindles 1&2 compared with spindles 3&4 as per

Figure 4.4-1) comes from the shared cutting tools, holders and tool turrets. Preliminary investigation into the industrial partner's claim is discussed below.

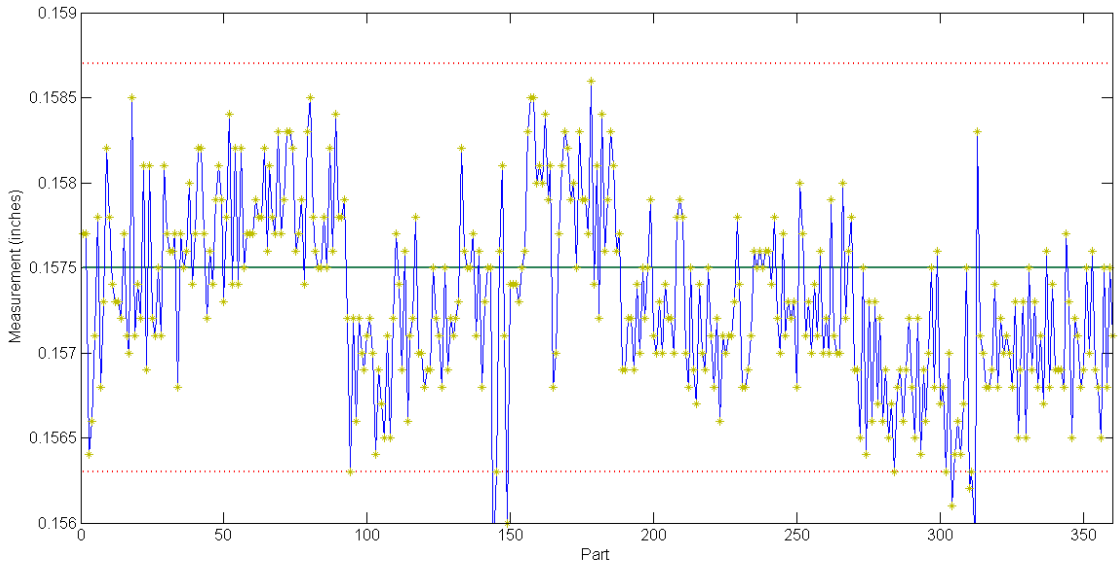

Figure 4.4-2 – Recorded data for production, showing height measurement data from Spindle 1 parts; red dotted lines represent upper and lower control limits, green solid line represents the nominal value

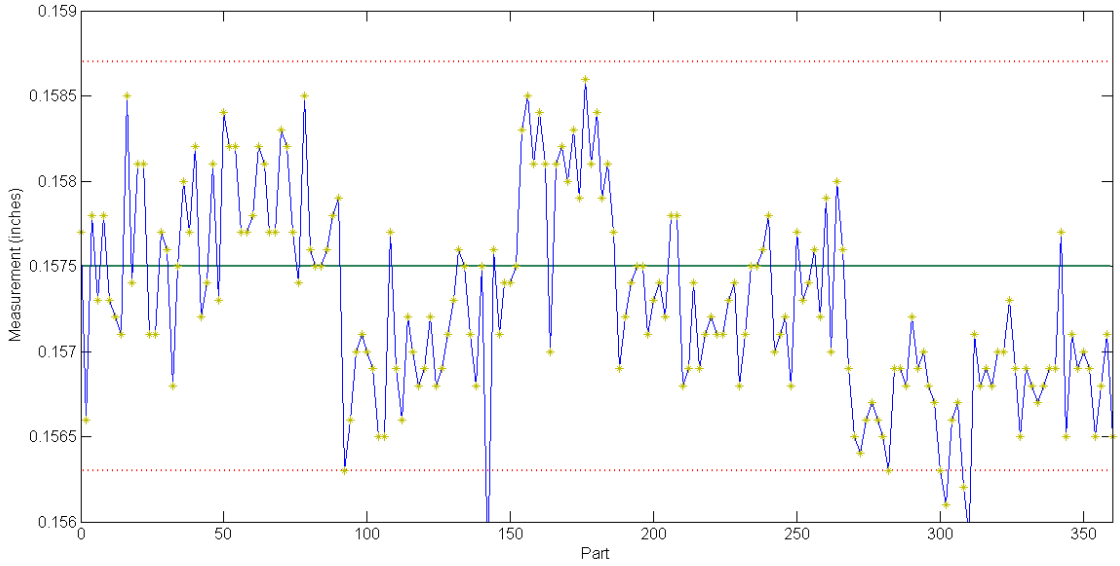

Figure 4.4-3 – Odd numbered values from Figure 4.4-2, representing spindle 1 of 4

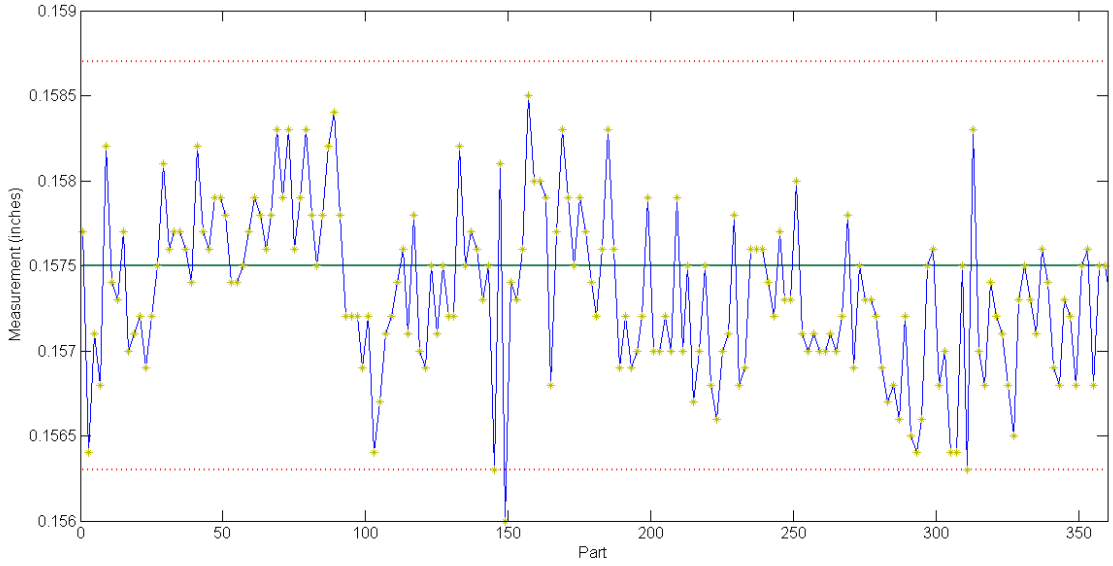

Figure 4.4-4 – Even numbered values from Figure 4.4-2, representing spindle 2 of 4

Figure 4.4-2 shows a set of recorded data from early in the project. Figure 4.4-3 and Figure 4.4-4 plot the same data in two sets; one plotting even numbered parts and the other plotting odd numbered parts. Some relevant statistical data from these plots are shown in Table 4.4-1.

Table 4.4-1 Mean and standard deviation for Spindle Grouping variation analysis

Data set	Modified Standard Deviation (inches)
Figure 4.4-2 (entire data set)	0.00065
Figure 4.4-3 (odd parts)	0.0013
Figure 4.4-4 (even parts)	0.0013

The modified standard deviation calculated above was found using the following method and acts as a suitable comparison for the variation in each data set:

1) A moving average (4-point window size and evenly weighted) was calculated for each data point in each set.
2) Each data point had its corresponding moving average value subtracted
3) The standard deviation of these new data sets was calculated

From viewing the entire data set, there appears to be an alternating pattern for data points which suggests pooling data from two spindles into one may be introducing significant variation due to differences in the spindles. To test if this is indeed the case; the data was split into sets for each separate spindle. It is then expected that there would be less variation in these sets, and smoother trends would appear. It would also be expected that the modified standard deviation would decrease, as a smoother trend would deviate less from the moving average, resulting in a lower variance and standard deviation.

However, separating these out as described above reveals that this variation is present in both spindles independently. The data in Table 4.4-1 supports this, as the modified standard deviations did not decrease as would be expected if a significant source of the variation in the combined data set was indeed due to the combination of the two spindles.

This preliminary analysis of variation between spindles sharing an offset has shown that there should be no significant variation introduced into data sets by the grouping of these spindles.

4.4.3 NORMALITY OF DATA

In order to use process capability metrics such as C_{PK}, the assumption of normally distributed data is required. However, making this assumption when data is in fact not normally distributed will lead to underestimating these values, and overstating the number of expected parts that will be out of tolerance and rejected. In short, the C_{PK} value will suggest a poorly performing process when in fact it is quite capable if data is not normally distributed.

In order to be sure that C_{PK} values calculated in the results section of this chapter are indeed representative of the process, normality tests were conducted on several sets of production data and are outlined below. Four sets were selected, spread roughly evenly over the duration of the project. Graphical methods as well as Chi Square normality tests were used.

Table 4.4-2 – Normality Test Results

Data Collection Date	Chi Square Normality P-values	
	Height	Diameter
May 4, 2011	0.143	0.00005
February 22, 2012	0.105	0.085
May 14, 2012	0.030	0.585
July 12, 2012	7.75E-29*	6.1E-22*

*These values are suspiciously low, however extensive investigation into the calculations could not reveal an error, and graphical means suggest the distribution is very close to normal, and so they are reported as calculated.

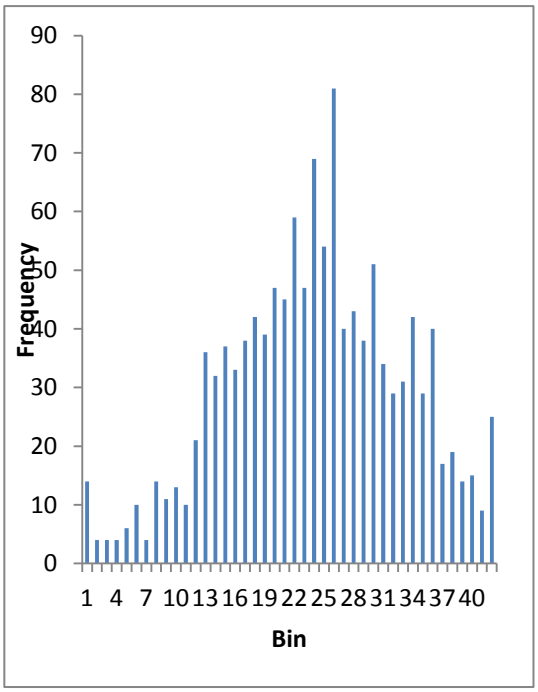

Figure 4.4-5 – Frequency histogram for May 4, 2011 data; height data

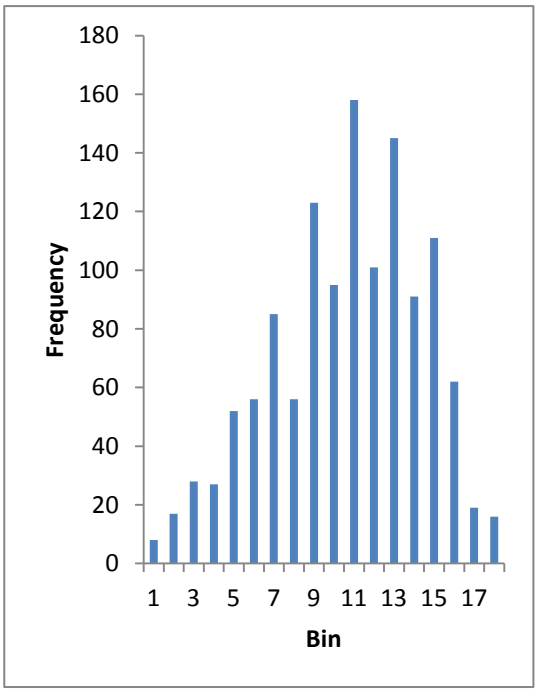

Figure 4.4-6 – Frequency histogram for May 4, 2011 data; diameter data

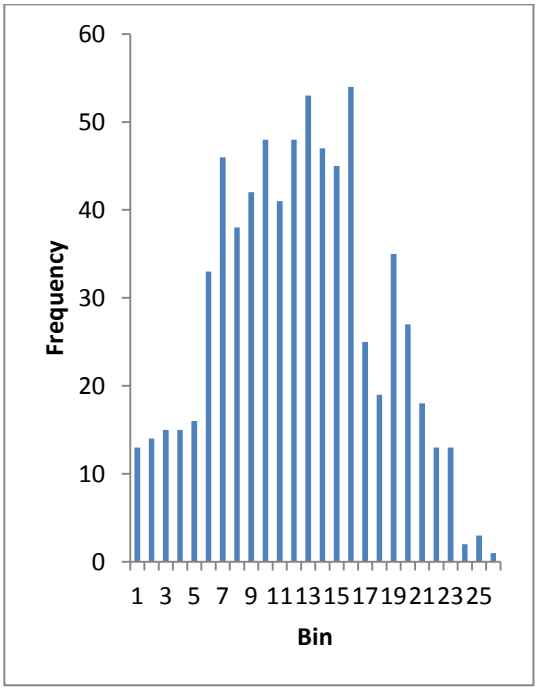

Figure 4.4-7 – Frequency histogram for February 22, 2012 data; height data

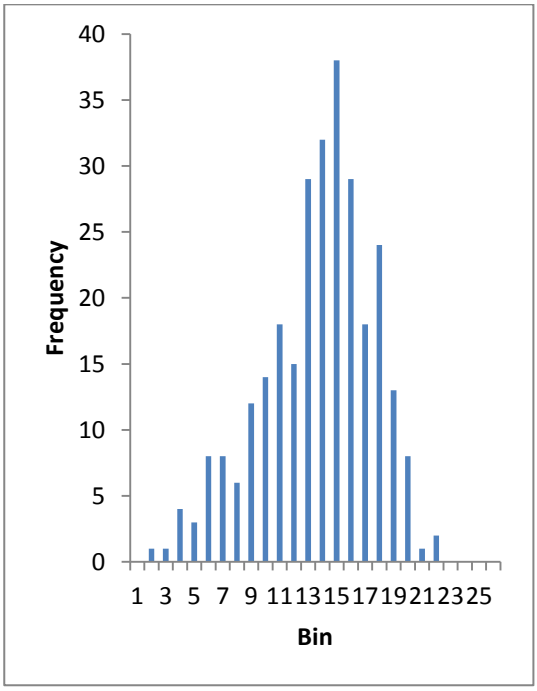

Figure 4.4-9 – Frequency histogram for May 14, 2012; height data

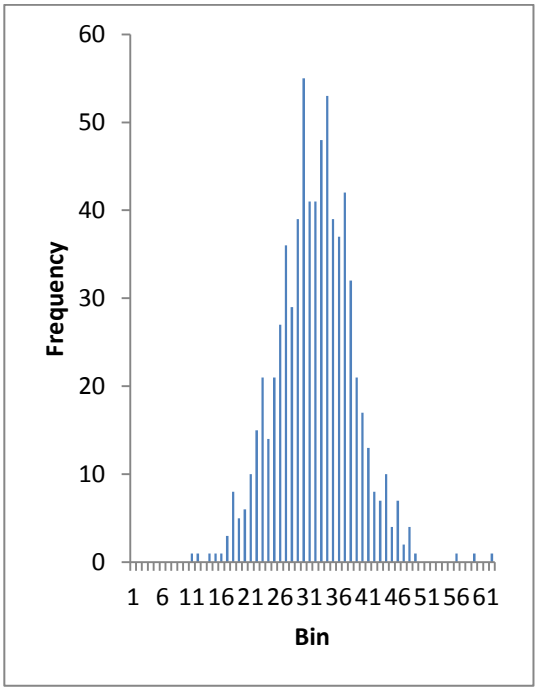

Figure 4.4-8 – Frequency histogram for February 22, 2012; diameter data

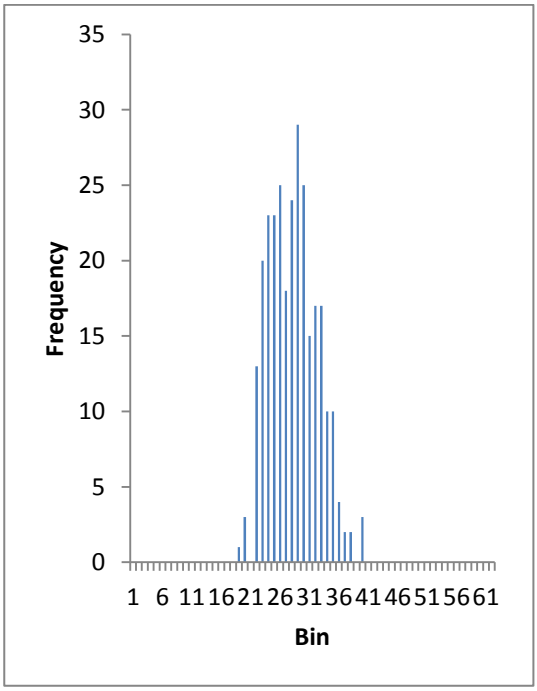

Figure 4.4-10 – Frequency histogram for May 14, 2012; diameter data

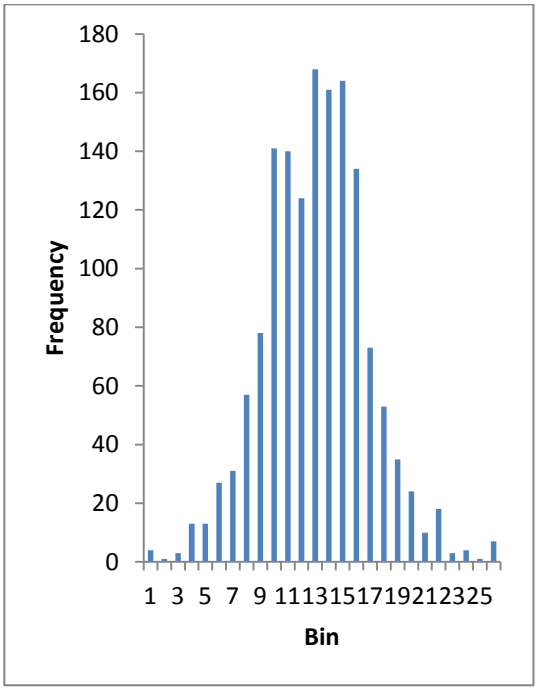

Figure 4.4-11 – Frequency histogram for July 12, 2012; height data

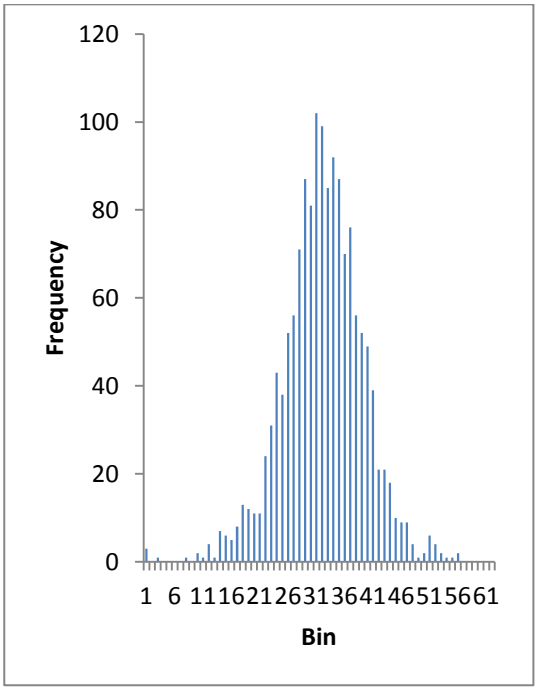

Figure 4.4-12 – Frequency histogram for July 12, 2012; diameter data

Figure 4.4-5 to Figure 4.4-10 clearly demonstrate that production data distribution is approximately normal. The chi-square normality test results, shown in Table 4.4-2 generally agree with this.

Therefore, the assumption of normally distributed data used in the following sections is acceptable and will not introduce unacceptable levels of error into process capability calculations.

4.4.4 Removal of Outliers

As discussed in previous sections, infrequent outliers occurred in some data sets due to known production anomalies such as swarf material impeding the proper mounting of parts on the spindle. These data points are removed from the production data when calculating process metrics such as C_{PK} as including them would artificially deflate these values.

4.4.5 OPERATOR TECHNIQUES

As with any manual process completed by more than one operator, part measurements will suffer from some variability introduced by human factors. Due to limitations common to industrial projects, the industrial partner was unable to use the same operator for all data collection dates. Therefore, some unavoidable variability in results will be naturally introduced by differences in both ability and technique of the operators.

4.5 RESULTS AND DISCUSSION

This section discusses the progressive improvements in the test production cell which are a direct result of implementing the software. By using the software, a number of areas of potential improvement were identified by the MMRI, which otherwise would have gone unnoticed. These progressive steps of improvement are organized into phases and discussed below.

Results are shown primarily in the form of control charts. In this process there are two spindles and three measurements per part; two height measurements measuring the same feature at different circumferential locations, and one diameter measurement. This results in six control charts for each data collection session.

4.5.1 PHASE 1: INITIAL IMPLEMENTATION – MAY 4, 2011

Software installation and implementation began in early 2011 and continued through to May 2011. On May 4, 2011 the software and our industrial partner had developed enough to capture a first set of production data. The data is displayed in Figure 4.5-1 to Figure 4.5-6. Summary statistics are also displayed for this data in

Table 4.5-1.

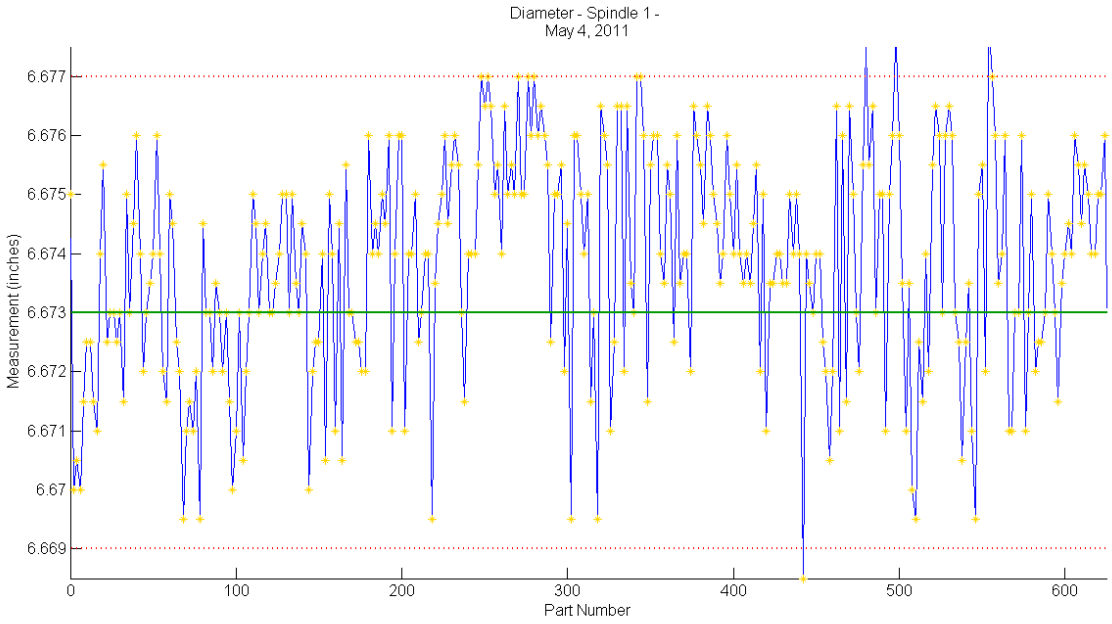

Figure 4.5-1 – Control chart for May 4 data collection, showing diameter measurements from parts produced on spindle 1

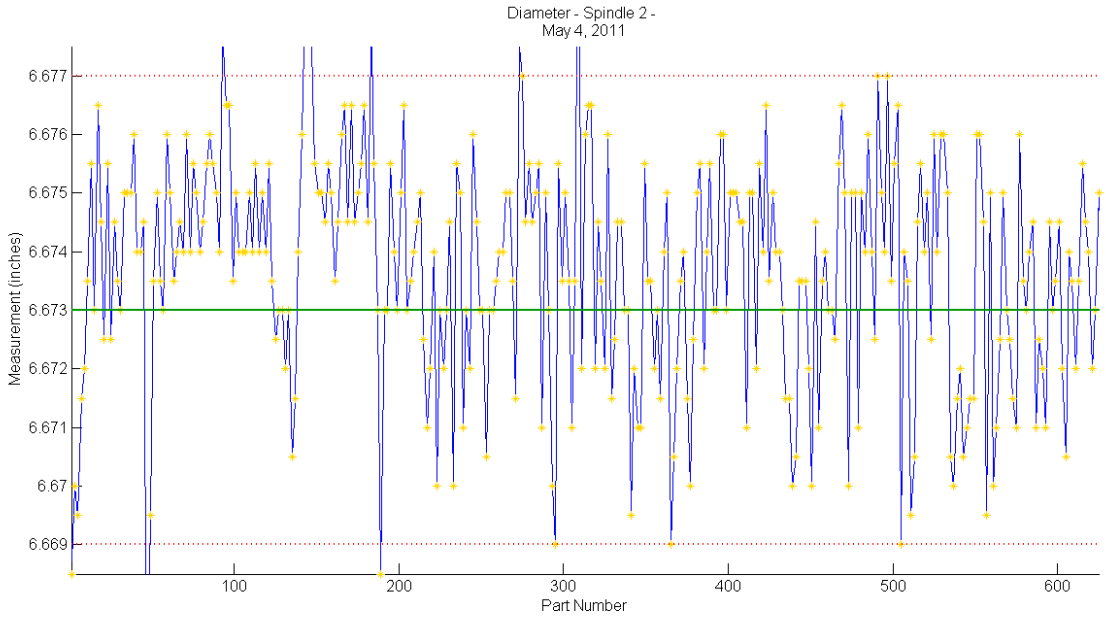

Figure 4.5-2 – Control chart for May 4, 2011 data collection, showing diameter measurements from parts produced on spindle 2

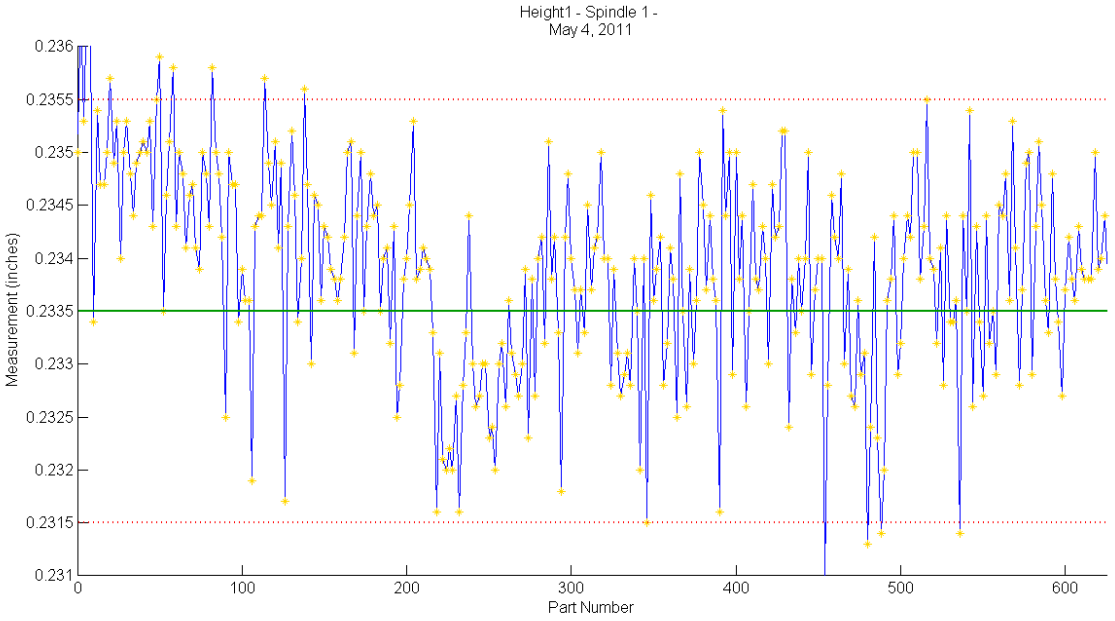

Figure 4.5-3 – Control chart for May 4, 2011 data collection, showing height 1 measurements from spindle 1

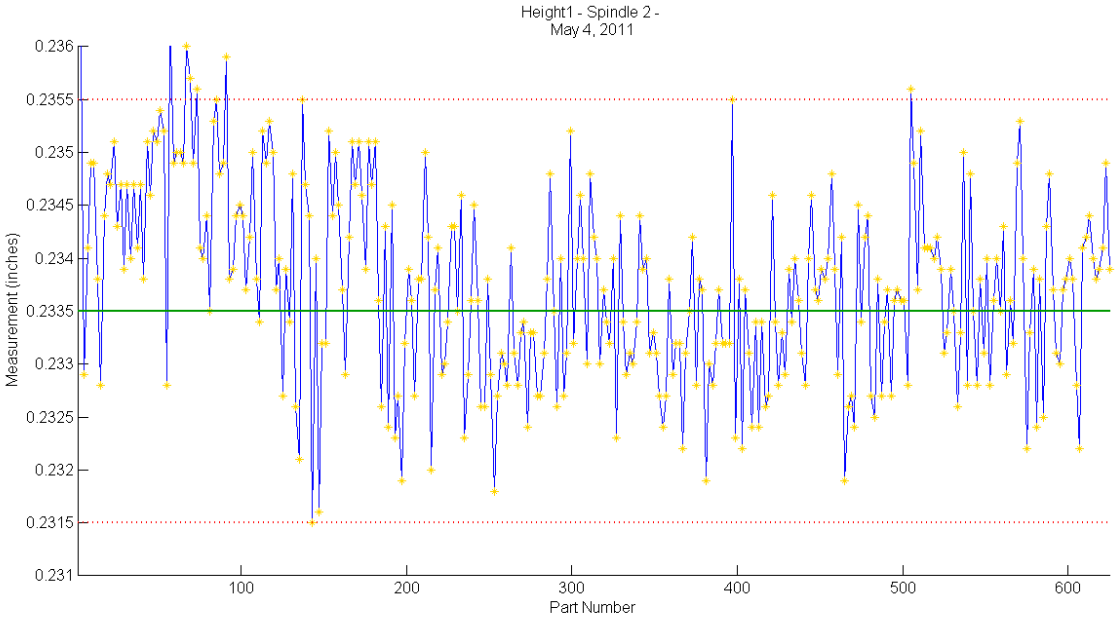

Figure 4.5-4 – Control chart for May 4, 2011 data collection, showing height 1 measurements from spindle 2

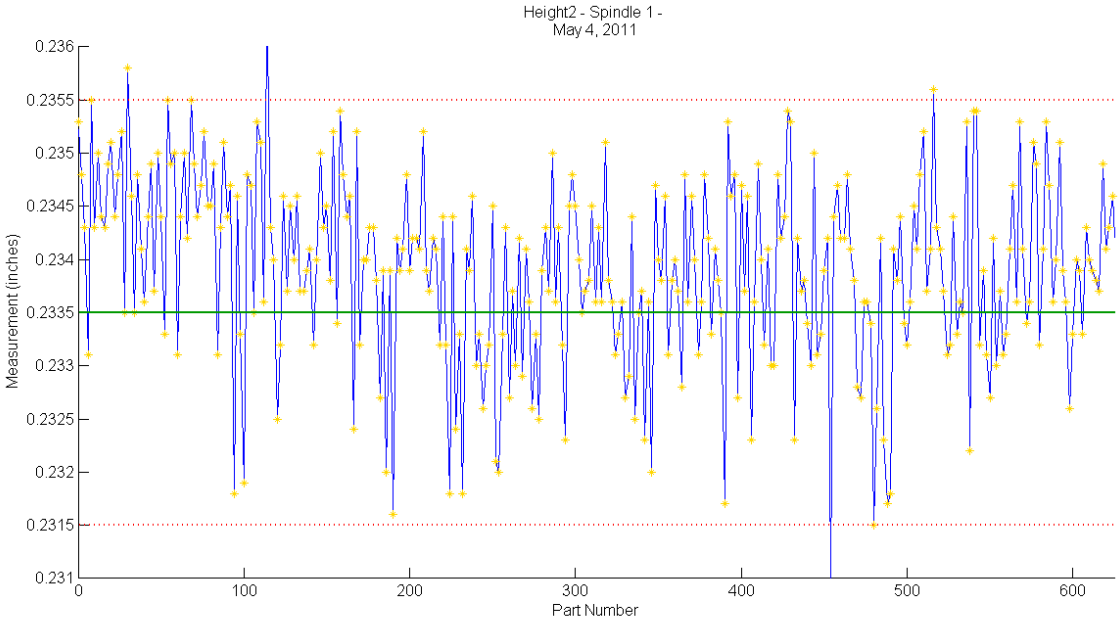

Figure 4.5-5 – Control chart for May 4, 2011 data collection, showing height 2 measurements from spindle 1

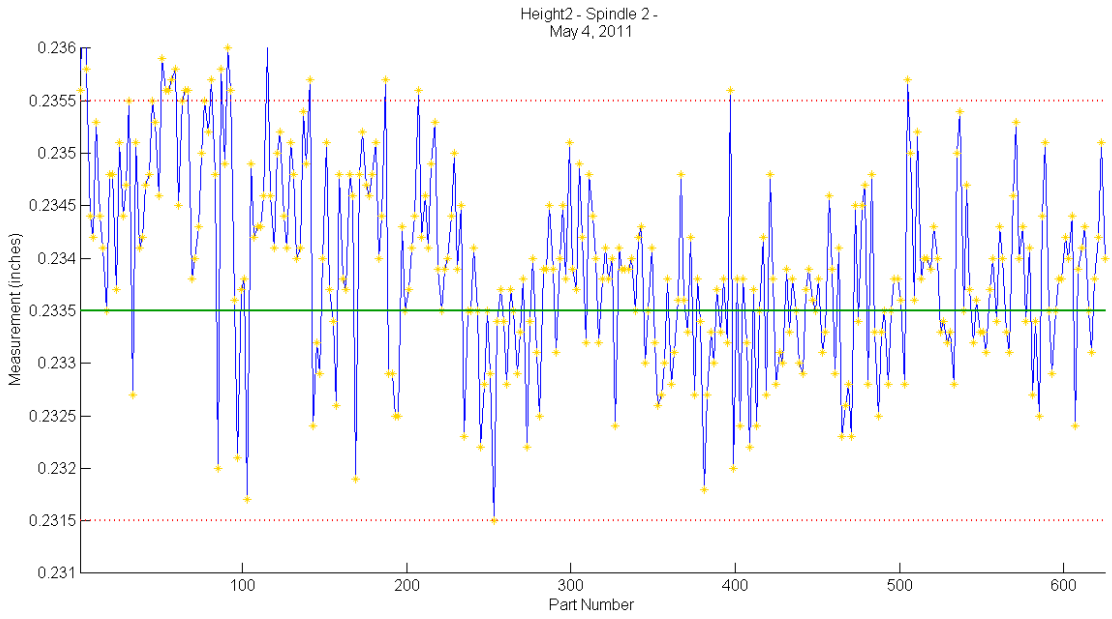

Figure 4.5-6 – Control chart for May 4, 2011 data collection, showing height 2 measurements from spindle 2

Table 4.5-1 – Summary statistics for May 4, 2011 data collection

Data Set		Mean (inches)	Std. Dev. (inches)	C_{pk}
Height*	Spindle 1	0.2338	0.00095	0.60
	Spindle 2	0.2339	0.00090	0.59
Diameter	Spindle 1	6.6739	0.0018	0.57
	Spindle 2	6.6737	0.0021	0.52

*Height stats are the average of height 1 and height 2 from each spindle

These figures demonstrate the significant potential for improvement in this process. As can be seen in the control charts, consecutive part measurements regularly vary by up to 50% of the entire tolerance range, which is reflected in the standard deviation and C_{pk} values.

As per Section 4.2.2, Goal 4 is to provide automated statistical process control which will make offsets to the CNC automatically. In order to achieve this, the dominant source of variation in parts must be from non-random sources so that trends can be identified, analyzed, and corrected. Therefore, process improvements were necessary to remove the apparent random variation which is present in this data set.

The process improvement initiatives prompted by this data are discussed in the next section.

4.5.2 PHASE 2: CORRECTIONS – AUGUST 18, 2011

After analysing the first set of collected data, it was clear that improvements were required before advancing implementation to the offset recommendation stages. Analysis of the process revealed the two major areas which required improvement. These areas align with Goals 1 and 2, as discussed in Section 4.2.2.

1) Remove part confusion: Operator duties in production sometimes require them to fall behind the CNC, allowing several parts to be produced before they can measure them. When this occurs, it is impossible to discern the sub-group a part was produced from. In order to correct this, a divider was installed on the conveyer as shown in Figure 4.2-5. This allowed the operator to discern which spindle parts were machined on and allowed them to designate the spindle appropriately when measuring them. This effectively accomplished Goal 1.
2) Gauge Improvement: In order for measurement variation to be corrected, the source of the variation needs to trend. For example, random cause variation introduced by a gauge with repeatability problems will mask trends in data. Due to the geometry of the part blanks, flatness or “waviness” error is common. In order to reduce this random variation, improvements were made to the gauge. Instead of surface-contact with the bottom face of the part, pins were installed and the gauge bottom surface was under-cut to allow clearance for the parts. In this way, the part was located using three point supports which were positioned directly under measurement locations, as depicted in Figure 4.2-7. This meant that reasonable levels of flatness error in the parts would no longer impact height measurements, effectively removing this source of variation. These improvements accomplished Goal 2.

After completing these improvements, data collection was conducted again on August 18, 2011.

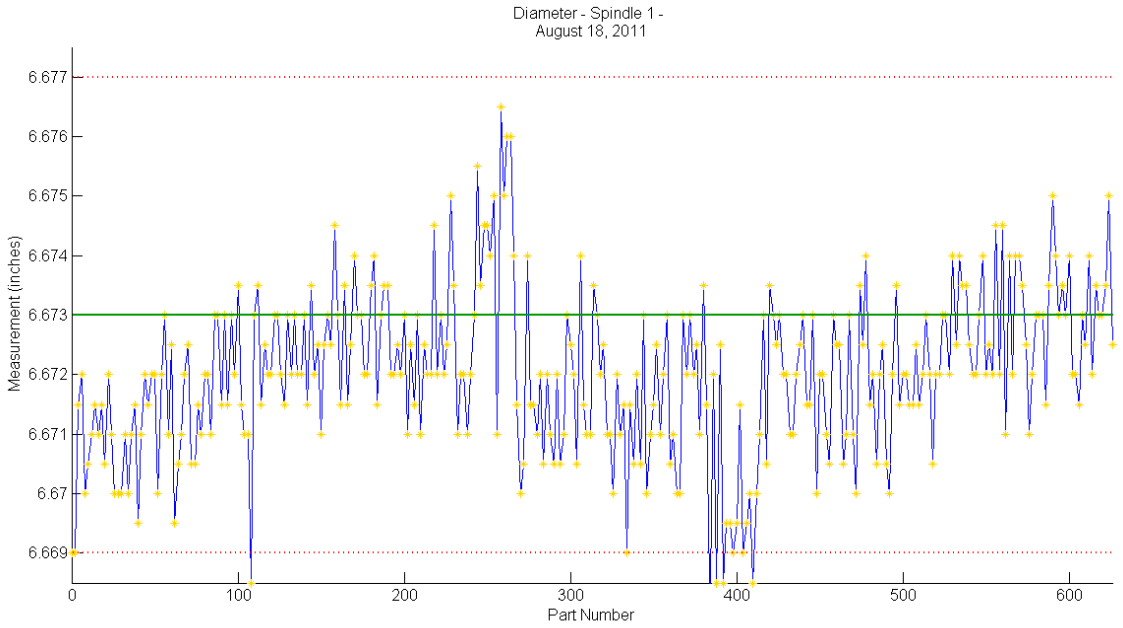

Figure 4.5-7 – Control chart for August 18, 2011 data collection, showing diameter measurements from spindle 1

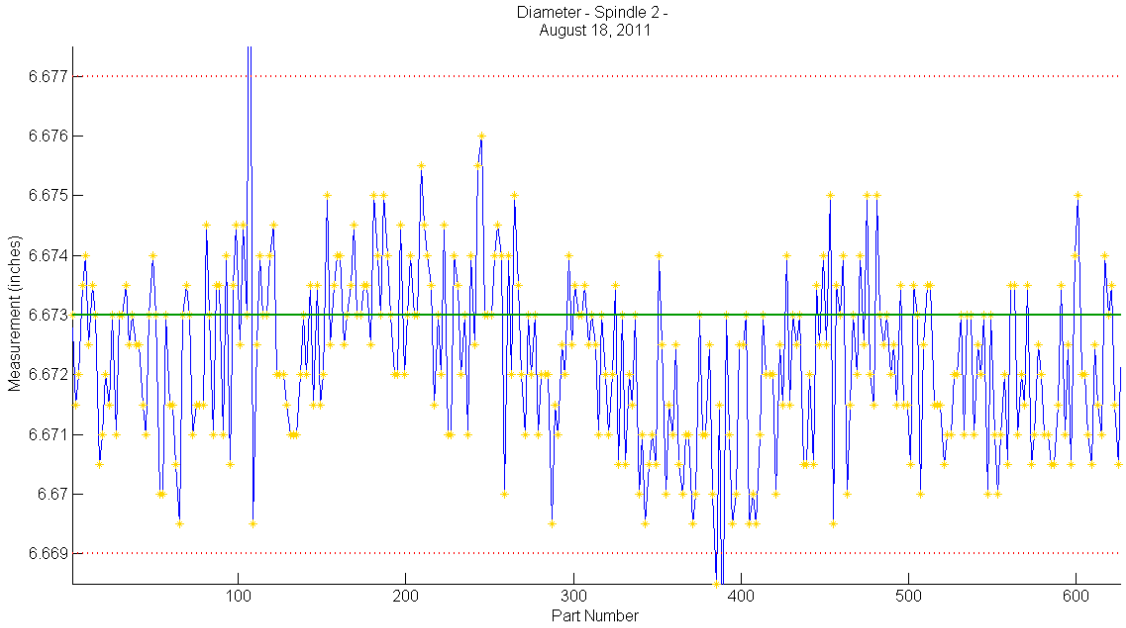

Figure 4.5-8 – Control chart for August 18, 2011 data collection, showing diameter measurements from spindle 2

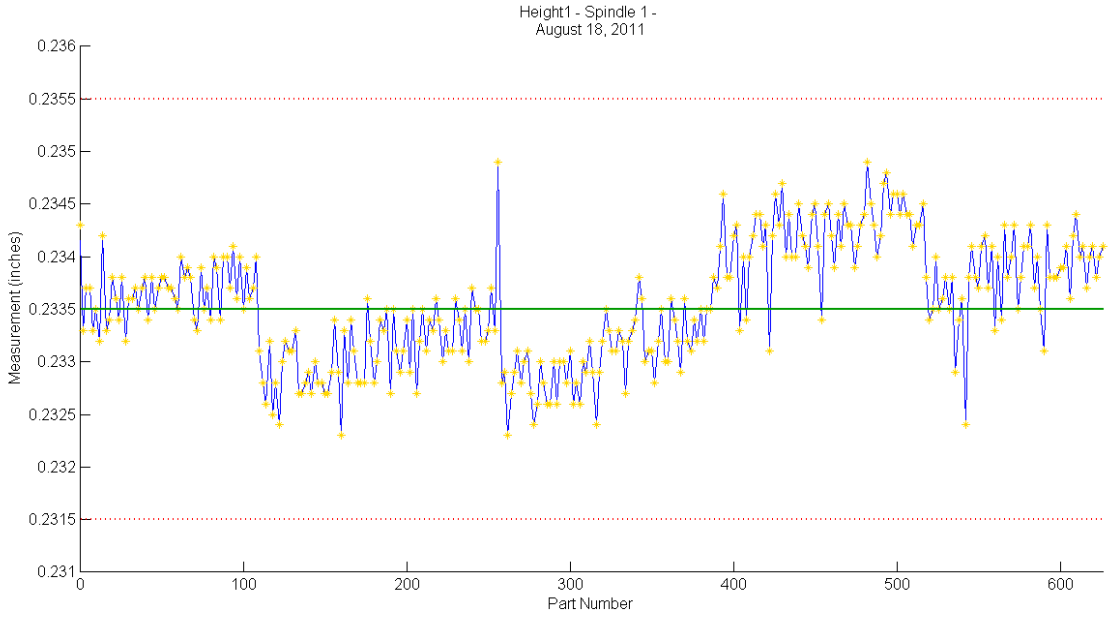

Figure 4.5-9 – Control chart for August 18, 2011 data collection, showing height 1 measurements from spindle 1

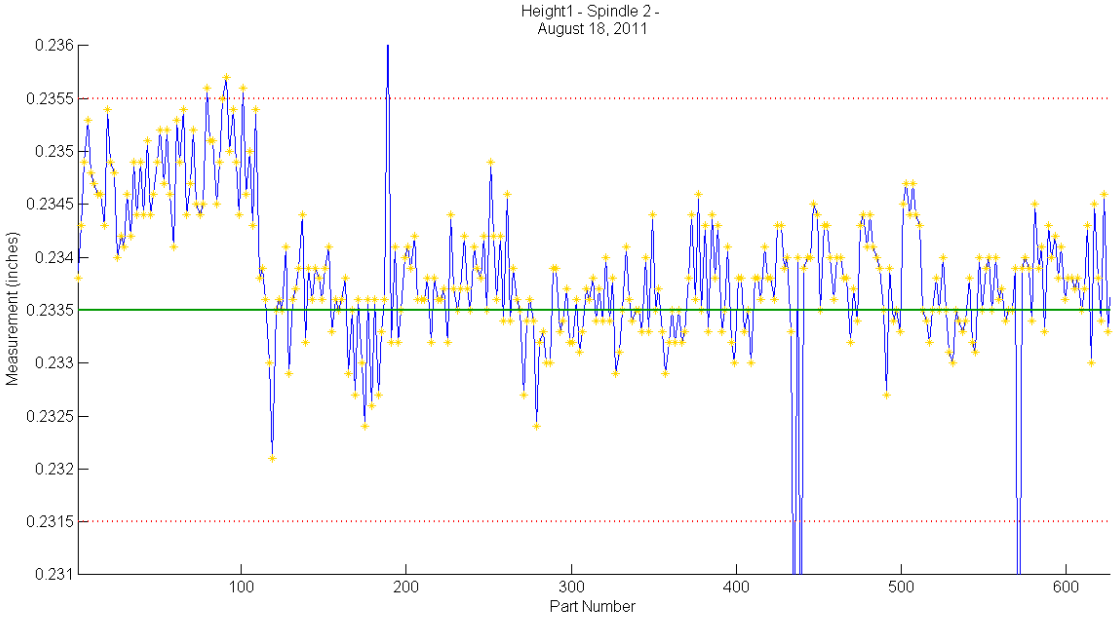

Figure 4.5-10 – Control chart for August 18, 2011 data collection, showing height 1 measurements from spindle 2

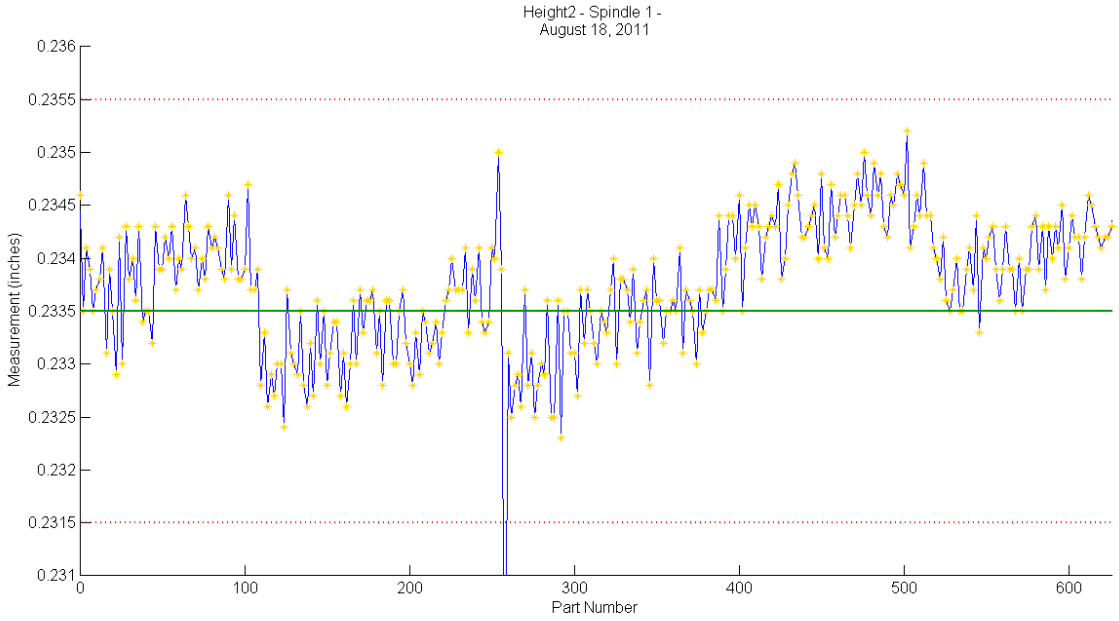

Figure 4.5-11 – Control chart for August 18, 2011 data collection, showing height 2 measurements from spindle 1

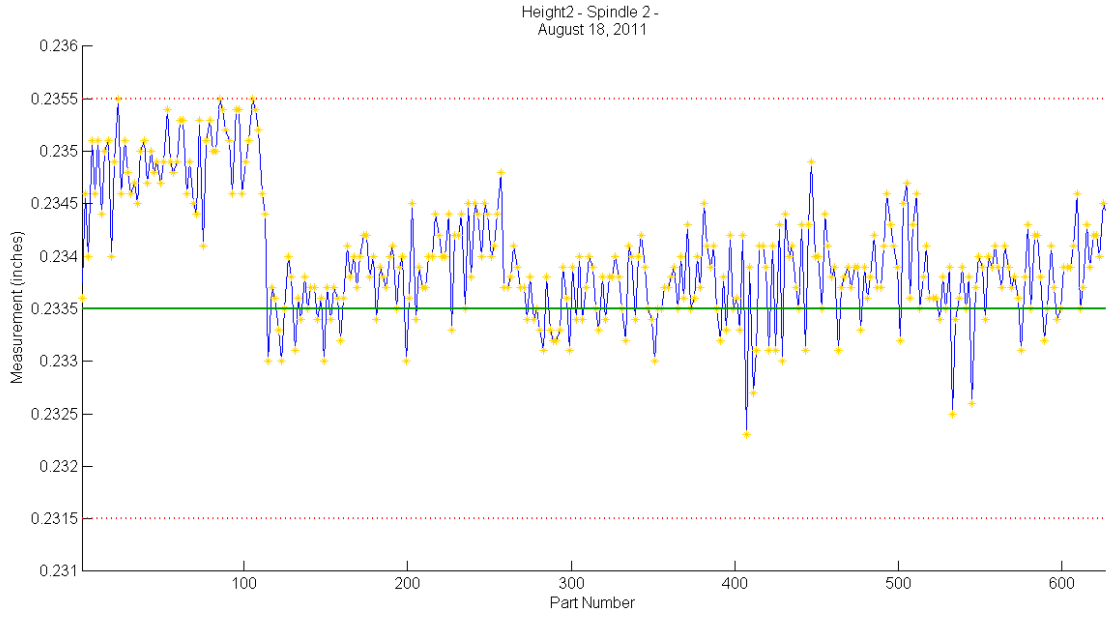

Figure 4.5-12 – Control chart for August 18, 2011 data collection, showing height 2 measurements from spindle 2

Table 4.5-2 – Summary statistics for August 18, 2011 data collection

Data Set		Mean (inches)	Std. Dev. (inches)	C_{pk}
Height*	Spindle 1	0.2336	0.00058	1.09
	Spindle 2	0.2337	0.00071	0.85
Diameter	Spindle 1	6.6721	0.0016	0.65
	Spindle 2	6.6722	0.0017	0.63

*Height stats are the average of height 1 and height 2 from each spindle

Visual inspection of Figure 4.5-7 through Figure 4.4-12 compared to Phase 1 reveal that less variation is occurring in the measurements, and indeed the C_{PK} and standard deviations shown in Table 4.5-2 confirm this. C_{pk} values for height have improved from 0.60 to 1.09 and 0.59 to 0.85 for Spindles 1 and 2 respectively.

Diameter data saw only minor improvement, though this is expected as the major impact of improvements was on height measurement only.

Note that Figure 4.5-10 and Figure 4.5-11 have data points which are far below the lower specification limit. These are due to swarf material becoming lodged on the spindles while parts are being mounted, causing the parts to not seat properly and thus be over-machined and undersized.

4.5.3 PHASE 3: SOFTWARE DEVELOPMENT – SEPTEMBER 2011 TO FEBRUARY, 2012

During this phase several software updates were made to include new features such as tool change and offset logging as well as gauge calibration reminders. Data collection was completed on several occasions, though the results were skewed by software bugs, hardware errors and operator error and so these results are not discussed here.

This phase also allowed operators to become comfortable with using the software through extensive usage.

Data was collected towards the end of this phase; in the interest of brevity the control charts are not included here as the summary statistics for this data set are sufficient for discussion.

Table 4.5-3 - Summary statistics for January 5, 2012 data collection

Data Set		Mean (inches)	Std. Dev. (inches)	C_{pk}
Height*	Spindle 1	0.2337	0.00094	0.64
	Spindle 2	0.2335	0.00010	0.67
Diameter	Spindle 1	6.6736	0.0012	0.94
	Spindle 2	6.6734	0.0013	0.92

*Height stats are the average of height 1 and height 2 from each spindle

As can be immediately seen, the CP values for this most recent set of data collection have become significantly worse for the height measurements. There is some improvement in the diameter though the reasons for this were not clear.

After some investigation using flatness gauges, the industrial partner had determined that flatness issues in incoming material had become significantly worse. The improvements to the gauge could only handle flatness variations below a certain threshold which parts were now regularly exceeding. Therefore complete redesign of the gauge would have been required to account for this error, a costly and time consuming endeavour. Therefore, the decision was made to move the software implementation to a different production cell. The new cell produced similar parts using a similar machine, gauge and process; the only differences being that the parts were approximately 30% smaller and did not suffer from any flatness issues. The parts also had a tighter tolerance on feature height, but a much wider tolerance on diameter.

4.5.4 PHASE 4: NEW PART – FEBRUARY 2012 TO MAY 2012

The dimensions and specification limits of the new parts compared to the parts used in previous phases are shown below in Table 4.5-4.

Table 4.5-4 – Comparison of new and old parts

Part	Specification Limits (inches)			
	Height		Diameter	
	Nominal	Tolerance	Nominal	Tolerance
Original	0.2335	± 0.002	6.673	± 0.004
New	0.1575	± 0.0012	4.752	± 0.006

As discussed in Section 2.5, C_{pk} is a function of the tolerance range. Therefore, it would be misleading to compare the C_{pk} values from original parts with the new parts as the tolerance ranges differ. For example, because both parts are produced on similar machines, it is a reasonable assumption that it is more challenging to produce the new part's height feature, as it requires a tighter tolerance. Therefore, if two sets of production have identical C_{pk} values, one for the old parts and one for the new, the process producing new parts is actually showing superior performance, according to Equation 4.5-1. This is because the new parts have a 40% smaller tolerance range, and so to achieve the same C_{pk} value, the standard deviation in the measurements (variation) must be proportionally smaller. Therefore, either: the process is under tighter control, the measurement methods are introducing less significant errors, or the blank material for the parts is more consistent.

$$C_{PK} \propto \frac{USL}{\sigma}, \frac{LSL}{\sigma} \qquad \textbf{Equation 4.5-1}$$

The software was now fully functional and significant sources of process variation such as error in the gauge, operator error, part confusion and variation in part blanks had been corrected. Data collection for new parts was collected on six dates over several months to track the performance of the process and to

confirm that the majority of variation in measurements was now coming from the machining process itself. Showing control charts for all collected data during this phase would require a great deal of space; therefore summary data is shown for all collection dates as well as select control charts of interest.

Table 4.5-5 - Summary statistics for February 22, 2012 data collection

Data Set		Mean (inches)	Std. Dev. (inches)	C_{pk}
Height*	Spindle 1	0.1573	0.00050	0.67
	Spindle 2	0.1575	0.00052	0.77
Diameter	Spindle 1	4.7523	0.0012	1.58
	Spindle 2	4.7518	0.0014	1.38

*Height stats are the average of height 1 and height 2 from each spindle\

Table 4.5-6 - Summary statistics for March 22, 2012 data collection

Data Set		Mean (inches)	Std. Dev. (inches)	C_{pk}
Height*	Spindle 1	0.1575	0.00035	1.14
	Spindle 2	0.1575	0.00070	0.43
Diameter	Spindle 1	4.7523	0.0010	1.90
	Spindle 2	4.7531	0.00089	1.84

*Height stats are the average of height 1 and height 2 from each spindle

Table 4.5-7 - Summary statistics for April 6, 2012 data collection

Data Set		Mean (inches)	Std. Dev. (inches)	C_{pk}
Height*	Spindle 1	0.1577	0.00051	0.65
	Spindle 2	0.1577	0.00057	0.58
Diameter	Spindle 1	4.7526	0.0015	1.20
	Spindle 2	4.7523	0.0014	1.36

*Height stats are the average of height 1 and height 2 from each spindle

Table 4.5-8 - Summary statistics for April 30, 2012 data collection

Data Set		Mean (inches)	Std. Dev. (inches)	C_{pk}
Height*	Spindle 1	0.1576	0.00026	1.41
	Spindle 2	0.1577	0.00033	1.01
Diameter	Spindle 1	4.7526	0.0015	1.20
	Spindle 2	4.7523	0.00097	1.96

*Height stats are the average of height 1 and height 2 from each spindle

Table 4.5-9 - Summary statistics for May 9, 2012 data collection

Data Set		Mean (inches)	Std. Dev. (inches)	C_{pk}
Height*	Spindle 1	0.1575	0.00022	1.82
	Spindle 2	0.1575	0.00023	1.74
Diameter	Spindle 1	4.7515	0.0018	1.02
	Spindle 2	4.7515	0.0018	1.02

*Height stats are the average of height 1 and height 2 from each spindle

Table 4.5-10 Summary statistics for May 14, 2012 data collection

Data Set		Mean (inches)	Std. Dev. (inches)	C_{pk}
Height*	Spindle 1	0.1576	0.00034	1.08
	Spindle 2	0.1575	0.00037	1.08
Diameter	Spindle 1	4.7515	0.00086	2.13
	Spindle 2	4.7511	0.00072	2.36

*Height stats are the average of height 1 and height 2 from each spindle

The average of the C_{pk} values from these six data sets is summarized in Table 4.5-11. Data for the dates of February 22, 2012 and March 22, 2012 were subject to production anomalies which affected their C_{pk} values significantly. Therefore, data from these dates is not included in the averages. As well, a modified C_{pk} is also calculated. This C_{pk} is calculated by using unaltered standard deviations from these data sets, but with the tolerance ranges from the original parts. While technically meaningless, these modified values will serve to highlight the effect that the differing tolerance ranges of the new parts have on C_{pk} calculations and that indeed the process is performing significantly better than a C_{pk} value comparison may indicate. This is a valid comparison because both parts are produced in similar production cells.

Table 4.5-11 – Average and Modified Average CP values for Phase 4

Data Set		C_{pk}	Modified C_{pk}
Height	Spindle 1	1.24	2.07
	Spindle 2	1.10	1.83
Diameter	Spindle 1	1.39	0.93
	Spindle 2	1.67	1.11

Below are control charts for April 30, 2012, which are representative of the data collected through this entire phase and highlight the improvements made.

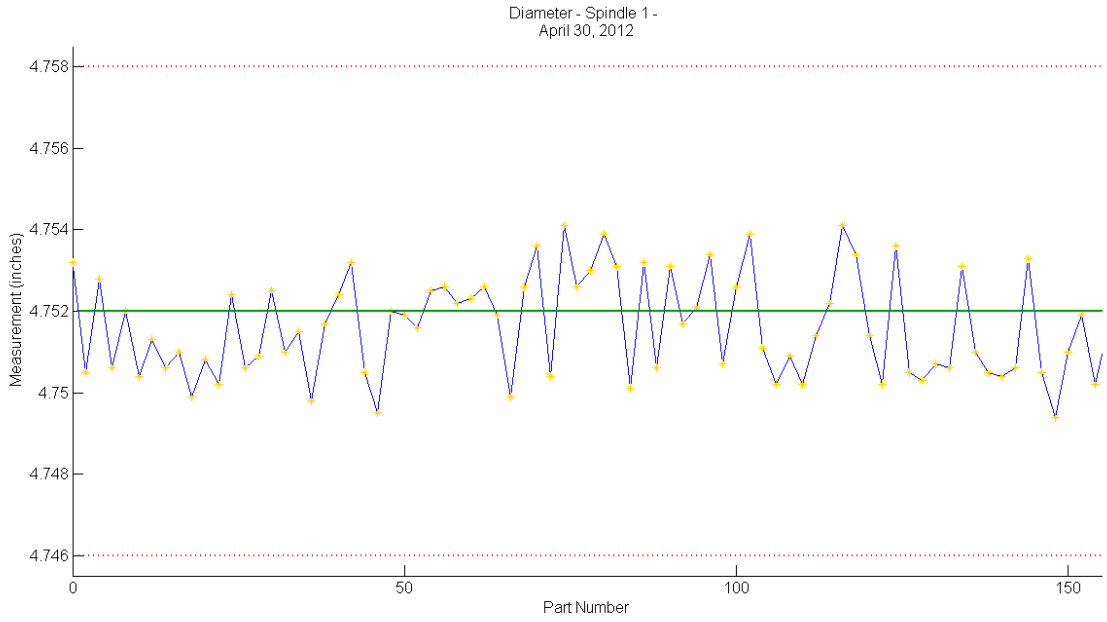

Figure 4.5-13 – Control chart for April 30, 2012 data collection, showing diameter measurements from spindle 1

Figure 4.5-14 – Control chart for April 30, 2012 data collection, showing diameter measurements from spindle 2

Figure 4.5-15 – Control chart for April 30, 2012 data collection, showing height 1 measurements from spindle 1

Figure 4.5-16 – Control chart for April 30, 2012 data collection, showing height 1 measurements from spindle 2

Figure 4.5-17 – Control chart for April 30, 2012 data collection, showing height 2 measurements from spindle 1

Figure 4.5-18 – Control chart for April 30, 2012 data collection, showing height 2 measurements from spindle 2

Note that in Figure 4.5-14 there is an outlier measurement which is massively undersized. These occur sporadically through the data sets. The cause of these was investigated and identified, and is due to worn bristle seals which prevent swarf material from leaving the machining chamber of the machine and entering the area where parts are mounted on the idle spindles. Due to this, chips occasionally pass through into the mounting area and land on the spindle before a part is mounted on it. Therefore, when the part is mounted on the chuck, the chip causes it to seat improperly and sit high on the spindle. Once machined, the part must be scrapped. Because the cause of these errors is known and is not a common-cause variation, these measurements are ignored in C_{pk} and other statistical assessments as they artificially affect these values.

4.5.5 PHASE 5: OFFSET IMPLEMENTATION – JUNE 2012 TO OCTOBER 2012 (ONGOING)

The final phase of this project begins implementation of the offset recommendation feature of the software. This feature, aligned with accomplishing Goal 4, tracks the part measurements in real time and when the process begins to violate pre-determined control limits, the software takes action by making an offset adjustment to the CNC machine, effectively implementing statistical process control (SPC) as described in Section 2.5. However, to reach this stage of full implementation, several steps are required as immediately implementing automatic offset adjustments without operator or intelligent oversight could have disastrous results; an erroneously large offset could cause the machine to crash. Therefore, the following plan for implementation is being followed:

--- Step 1: Offset recommendations to Operator, advisory only

The purpose of this step is to begin notifying the operator through a software “pop-up” window that the process has violated a control limit and

provides a recommended offset. In this step the operator takes no action beyond noting whether the offset is appropriate or not.

The goal of this step is to ensure that the software is making reasonable judgements and to tune control limit parameters.

--- Step 2: Offset recommendations to Operator, implemented

In this step, the operator will be required to make an offset adjustment when the software makes a recommendation, if they agree that the magnitude of the recommendation is reasonable. Production data can then be collected to determine if control limits have been set appropriately and if improvements are observed.

--- Step 3: Offset Recommendations to Machine, Semi-Automated

This step will be identical to previous steps, though now the operator will simply be required to accept or reject an offset recommendation through the software. If accepted, the software will make the offset directly through a data connection to the CNC controller. This interface also avoids data entry errors by the operator and greatly speeds up the offset update activity.

--- Step 4: Offset Recommendations to Machine, Fully Automated

This step represents full implementation of statistical process control for this production cell. The software will make automatic offsets to the CNC without requiring operator approval or influence.

At the time of this writing, Phase 5 is at Step 1. Feedback on offset recommendations is being collected from operators. Based on this feedback, along with production data and software logs, the control limits are being tuned.

4.5.6 OFFSET RECOMMENDATION LOGIC

At the time of writing, the offset recommendations are based on a simple moving average calculation completed according to the process described in Section 2.5. Upper and lower control limits are set at appropriate values, which are set at 75% of the specification limits (tolerances). When the moving average exceeds either the upper or lower control limit, an offset recommendation is made. The recommendation is also subject to a scaling factor to prevent over-compensation which may result in unstable behaviour.

Additional logic is used to suppress recommendations when they would not be appropriate. Changes inherent to the process which may artificially affect the moving average should not immediately trigger an offset recommendation. For example, after a tool change it is likely that the next produced part will vary significantly from the trends of the parts immediately before it. The software should wait several measurements before making a judgement on whether an offset is necessary in order to prevent data points from the previous tool improperly influencing the recommendation.

4.6 SUMMARY

This section will discuss the impacts of the work on the industrial partner's production, as well as summarize the improvements made to the software.

4.6.1 SUMMARY OF PRODUCTION STATS

This section summarizes the C_{pk} production metric for all phases. It is visible from Figure 4.6-1 that the implementation of the software in the industrial partner's production cell had a significant and positive effect on process capability (C_{pk}). Though production and quality control data was not available to verify scarp rates associated with calculated C_{pk} values, anecdotal evidence gleaned from

conversations with operators and quality control personnel supported the conclusions drawn based on C_{pk} values.

Table 4.6-1 – Summary of production data

Date	C_{pk}			
	H-S1	H-S2	D-S1	D-S2
04-May-11	0.60	0.59	0.57	0.52
18-Aug-11	1.09	0.85	0.65	0.63
05-Jan-12	0.64	0.67	0.94	0.92
22-Feb-12	0.67	0.77	1.58	1.38
22-Mar-12	1.14	0.43	1.90	1.84
06-Apr-12	0.65	0.58	1.20	1.36
30-Apr-12	1.41	1.01	1.20	1.96
09-May-12	1.82	1.74	1.02	1.02
14-May-12	1.08	1.08	2.13	2.36
11-Jul-12	1.14	1.08	1.53	1.33
12-Jul-12	0.96	0.99	1.38	1.49

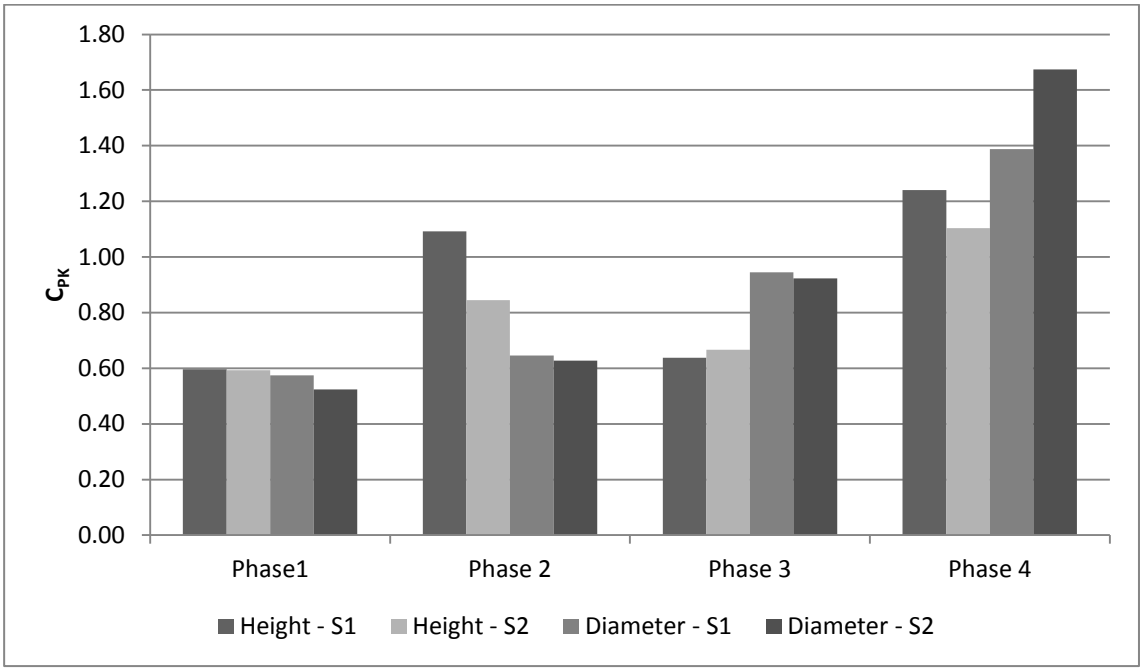

Figure 4.6-1 – Plot of average C_{pk} values for production value sorted by phase

Table 4.6-2 – Average C_{pk} values for production value sorted by phase

Phase	H-S1	H-S2	D-S1	D-S2
Phase1	0.60	0.59	0.57	0.52
Phase 2	1.09	0.85	0.65	0.63
Phase 3	0.64	0.67	0.94	0.92
Phase 4	1.24	1.10	1.39	1.67
Phase 5	N/A	N/A	N/A	N/A

4.6.2 GOAL COMPLETION

Goal 1 – Remove Part Confusion - Complete

This goal was completed after phase 1 when the conveyor divider was installed. There can still be confusion about sequence of parts being produced when parts stack up, however the difficulty in determining sequence of production, which becomes important in offset recommendation, is only a minor challenge for a competent operator.

Goal 2 – Gauge Improvement - Complete

Goal 2 was accomplished after the modification of the Gauge in Phase 2. Flatness errors no longer influence height measurements in parts and repeatability of the gauges has improved markedly as demonstrated by the improvements between phase 1 and phase 2 in Figure 4.6-1.

Goal 3 – Eliminate Operator Part Judgement – In Progress

The completion of this goal is still in progress and was not discussed heavily in this section. The capability to make judgments on whether a part is in tolerance or not is currently developed, but not yet implemented as this function was not a priority for the industrial partner.

This feature functions by displaying a visual and audio cue to the operator when the dial measurements are all within the specification limits. Therefore, rather than read all three dials and make this judgement, the operator simply

needs to look or listen for the visual or auditory cue, eliminating error in reading the dials or in mental math.

Therefore, this goal has not been completed as of this writing but could be implemented in a very short period.

Goal 4 – Automate Offset Judgement – In Progress

As discussed in Phase 5, this capability is currently being implemented in the test production cell and is progressing well. Therefore, the completion of this goal is currently in progress at the time of this writing.

4.6.3 FINAL REMARKS

Through this project, statistical process control and process monitoring were implemented in an industrial process to achieve real-world improvements. The process monitoring abilities of the software allowed the improvement process described in Section 4.1 to be applied. Several potential areas for improvement were identified and action was taken to exploit these opportunities.

Through this work, the C_{PK} of the process was improved by 236%, which corresponds to a theoretical reduction in scrap rates from 85,000 ppm to 30 ppm. Of course, this is an over-estimation of real-world scarp rates, but provides a sense of how substantial the improvement can potentially be.

4.7 FUTURE WORK AND GOALS

Aside from the completion of phase 5, there remain some potential improvements, recommendations and applications for this software which have not yet been developed. These are discussed in this section.

4.7.1 MMRI IMPROVEMENT VALIDATION TOOL

One of the future goals for this software is to track performance of other MMRI projects or work. The ability of this software to passively track the performance of a process over weeks or months is extremely valuable. Ideally, this software would be provided, packaged with industry research projects as a tool for validation of improvements.

For example, in a tool wear research project, once the testing has been done in our lab and recommendations are made, it is often difficult to track the performance of tooling in industry. Typically industry will report an improvement, sometimes substantially so, but it is rare that it is assessed quantitatively. However, if as a part of research collaboration this software is installed on the production cell where the improvements are being made, it can be used as a validation tool. Part measurements, production rates or other relevant metrics before and after the improvement can be tracked and analyzed.

This ability would be extremely useful in quantifying the value to industrial partners, as well as providing large data sets for researchers to determine if production results match expected results from lab-scale research.

4.7.2 SPINDLE INDEPENDENCE

As discussed extensively in section 4.4.2, the current implementation only requires the tracking of two offsets. The reason for this is that during the design of the production cell, the operator was responsible for tracking these, and tracking 4 separate trends was simply too difficult for one operator to handle. Therefore, the four spindles were grouped together to require only two offsets to be tracked.

With the implementation of the software, tracking four separate sub-groups is no longer challenging. It would be trivial to change the software to track each spindle separately for a total of four offsets and update them automatically.

Tracking all four spindles would allow for a more precise tracking of trends, and so there is potential improvement to be realized from pursuing this.

4.7.3 FULL AUTOMATION OF SOFTWARE

Currently the operator is required to interact with the software frequently through the button pad. In order to decrease the amount of time the operator spends interacting with the software, these interactions could be automated.

Installing a sensor or switch on the gauge to detect when a part has been inserted could replace the need for the operator interaction. The technical challenge in this would be preventing unintentional data collections.

Implementing this would require significant modifications to the gauge, which is costly and time consuming. As well, some operators may actually prefer to have precise control over when the data is collected through push-button control. Therefore, this is unlikely to be implemented without significant interest from the industrial partner.

CHAPTER 5. CONCLUSIONS AND FUTURE WORK

This body of work described the efforts made with two industrial partners to further knowledge in the areas of tooling and coating design, as well as process monitoring and control. The detailed results of these studies can be found in the summary sections (Section 3.5 and Section 4.6) of Chapter 4 and Chapter 5.

In collaboration with Siemens, their material and tooling was investigated in detail to identify causes of accelerated wear in machining of very high value parts. The use of both characterisation methods and empirical testing resulted in the identification of tooling having a more aggressive rake angle and a better performing coating. This superior tool provided over 300% improvement in tool life. Investigation revealed that neither the rake angle nor coating alone was enough to fully account for the best performance. While the coatings provided lubricity as well as thermal and oxidation protection, the rake angle served to decrease the forces seen during cutting. The synergistic combination of these two was required to achieve the highest tool life among the inserts tested.

This work resulted in a potential savings of $18,400 per part through increased productivity and decreased tooling cost. This opportunity also allowed the MMRI to improve its knowledge in machining of stainless steel like materials and develop data relating rake angle and coatings to tooling performance. These developments are also of value to other efforts within the MMRI, such as verification and development of Tribometer work completed by Dr. Stephen Veldhuis, Jeremy Boyd and Andrew Biksa (Biksa, et al., 2010) (Biksa, 2010).

In collaboration with another industrial partner, software was developed to monitor and control a mid-volume CNC production cell. By implementing the software, a number of potential areas of improvement were identified which otherwise would have gone un-noticed. These included improving gauge repeatability and identifying incoming material inconsistencies. These

improvements also represent the necessary steps to achieving collection of useful data, as data containing significant and preventable variation makes useful online-feedback impossible. A widely used and accepted measure of variation in a process, C_{PK}, was used as the metric to measure improvements in the process.

Through these improvements, a direct result of the software implementation, a 230% improvement in process capability was achieved. This, in theory, results in an order of magnitude reduction in out of specification parts.

In addition, the MMRI now has process monitoring software that it can implement with other projects to quantify their impacts on productivity, quality and cost over long term production. This data is extremely valuable to both research efforts and the industrial partner.

CHAPTER 6. BIBLIOGRAPHY

Altintas, Y., 2012. *Manufacturing Automation.* Second ed. New York: Cambridge University Press.

ASM, 2004. *Metallography and Microstructures Vol. 9.* 9 ed. Metals Park: ASM International.

Astrand, M., Selinder, T. I., Fietzke, F. & Klostermann, H., 2004. PVD-AL2O3-coated cemented carbide cutting tools. *Surface and Coatings Technology,* Volume 188-189, pp. 186-192.

Bachelet, E., 1990. *High temperature materials for Power Engineering.* Liege, Belgium, s.n., p. 595.

Barshilia, H. C. & Rajam, K. S., 2004. Raman spectroscopy studies on the thermal stability of TiN, CrN, TiAlN coatings and nanolayered TiN/CrN, TiAlN/CrN multilayer coatings. *Journal of Materials Research,* Volume 19, pp. 3196-3205.

Bhattacharyya, A., 2000. *Metal Cutting Theory and Practice.* s.l.:New Central Book Agency.

Biksa, A., 2010. *Tribological characterization of surface engineered tooling for metal cutting applications (Thesis).* Hamilton(Ontario): s.n.

Biksa, A., Boyd, J. & Veldhuis, S., 2010. Tribological characterisation of surface engineered tooling for metal cutting applications. *Proceedings of the Eight international conference in High Speed Machining.*

Boothroyd, G., 1981. *Fundamentals of Metal Machining and Machine Tools.* 9th ed. s.l.:McGraw-Hill.

Box, G. E., Hunter, W. G. & Hunter, J. S., 1978. *Statistics for Experiments - An Introduction to Design, Data Analysis, and Model Building.* New York: Wiley.

British Steel, 2006. [Online]
Available at: http://www.threeplanes.net/

Brookes, K., 2005. MIM marches on into hardmetal tool manufacture. *Metal Powder Report,* 60(14-16), pp. 18-19.

Cava, S. et al., 2007. Structural characterization of phase transition of Al2O3 nanopowders obtained by polymeric precursor method. *Materials Chemistry and Physics,* Volume 103, pp. 394-399.

Chamritski, I. & Burns, G., 2005. Infrared- and Raman-active phonons of magnetite, maghemite, and hematite: a computer simulation and spectroscopic study. *Journal of Physical Chemistry B,* Volume 109, pp. 4965-4968.

Chandra, M. J., 2001. *Statistical Quality Control.* s.l.:CRC Press.

Cheng, Y. H. et al., 2002. Substrate bias dependence of Raman spectra for TiN films deposited by filtered cathodic vacuum arc. *Journal of Applied Physics,* Volume 92, pp. 1845-1849.

Chen, M., Li, J. & Gou, G., 2001. An experimental and FEM study on dry turning of rotor steel 26NiCrMoV145 using multilayer coated carbide tool. *Mechanical Science and Technology,* Volume 15, pp. 243-261.

Chen, R. K., Gu, G. F., Han, L. Z. & Plan, J. S., 2011. Novel process to refine grain size of NiCrMoV steel. *Materials Science and Technology.*

Constable, C. P., Yarwood, J. & Munz, W. D., 1999. Raman microscopic studies of PVD hard coatings. *Surface and Coatings Technology,* Volume 116-119, pp. 155-159.

Constable, C. P. et al., 2001. Investigation of wear processes on worn tools using Raman microscopy. *Surface Engineering,* Volume 17, pp. 153-158.

Coutsouradis, D., ed., 1994. *Materials for advanced power engineering 1994.* s.l.:Springer.

Dogra, M., Sharma, V. S. & Dureja, J., 2011. Effect of tool geometry variation on finish turning - a review. *Journal of Materials Science and Technology,* Volume 4, pp. 1-13.

Dreiling, I., Stiens, D. & Chasse, T., 2010. Raman spectroscopy investigations of TiBxCyNz coatings deposited by low pressure chemical vapor deposition. *Surface and Coatings Technology,* Volume 205, pp. 1339-1344.

Edlmayr, V., Moser, M., Walter, C. & Mitterer, C., 2010. Thermal stability of sputtered Al2O3 coatings. *Surface and Coatings Technology,* Volume 204, pp. 1576-1581.

Eggleston, D. M., Herzog, R. & Thomsen, E. G., 1959. Observations on angle relationships in metal cutting. *ASME Journal of Industrial Engineering,* Volume 81, pp. 263-279.

Fietzke, F., Goedicke, K. & Hempel, W., 1996. The deposition of hard crystalline Al2Or layers by means of bipolare pulsed magnetron sputtering. *Surface and Coatings Technology,* pp. 657-663.

Fila, P. et al., 2005. Evaulation of super clean steels according to chemical composition. *Metalurgija,* 44(3), pp. 183-188.

Fox-Rabinovich, G. S. & Totten, G. E. eds., 2007. *Self-Organization During Friction.* Boca Raton: CRC Press.

Gates, J. D., Atrens, A. & Smith, I. O., 1987. Microstructure of As-quenched 3.5NiCrMoV Rotor Steel. *Z. Werkstofftech,* Volume 18, pp. 165-170.

Grzesik, W., 1999. Experimental investigation of the cutting temperature when turning with coated indexable inserts. *International Journal of Machine Tools and Manufacture,* Volume 39, pp. 355-369.

Gunay, M., Aslan, E., Korkut, I. & Seker, U., 2004. Investigation of the effect of rake angle on main cutting force. *International Journal of Machine Tools and Manufacture,* pp. 953-959.

Guo, Z. et al., 2010. Characterization and properties of MTCVD Ti(C,N) coated cemented carbide sbustrates with Fe/Ni binder. *International Journal of Refractory Metals and Hard Materials,* Volume 28, pp. 238-242.

Gupta, A. et al., 2010. Grain growth behavior of Al2O3 nanomaterials; a review. *Materials Science Forum,* Volume 653, pp. 87-130.

Jallad, K. N. & Ben-Amotz, D., 2002. Raman chemical imaging of tribological nitride coated (TiN, TiAlN) surfaces. *Wear,* Volume 252, pp. 956-969.

Jayaprakash, M. et al., 2010. Effect of contact pad rigidity on fretting fatigue behavior of NiCrMoV turbine steel. *International Journal of Fatigue,* Volume 32, pp. 1788-1794.

Kalpakjian, S. & Schmid, S. R., 2006. *Manufacturing Engineering and Technology.* Fifth ed. Upper Saddle River: Pearson Prentice Hall.

Kearney, M. G., 1985. The Structure and Properties of High Purity Ni-Cr-Mo-V Steels. *University of Leeds.*

Klocke, F., Gerschwiler, K., Cordes, S. E. & Fritsch, R., 2008. Analyses of the performance potencil of oxidic PVD wear-protection coatings on cutting tools using the example of crystalline γ-Al2O3. *Advanced Engineering Materials,* Volume 10, pp. 622-627.

Kohara, T., Tamagaki, H., Ikari, Y. & Fujii, H., 2004. Deposition of α-Al2O3 hard coatings by reactive magnetron sputtering. *Surface and Coatings Technology,* Volume 185, pp. 166-171.

Liew, W. H., 2010. Low-speed milling of stainless steel with TiAlN single-layer and TiAlN/AlCrN nano-multilayer coated carbide tools under different lubrication conditions. *Wear,* Volume 269, pp. 617-631.

Maranhao, C. et al., 2010. FEM machining analysis: influence of rake angle in cutting of aluminum alloys using polycristallyne diamond cutting tools. *International Journal of Materials and Product Technology,* Volume 37, pp. 199-213.

Martínez-Martínez, D. et al., 2009. Self-lubricating Ti–C–N nanocomposite coatings prepared by double magnetron sputtering. *Solid State Sciences,* Volume 11, pp. 660-670.

McHaughton, W. P., Richman, R. H. & Jaffee, R. I., 1991. "Superclean" 3.5NiCrMoV turbine rotor steel: A status report - Part I: Steelmaking practice, heat treatment and metallurgical properties. *Journal of Materials Engineering,* 13(1), pp. 9-18.

Meyer, W., 1984. *Presentation of the status of production of high purity rotor for advanced steam power plant.* s.l.:s.n.

Mohrbacher, H. et al., 1995. Oxidational wear of TiN coatings on tool steel and nitrided tool steel in unlubricated fretting. *Wear,* 188(1-2), pp. 130-137.

Moura, C. et al., 2006. Raman spectra and structural analysis in ZrOxNy thin films. *Thin Solid Films,* Volume 515, pp. 1132-1137.

M'Saoubi, R. & Ruppi, S., 2009. Wear and thermal behaviour of CVD α-Al2O3 and MTCVD Ti(C,N) coatings during machining. *CIRP Annals Manufacturing Technology,* Volume 58, pp. 57-60.

Nagabhushana, K. R., Lakshminarasappa, B. N. & Singh, F., 2009. Photoluminescence and Raman studies in swift heavy ion irradiated polycrystalline oxide. *Bulletin of Materials Science,* Volume 32, pp. 515-519.

Oomen-Hurst, S. M., Abad, M. D., Khanna, M. & Veldhuis, S. C., 2012. Comparative wear behavior studies of coated inserts during milling of NiCrMoV steel. *Tribology International,* Volume 53, pp. 115-123.

Parthasarathy, M., 2011. *Lab Manual for Manufacturing Technology II,* s.l.: s.n.

Rabinowicz, E., 1995. *Friction and Wear of Materials.* 2 ed. New York: Wiley.

Ruppi, S., 2005. Deposition, microstructure and properties of texture-controlled CVD α-Al2O3 coatings. *International Journal of Refractory Metals and Hard Materials,* Volume 23, pp. 306-316.

Ryu, S. H., Yu, J. & Hong, S. H., 1997. Quasi-steady-state creep crack growth in a 3.5NiCrMoV steel. *Metallurgical and Taterials Transactions,* Volume 28A, pp. 629-635.

Salemi, A. & Abdollah-zadeh, A., 2008. The effect of tempering temperature on the mechanical properties and fracture morphology of NiCrMoV steel. *Materials Characterization,* Volume 59, pp. 484-487.

Schiller, S. et al., 2004. *PVD Al2O3 coated cutting tool.* United States, Patent No. 6673430B2.

Schlicht, H., Schreiber, E. & Zwirlein, O., 1988. Effect of steel manufacturing process on the quality of bearing steels. *American Society for Testing Materials,* pp. 81-101.

Shaw, M. C., 1997. *Metal Cutting Principles.* New York: Oxford University Press.

Shige, T. et al., 2001. Development of large-capacity, highly efficient welded rotor for steam turbines. *Mitsubishi Heavy INdustries Ltd. Technical Review,* Feb., 38(1), pp. 6-11.

Shim, S. H. & Duffy, T. S., 2001. Raman spectroscopy of Fe2O3 to 62 GPa. *American Mineralogist,* Volume 87, pp. 318-326.

Silva, E. et al., 2010. Structure-property relations in ZrCN coatings for tribological applications. *Surface and Coatings Technology,* Volume 205, pp. 2134-2141.

Spengler, W. & Kaiser, R., 1976. First and second order Raman scattering in transition metal compounds. *Solid State Communications,* Volume 18, pp. 881-884.

Spengler, W., Kaiser, R., Christensen, A. N. & Muller-Vogt, G., 1978. Raman scattering, superconductivity, and phonon density of states of stoichiometry and nonstoichiomestry TiN. *Physical Review B,* Volume 17, pp. 1095-1101.

Spink, G. M., 1990. Fretting fatigue of a 2.5NiCrMoV low pressure turbine shaft steel - the effect of different contact pad materials and variable slip amplitue. *Wear,* Volume 136, pp. 281-297.

Statistics Canada, 2012. *Manufacturing sales, by subsector, by province and territory,* s.l.: s.n.

Stephenson, D. A. & Agapiou, J. S., 1997. *Metal Cutting Theory and Practice.* New York: Marcel Dekker.

Subramanian, B., Muraleedharan, C. V., Ananthakumar, R. & Jayachandran, M., 2011. A comparative study of titanium nitride (TiN), titanium oxy nitride (TiON) and titanium aluminum nitride (TiAlN), as surface coating for bio implants. *Surface and Coatings Technology,* Volume 205, pp. 5014-5020.

Tchizhik, A. A., Tchizhik, T. A. & Tchizhick, A. A., 1998. Optimization of the heat treatment for steam and gas turbine parts manufactured from 9-12% Cr steels. *Journalmof Materials Processing Technology,* Volume 77, pp. 226-232.

Tennant, G., 2001. *Six Sigma: Spc and Tqm in Manufacturing and Services.* s.l.:Gower Publishing Ltd..

Tlusty, G., 2000. *Manufacturing Processes and Equipment.* Upper Saddle River: Prentice-Hall.

Trent, E. M. & Wright, P. K., 2000. *Metal Cutting.* fourth ed. Woburn: Butterworth-Heinemann.

Votsch, W., Drobiniewski, J. & (assignee), W. A., 2004. *Cutting inserts with wear detection.* Unitied States, Patent No. 6682274B2.

Walter Tools, 2007. *Walter Tools General Catalogue,* s.l.: s.n.

Wermelinger, T., Borgia, C., Solenthaler, C. & Spolenak, R., 2007. 3-D Raman spectroscopy measurements of the symmetry of residual stress fields in plastically deformed sapphire crystals. *Acta Materialia,* Volume 55, pp. 4657-4665.

Wittig, J. E. & Joshi, A., 1990. High-resolution auger electron spectroscopy of grain boundary phosphorus segregation in NiCrMoV and NiCr Steels. *Metallurgical Transactions,* Volume 21A, pp. 2817-2821.

Yang, S., Wiemann, E. & Teer, D. G., 2004. The properties and performance of Cr-based multilayer nitride hard coatings using unbalanced magnetron sputtering and elemental metal targets. *Surface and Coatings Technology,* Volume 188-189, pp. 662-668.